Novel Materials for Cellular Nanosensors

Sasso, Luigi; Svendsen, Winnie Edith; Emnéus, Jenny; Castillo, Jaime

Publication date:
2012

Document Version
Publisher's PDF, also known as Version of record

DTU Nanotech
Department of Micro- and Nanotechnology

DTU

Novel Materials for Cellular Nanosensors

Luigi Sasso

Supervisors:
Winnie E. Svendsen
Jenny Emnéus
Jaime Castillo-León

June 1, 2012

Abstract

The monitoring of cellular behavior is useful for the advancement of biomedical diagnostics, drug development and the understanding of a cell as the main unit of the human body. Micro- and nanotechnology allow for the creation of functional devices that enhance the study of cellular dynamics by providing platforms that offer biocompatible surfaces for the cell culturing in lab-on-chip devices integrated with optimized nanosensors with high specificities and sensitivities towards cellular analytes.

In this project, novel materials were investigated with a focus on providing suitable surface modifications for electrochemical nanosensors for the detection of analytes released from cells. Two type of materials were investigated, each pertaining to the two different aspects of such devices: peptide nanostructures were studied for the creation of cellular sensing substrates that mimic *in vivo* surfaces and that offer advantages of functionalization, and conducting polymers were used as electrochemical sensor surface modifications for increasing the sensitivity towards relevant analytes, with focus on the detection of dopamine released from cells via exocytosis.

Vertical peptide nanowires were synthesized from diphenylalanine via a high temperature, aniline vapor assisted self-assembly process, yielding biological nanostructures 3-8 μm high and 200-300 nm in diameter grown from nanosensor surfaces and able to withstand cell culturing conditions. Several methods have been tested and optimized for the peptide nanowires' functionalization with biomolecules, metal nanoparticles and chemical functional groups such as thiols, showing the versatility and flexibility of this material's applications. A technique for the patterning of these nanostructures using soft lithography was also developed and tested for suitable cell sensing and culturing conditions. A study of the effect of these structures on the behavior of cell populations was carried out *in vitro*, utilizing PC12 cells as a differentiating stem cell neuronal model. The cells' growth, adhesion and morphology were characterized when cultured upon a surface of peptide nanowires. An *in vivo* investigation also gave evidence of how the peptide nanowires can be used as surface modification in implantable electrodes for neurological measurements.

Conducting polymers were utilized in electrode modifications for electrochemical sensor surfaces. Both chemical and electrochemical deposition methods were used to optimize the polymer film with respect to sensitivity towards cellular analytes, each method chosen accordingly to specific electrode geometry and shape. Chemical polymerization of pyrrole was used to achieve conductive polymer film coatings for out-of-plane electrode structures without or with poor surface conductivity,

providing a patternable conducting polymer deposition technique integrated with standard microfabrication techniques. Electropolymerization of pyrrole on planar interdigitated electrodes resulted in the creation of doped conducting polymer films. Different counter-ion dopants were tested, and the process was optimized in terms of electrochemical sensitivity towards dopamine. The doped polypyrrole modification was used for the *in vitro* detection of dopamine released via cellular exocytosis.

Combinations of these materials were tested, and an integrated surface modification consisting of both peptide nanowires and conducting polymers was applied to an *in vitro* cell culturing and sensor platform for the detection of dopamine from PC12 cell populations, showing how the advantages of each material type can be united into a joint cellular nanosensor modification.

Résumé

Den overvågning af cellulær adfærd er nyttig til fremskridtet af den biomedicinske diagnostik, lægemiddeludvikling og forståelsen af en celle som hovedenhed af det menneskelige legeme. Mikro- og nanoteknologi giver mulighed for oprettelsen af funktionelle enheder, der forbedrer studiet af cellulære dynamik ved at give platforme, der tilbyder biokompatible overflader til celledyrkning i lab-on-chip enheder integreret med optimerede nanosensorer med høje specificiteter og følsomhed over for cellulære analytter.

I dette projekt, blev nye materialer undersøgt med fokus på at give egnede overfladeændringer for elektrokemiske nanosensorer for detektion af analytter frigivet fra cellerne. To typer af materialer blev undersøgt, hver vedrørende de to forskellige aspekter af sådanne enheder: peptid nanostrukturer blev undersøgt for oprettelsen af cellulære aflæsning substrater, der efterligner in vivo overflader, og som byder på fordele ved funktionalisering, og ledende polymerer blev brugt som elektrokemiske sensor-overfladeændringer for at øge følsomheden over for relevante analytter, med fokus på påvisning af dopamin frigivet fra celler via exocytose.

Vertikale peptid nanotråde blev syntetiseret ud fra diphenylalanine via en høj temperatur, anilin damp assisteret selvsamling proces, hvilket gav biologiske nanostrukturer 3-8 μm høj og 200-300 nm i diameter dyrket fra nanosensor-overflader og i stand til at modstå celle dyrkningsbetingelserne. Adskillige fremgangsmåder er blevet testet og optimeret for at funktionalisere peptid nanotråde med biomolekyler, metalliske nanopartikler og kemiske funktionelle grupper, såsom thioler, der viser alsidigheden og fleksibiliteten af dette materiales påførelse. En teknik til at lave mønster af disse nanostrukturer ved hjælp af blød litografi blev ogsåudviklet og testet for egnede celle aflæsning og dyrkningsbetingelser. En undersøgelse af virkningen af disse strukturer på opførslen af cellepopulationer blev udført *in vitro* ved brug af PC12-celler som en differentierende stamcelle neuronal model. Cellernes vækst, adhæsion og morfologi var karakteriseret ved dyrkning på en overflade af peptid nanotråde. En *in vivo* undersøgelsen gav ogsåbeviser på, hvordan de peptide nanotråde kan bruges som overfladebehandling i implanterbare elektroder til neurologiske målinger.

Ledende polymerer blev anvendt i elektrode modifikationer for elektrokemisk sensoroverflader. Både kemisk og elektrokemisk deponeringsmetoder blev anvendt til at optimere polymerfilm med hensyn til følsomhed over for cellulære analytter, idet hver metode vælges i overensstemmelse med den specifikke elektrodes geometri og form. Kemisk polymerisation af pyrrol blev anvendt til at opnåledende polymerfilmbelægninger til ude-af-planet elektrodestrukturerne med eller uden dårlig overfladeledningsevne, hvilket giver en mønstret ledende polymer udfældningsteknik in-

tegreret med standard microfabricationsteknikker. Elektropolymerisation af pyrrol på plane interdigiterede elektroder resulterede i etableringen af doterede ledende polymerfilm. Forskellige mod-ioner doteringsstoffer blev testet, og processen blev optimeret med hensyn til elektrokemisk følsomhed overfor dopamin. Den doterede polypyrrol modifikation blev anvendt til *in vitro* påvisning af dopamin frigivet via cellulær eksocytose.

Kombinationer af disse materialer blev testet, og en integreret overflademodifikation bestående af både peptid nanotråde og ledende polymerer blev påført en *in vitro* celledyrkning og sensorplatformen til påvisning af dopamin fra PC12 cellepopulationer, der viser, hvordan fordelene ved hvert materiale type kan blive forenet i en fælles cellulær nanosensor modifikation.

Preface

This thesis is presented as a partial requirement for obtaining a Ph.D. degree from the Technical University of Denmark (DTU). The research was financed by the EU Commission within the framework of the project "Excell" (NMP4-SL-2008-214706) and carried out at the Department of Micro- and Nanotechnology (DTU Nanotech) in the period from June 2009 to May 2012.

The Ph.D. project was supervised by Associate Professor Winnie E. Svendsen, leader of the Nano-Bio Integrated Systems (NaBIS) group, and co-supervised by Professor Jenny Emnéus, leader of the Bioanalytics group, and Assistant Professor Jaime Castillo-León.

Kgs. Lyngby,
1st June, 2012

Luigi Sasso

Acknowledgments

This project would not have been possible without the support of a large number of people, a collection of brilliant minds that have touched my life and have inspired me with their curiosity and thirst for knowledge.

I would first like to express my gratitude to my supervisors, for their professional, social and moral support during the last three years, and for having contributed with superior guidance to this thesis. To Winnie Svendsen, for giving me the opportunity to carry out this project in her research group, for always believing in me, for always letting me make my own decisions, for the enthusiasm she has shown towards my work, for her adventurous scientific spirit, and for always being able to point out the forest when all I could see were trees. To Jenny Emnéus, for welcoming me into the Excell project with warmth, for the contagiousness of her creativity and spontaneity, for having shown me how to do "good analytical science", and for the many philosophical discussions during airplane trips to project meetings. Also, to both Winnie and Jenny, thank you for teaching me how to ski. To Jaime Castillo, for introducing me to the world of peptide self-assembly, for being a point of reference during my work, always available when I needed help, for always pointing out the one data point I was missing, for the many scientific email discussions at 4 a.m. when I was going to sleep and he was waking up.

A special thanks goes to the current and previous members of the NaBIS group, for spicing up the workplace with their many different cultures and personalities. Particularly to Maria Dimaki for being my guru in microfabrication and for supporting this project by being an unofficial supervisor, to Patricia Vazques for the complicity we have found while working together, to Karsten Andersen for sharing my vision of a better world and for the the many brainstorming sessions all around the world, scribbling our ideas on napkins and hotel brochures at odd hours of the night, to Indu Vedarethinam, for teaching me the secrets of cell culturing, for her smiles and positive attitude towards life, for being a ray of sunshine on those dark Danish evenings in the lab. To the Masters students, especially the ones I have had the opportunity to help supervise: Mohammed Abaddi, Francesco Diazzi, Mehmet Taskin, Tanya Bakmand, thanks for your innovative perspectives and all your hard work. To Casper Clausen and Mohammad Ajine, for sharing an office and a lot of chocolate with me during these years. To Dorota Kwasny for all the fruitful scientific discussions, and for donating her old sofa to my office. To Romén Rodriguez, for his sweet and caring personality that is so useful in times of stress. To the rest of the NaBIS group, each of whom has influenced me greatly during the project, thank you for letting me feel part of this research family.

To the Excell consortium, for providing a professional network of researchers with

expertise in many scientific disciplines. Particular thanks to the "young" scientists: Tania Ramos, Natalia Avaliani, Marco Vergani, Ettore Landini, Miklos Mohos and all the rest, for the constant communication throughout the project and for sharing a common drive for the collaborative work. To the "young-at-heart" scientists: Marco Sampietro, Zsofia Keresztes, Ulla Wollenberger, Roberto Raiteri and the rest, for making the project meetings fun and enjoyable while maintaining a high level of scientific professionalism that I very much admire.

To Arto Heiskanen, a true dragon in electrochemistry, thanks for being my default hotel roommate in all the project meetings, for the many inspiring and enlightening late-night conversations, for all the weekends spent in the lab together, for all the breaths of fresh air we have shared, for being a solid rock in this tortuous river of scientific research. This world needs more Artos.

I wish to thank all the people at DTU Nanotech who have somehow been part of my every day life during these past years, greeting me with a smile on the way down the stairs or chatting with me while waiting in line for coffee. I cherish the friendship that some of them have shown me. I'm grateful to them for making the department a place I will miss.

Last but not least, I would like to thank all my loved ones, both family and friends who are scattered across the world, who show constantly their love for me without limitations from small details such as geographical distance. I could not have done this without their support.

Contents

Chapter 1

Introduction

Modern trends in micro- and nanotechnology offer relevant features and functionalities for the monitoring of cellular responses [1], both in terms of providing suitable cell culturing substrates [2, 3] and electrochemical sensor modifications for the detection of specific cellular analytes [4]. Microtechnology offers powerful circuits and sensor systems for the development of innovative solutions to biological questions [5, 6, 7], for example by providing the miniaturization of electrochemical sensor electrodes to sizes comparable to single cells or cell populations. This miniaturization allows for a more efficient transport of the cellular analytes to the sensor surface, therefore resulting in devices with higher sensitivities. There is also a focus towards obtaining functional platforms that do not alter the cellular behavior but offer possibilities for the biological study of cells. Finding the correct materials for the development of these devices, though, is often cumbersome and requires the right combination of biocompatibility and sensor performance.

The scientific study of cellular behavior in *in vitro* and *in vivo* systems gives us the opportunity to gain insights about the complex biological mechanisms behind cellular dynamics, in order to obtain crucial information for the development of medical diagnostics techniques, drug development and overall a better biological understanding of the human body and its functional components.

The PhD project behind this thesis has been carried out within the framework of the EU financed project "Excell" (NMP4-SL-2008-214706). The project focused on finding innovative approaches for investigating cellular dynamics, by exploring the interaction mechanisms between live cells and micro- and nanostructures. It goes without saying that a project of this kind asks for the integration of various inter-disciplinary scientific fields, and the many partners of this project were involved according to their technological and scientific specializations, including cell

and molecular biology, nano- and microelectronics, analytical chemistry, material engineering, biotechnology, and microfluidic engineering.

The main aim of the Excell project was to develop a novel microfluidic cell culture and nanosensor array system capable of studying cells and cell populations by investigating their dynamics with the use of electrochemical analytical sensors, among other types. The project was based on addressing key issues in stem cell research and studying the cellular differentiation mechanisms by sensing relevant analytes excreted from cells cultured in the developed platform. A major focus has been placed on the study of neuronal stem cell implantation into damaged brain tissue, by validation of stem cell differentiation and functionality via detection of neurotransmitters release, particularly dopamine. Because of the role of dopamine as a neurotransmitter, the study of the dopaminergic properties of stem cells has been a crucial topic in brain research tailored towards finding better treatments and eventually a cure for neurological diseases such as Parkinson's or Alzheimer's [8].

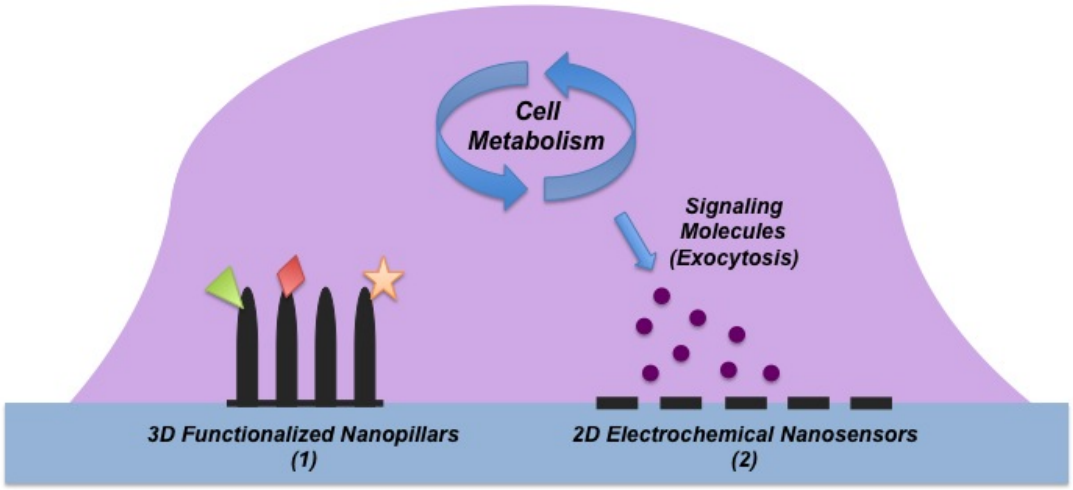

Figure 1.1: Schematic of the Excell platform, showing functionalized 3D nano pillars and 2D electrochemical sensors for the detection of analytes released from cells.

My part in this large project was to find novel suitable methods for both (1) the inclusion nanopillars in the platform that would mimic a biological surface and could be functionalized with various relevant molecules and chemical groups for the cellular sensing, and (2) the surface modification of electrochemical nanosensors to provide sensitivity towards specific analytes released from cells, with focus on dopamine exocytosis (see Fig. 1.1). In the context of this thesis, a *cellular*

nanosensor is defined as a sensor for the detection of cellular analytes with sensitivity to concentrations in the nM range and below.

1.1 Project Aim and Overview

The aim of this project was to investigate new materials for use in sensing platforms for the detection of cellular analytes, focusing on creating (1) *in vivo*-like cell sensing substrates that can offer culturing directly on a sensor surface with the possibility for facile functionalization and (2) electrode surface modifications to increase the sensitivity towards relevant analytes released from cells, particularly dopamine.

The material choices made for the investigations reflect the project aims, being (1) biological structures in the range of cell-like dimensions for creating *in vivo*-like sensing surfaces and (2) conducting polymer surface modifications for achieving an increase in sensitivity of the electrochemical sensing.

Self-assembled vertical peptide nanowires were chosen as a candidate material for mimicking a biological environment. These structures, that have proved to stay solidly attached to a surface and stable under cell culturing conditions, have typical dimensions of 200-300 nm in diameter and 3-8 μm in height. Various means for functionalization of these structures have been developed, including the possibility for their decoration with biomolecules, metal nanoparticles and relevant functional groups such as thiols. A visual *in vitro* biocompatibility assessment was carried out to study the effect of these structures upon cell populations in terms of cell growth, adhesion and morphology. By growing the peptide nanowires onto an implantable electrode, the effects of these structures in a live rat brain were investigated via an *in vivo* experiment.

Conducting polymers were chosen as the basis for electrode modifications for the sensitivity increase. Various film formation methods were studied, based on both chemical and electrochemical deposition of a polymer film. The deposition methods were chosen depending on their suitability towards specific electrode geometries and shapes. Chemical polymerization was used in the case of 3-dimensional electrode structures for cellular sensing, providing a polymer deposition method that does not require a conductive surface underneath, therefore showing how this material can be used to enhance current microfabrication techniques and be a solution to some of the issues encountered during the fabrication of such structures, specifically in terms of metal deposition. Electropolymerization was used on planar interdigitated electrodes, offering the possibility for doping the conducting

polymer film. Several counter-ion dopants were studied in terms of electrochemical activity towards dopamine, and an optimized modification was developed and used for the *in vitro* detection of dopamine released from cells via exocytosis.

Combining these materials demonstrated how these modifications can be integrated onto the same cellular sensing platform, holding the *in vivo*-like and functionalization properties of the peptide nanowires while retaining the sensitivity increase brought upon by the conducting polymer films.

1.2 Thesis Organization

The thesis has been divided in sectioned chapters, reflecting the work that has been carried out during the 3 years of the PhD project:

Chapter 2

This chapter gives a theoretical background needed for understanding the rest of the thesis. It is divided in a *Cell Biology* section, explaining the various properties of cells studied in this project, and an *Electrochemistry* section, discussing the electrochemical concepts and techniques used throughout the investigation.

Chapter 3

This chapter is focused on the use of peptide nanostructures for cellular studies. The experimental work describes optimal techniques for the creation of the structures and their functionalization. An *in vitro* investigation of cellular behavior on peptide nanostructure surfaces is presented, and results from the growth of the biological nanostructures onto an implantable electrode shows the structures' effects in an *in vivo* situation.

Chapter 4

This chapter concentrates on electrode modifications with conducting polymer films for electrochemical sensing of cellular analytes. The first section holds a description for the chemical deposition of polymer films onto 3-dimensional structures to enhance their conductive properties. The second section shows how electrochemical polymerization can be used to create polymer films doped with counter-ions

that increase the sensitivity towards dopamine in *in vitro* detections from cellular exocytosis.

Chapter 5

This combinatorial chapter includes the use of various techniques and methods described in the previous chapters, illustrating how the advantages of the conducting polymer modifications can be used in conjunction with peptide nanostructure based cell sensing substrates.

Chapter 6

A concluding chapter summarizes the results and offers perspectives on how to continue the work for a better optimization of the cellular sensing surface modifications developed as well as their combinations.

Appendices

A list of the publications and conference contributions that have been produced throughout the project can be found in Appendix A and B, respectively.

As described in each section, the materials and methods behind the research can be found in Appendix C.

Several kinds of microfabricated electrode structures, shapes and geometries have been utilized during the project, and each requires different cleanroom techniques and protocols. Microfabrication is not intended to be the focus of this thesis, and therefore details about these processes can be found in the respective publications cited throughout the document.

Chapter 2

Theoretical Background

2.1 Cell biology

Cell biology is a vast and complex scientific field dedicated to the study of cells and their properties, both on a microscopic and molecular level. Knowledge about mammalian cellular behavior and function, particularly, is an important key in understanding the way our body works. Understanding the factors that effect cell behavior can give us insights about the causes for the many diseases associated with cellular dysfunction, aiding the development of preventions and cures against related diseases.

What follows is a brief introduction to concepts from this field that are relevant to this thesis, with focus on the structural and morphological properties of mammalian cell cultures and the cellular dynamics related to the PhD project aim such as dopamine exocytosis.

2.1.1 Cell Adhesion and Morphology

Cellular adhesion in an important factor when studying new materials for use in cell culturing or sensing. The adhesion to surfaces influences in some way all cellular processes, and a cell's well-being is highly affected by the substrate it lives on. For this reason understanding the way that a cell perceives and reacts to a substrate is important for the development of new medically useful devices such as *in vitro* electrodes, where a cell population is cultured directly on the electrode surface, or *in vivo* studies with implantable electrodes. These devices can both

be useful in terms of drug delivery or stimulation as well as cellular analysis via measurements from live cells.

When a cell comes in contact with a surface, it starts by forming filaments that form the basis for cellular adhesion. These "finger-like" projections from the cell membrane are called *microvilli*, and are 100 nm wide structures ranging 1 to 2 μm in lenght [9] (see Fig. 2.1).

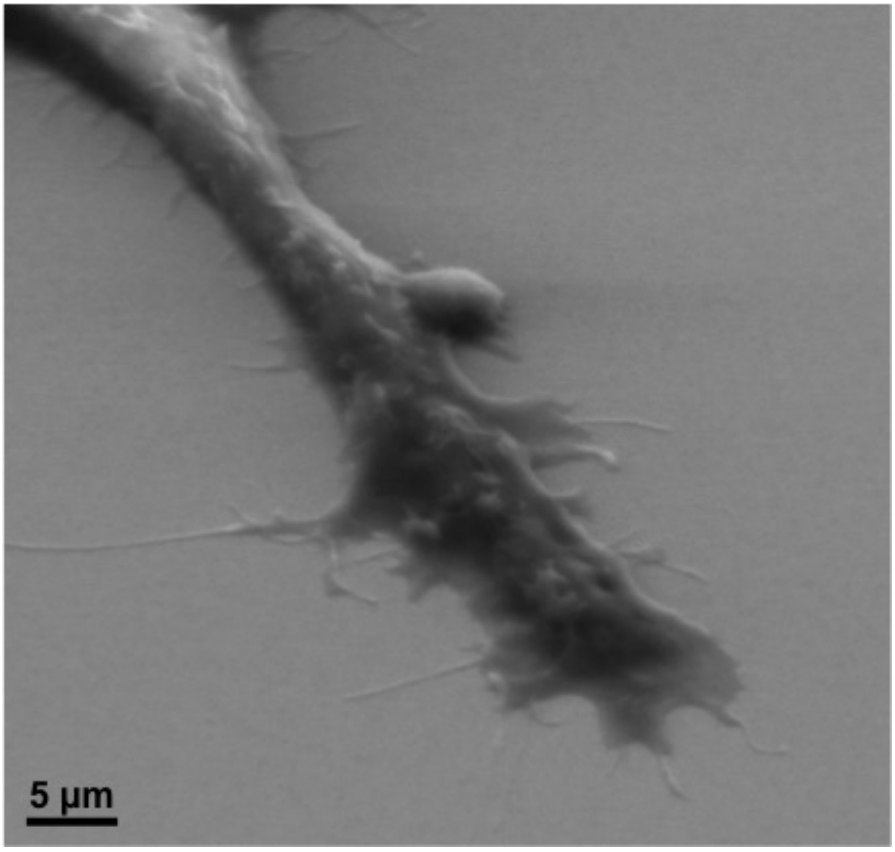

Figure 2.1: SEM image of projections from a HeLa cell membrane used as focal adhesion sites.

The attachment onto the suface is then strengthened by the formation of adhesion complexes on the cell membrane, mainly by the creation of an extracellular matrix composed of various proteins such as collagen, vitronectin, fibronectin, and laminin, as well as cell surface transmembrane glycoproteins to provide a strong binding between the extracellular matrix and the cell membrane [10]. Several of the extracellular matrix proteins are often used in cell culturing to increase the adhesion of cells to a particular substrate. Finally the cell reorganizes itself according to the surface both in terms of topology and protrusion generation. Cell morphology onto a surface is defined by the organization taken up by the cell's

cytoskeletal fibers, and this is highly influenced by the cell-surface interaction. If the surface is not suitable for the adhesion and culturing, cells will then exhibit unusual morphology (see Fig. 2.2).

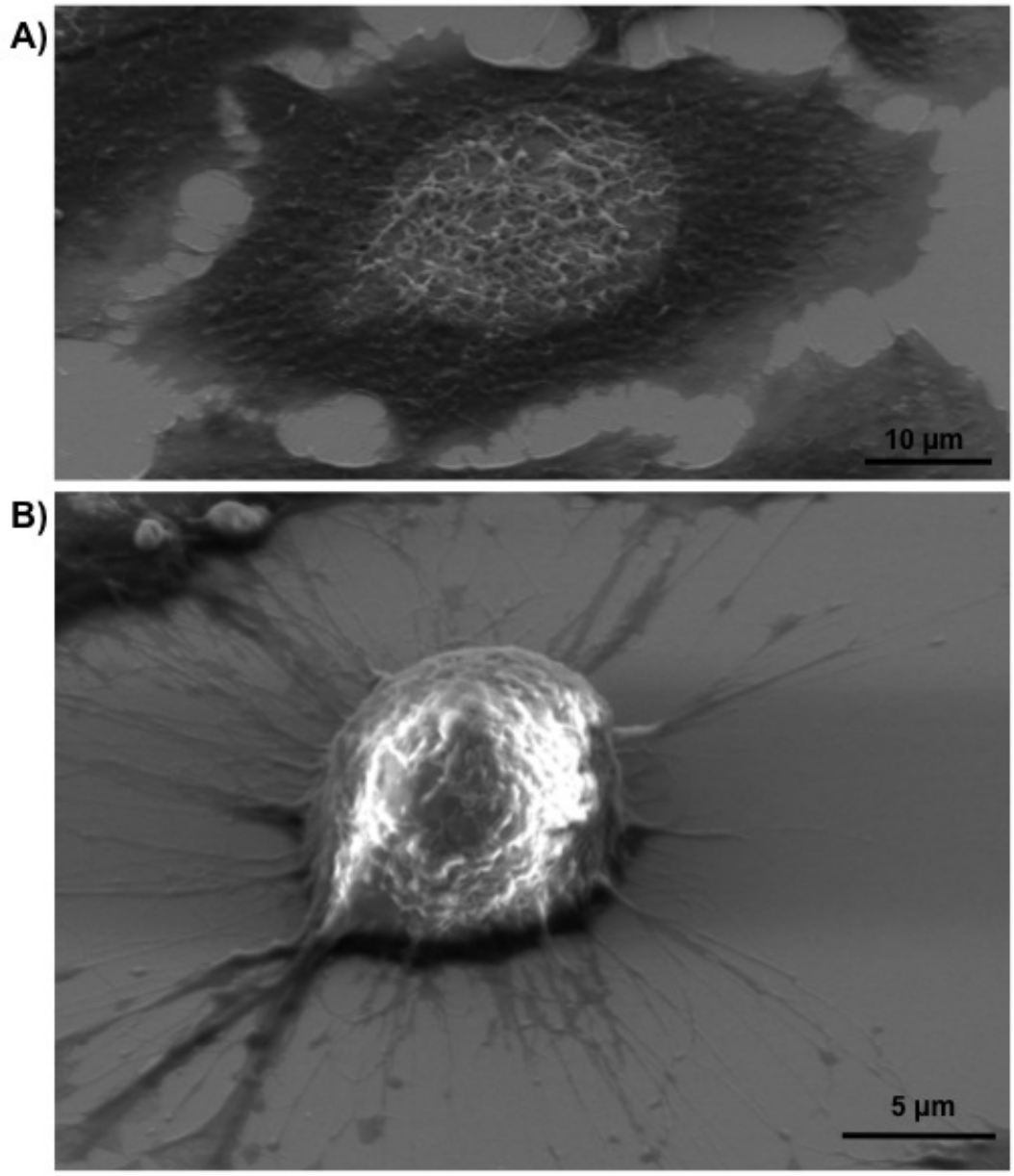

Figure 2.2: SEM images of A) a HeLa cell nicely adhered to a laminin coated gold surface and B) the same cell line, but cultured on a bare gold surface without adhesion enhancement protein coating.

2.1.2 Cell Differentiation

Stem Cells

Stem cells are defined as unspecialized biological cells found in multicelluar organisms that can *differentiate* into specialized cell types to be used in different parts of the body. They also have the ability to self-regenarate, meaning that they can divide and produce more copies of themselves many times, a process called *proliferation*. Stem cells are both present as embryonic stem cells, found in blastocyst structures in embryos, and adult stem cells, found in several tissues around the body and used as a repair system. Their use in clinical and biological laboratories has revolutionized the fields of genomics [11], the study of biological processes and the development of drug discovery [12].

Stem cell differentiation is the process by which these cells specialize into a specific function, and the differentiation mechanism is governed by the environment the cells are exposed to, particularly by specific growth factors related to the differentiation, which causes the cells to express different gene profiles.

Embryonic stem cells, or stem cells derived from embryos, that have proliferated in a cell culture without being differentiated, are called *pluripotent*, meaning that they have the ability to specialize into all the various cell types present in the body. *Adult* or *somatic stem cells*, on the other hand, are undifferentiated cells present in tissues or organs that have the ability to specialize into the limited cell types found in that particular tissue or organ. The roles of adult stem cells in the body are maintenance and repair of the specific tissue where they are found. Adult neuronal stem cells, for example, can give rise in the nervous system to neurons or glial cells like astrocytes or oligodendrocytes, but not to to bone marrow cells like osteoblasts [13].

PC12 Cells

Rat pheochromacytoma (PC12) cells were used throughout this project as a suitable model to study exocytotic dopamine release. There is an interest in the field of biology and in the Excell project to develop neuronal stem cells that can be differentiated into having dopaminergic properties, for future purposes of transplantation into damaged tissues in the human body [14, 15, 16]. PC12 cells were then used initially as a model to ensure the monitoring of dopamine from the developed sensing systems.

The differentiation of PC12 cells into neuronal models occurs by treatment with

nerve growth factor (NGF), a small protein present in the human body, responsible for the growth and survival of neurons discovered by Rita Levi-Montalcini in the 1950s, as a result of which she was awarded the Nobel Prize in Physiology or Medicine in 1986 [17].

The PC12 cell line was originally created as a cell model for neurochemical and neurobiological studies [18]. It has been widely used as a model to investigate neuronal functions like exocytosis [19], since these cells are known for their reliable dopamine release [20, 21].

2.1.3 Cellular Exocytosis

Exocytosis is the process by which cells release chemical contents out of their interior via vescicles. In the case of this project, exocytosis is intended as the release of neurotransmitter or other neuronal signaling related molecules like dopamine, that are further brought to neighbouring cells by diffusion, allowing for communication between neuronal cells.

Exocytosis in multicellular organisms can be either Ca^{2+} triggered (*non-constitutive*) or non-Ca^{2+} triggered (*constitutive*). Constituitive exocytosis is related to the cellular release of proteins to their plasma membrane or of other components of the extracellular matrix. Non-constituitive exocytosis, which is of primary interest to this research work, is instead based on the synaptic release of neurotransmitters for signaling between neurons [22], and is triggered by the interaction of Ca^{2+} ions with the outer axon membranes [23].

Upon stimulation from other cells by the means of ion exchange across the cell membrane, secretory vesicles present in the cytoplasm move to the cell membrane. With several protein-protein interactions and the localized rearrangement of the phospholipid bilayers in the membrane, the neurotransmitters or signalling molecules, e.g. dopamine, are then released into the extracellular medium via fusion pores that are created in the process (see Fig. 2.3). The final outcome of the vesicles, in other words whether the empty vesicles are then internalized by the cell and recycled for later use or they partially or fully fuse with the cell membrane, is not well understood and there are several theories that explain the details of this mechanism [24, 25, 26]. Within a population of cells, dopamine exocytosis occurs by the release of one vesicle at a time as small packages in what is known as quantal release [27]. The overall dopamine release, then, can for example be monitored electrochemically or chemically to elucidate on the behavior of the cell population.

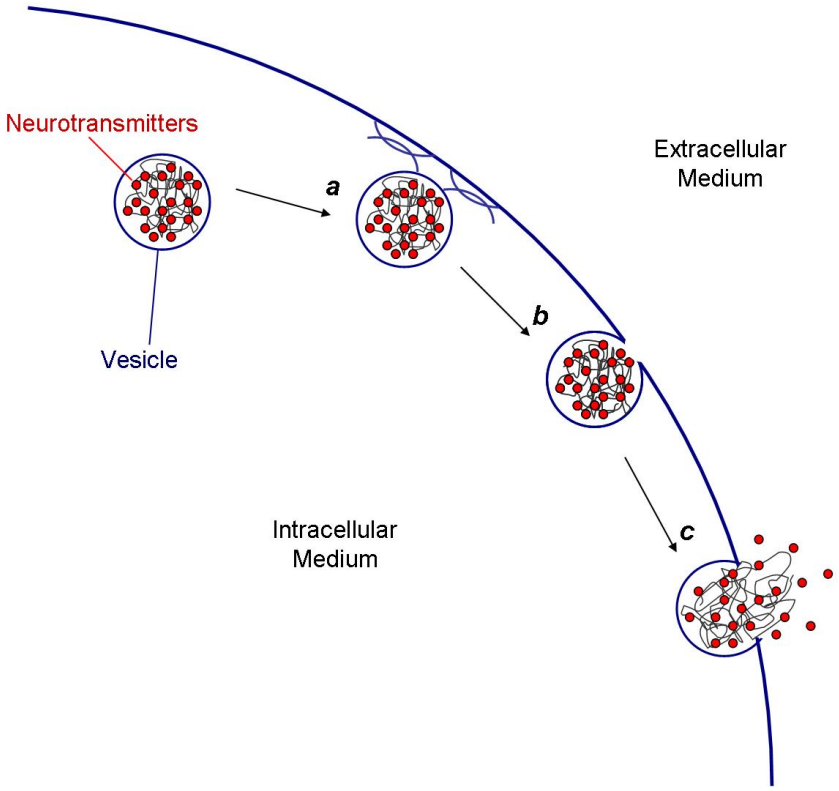

Figure 2.3: Schematic of the exocytosis process with (a) the movement of veciscles in the cytoplasm towards the cell membrane and the formation of protein complexes, (b) the formation of fusion pores and (c) the release of the vesicle content to the extracellular medium.

Dopamine

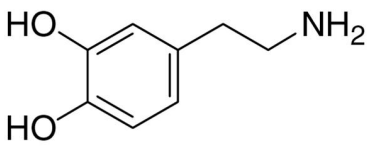

Figure 2.4: Schematic representation of a dopamine molecule.

Dopamine is a catecholamine (see Fig. 2.4) produced in several parts of the central and peripheral nervous system as well as the medulla of adrenal glands. It is involved in many physiological processes such as hormonal, cardiovascular and renal functionality [28], control of motorial functions [29] and is associated with feelings of sleep, pleasure, memory and learning [30]. In the brain and the remaining parts of the nervous system, dopamine acts as a neurotransmitter, being involved in signaling between neuronal cells. It is released by pre-synaptic neurons upon stimulation by an action potential and further received by receptors in post-synaptic neurons, causing a myriad of biochemical processes relevant to physiological functions. A typical dopamine nerve terminal holds about 200-300 vesicles [31], each containing approximately 1500-2500 dopamine molecules [32]. An abnormal level of dopaminergic activity is the cause of many neurological disorders, e.g. Parkinson's disease in the case of a dicrease in dopaminergic activity and schizophrenia in the case of an increase. The detection of dopamine exocytosis is an important topic in neurological reasearch, due to its tight relationship with the functionality of the human body and the diseases associated to this molecule's role in the central nervous system.

2.2 Electrochemistry

Electrochemistry is defined as the study of the interchange of chemical and electrical energy. This field has grown much throughout the past couple of centuries, and has found notable importance in the development of fuel cells (batteries), corrosion studies, and in the past couple of decades it seems to have found a new anchoring point around electrochemical sensors development.

This section is intented to present background information important for the understanding of the work carried out during this thesis relevant to the electrochemical sensor modifications applied to microelectrodes. The understanding of both the polymer electrode modifications as well as the cellular measurements lie heavily on the electrochemical concepts discussed in this section.

2.2.1 Electrode/Electrolyte Interfaces

An electrochemical oxidation-reduction (redox) reaction is one that takes place at the interface between an electrode, an electron conductor usually made of conductive or semiconductive material, and an electrolyte, a solution of any chemical compound dissociated into ions that have the ability to be oxidized or reduced. The latter is not to be confused with a "supporting electrolyte", which by definition is an electrolyte composed of species that are not electrochemically active in the potential ranges used during the study [33].

By applying a potential along the electrode/electrolyte interface, an electron (or charge) transfer happens between the two components, resulting usually in a redox reaction at the surface of the electrode (charge transfer can also occur between two molecules in solution, but for the purpose of this thesis let us disregard that for the moment). An electrode at which oxidation occurs is called an *anode*, and one at which a reduction occurs is referred to as a *cathode*.

In a galvanic cell, i.e. a device where chemical energy is transferred into electrical energy, the charge transfer between electron donors and acceptors happens spontaneously, because of a negative free energy of the redox reaction. The driving force that "pushes" electrons from anode to cathode is then the potential difference between the two electrodes, and is measured in units of volt (V). The potential reflecting the "work" of the electron transport from the electrode to the electroactive species in the solution is dependent on the energy level of the electron in the electrode, and therefore can be controlled by applying an externally caused potential to the electrode surface. For example, by applying a "more negative" potential to the electrode, the electrons are transferred from the electrode to

the electroactive species in the solution, creating a *reduction current*. Vice-versa, when applying a "more positive" potential to the electrode, an *oxidation current* is created because of electron transfer from the electroactive species in the electrolyte to the electrode surface, where the electrons' energy level are now lower than the energy levels of the molecular orbitals in the electrolyte redox molecules. The charge transfer in this interface can therefore be manipulated by tuning the balance between the electrons' energies in the electrode and the energy levels of the vacant electronic states in the redox species in the electrolyte. The current resulting from this charge transfer can be taken as a measure of the rate of the electrochemical reaction (in units of ampere, A), and together with the accumulated charge (a current over a period of time, in coulombs, C), is an important value in electrochemical techniques.

Electrode Reactions

Let us consider the simple reaction between the two species, O and R:

$$O + ne^- \rightleftharpoons R \tag{2.1}$$

occurring in the ideal electrochemical cell illustrated in Fig. 2.5, a container with two compartments separated by a porous material that does not allow the spontaneous mixing of the solutions but allows the migration of ions between the two compartments. A working electrode with an inert surface and small surface area is placed in one compartment, and in the other a reference normal hydrogen electrode (NHE), a large platinum electrode with hydrogen gas bubbled on its surface, whose potential is by convention taken as $0V$. The solutions are deoxygenated and contain relatively small concentrations of the redox species O and R, C_O^∞ and C_R^∞, respectively.

The equilibrium potential of the working electrode, E, is then expressed by the *Nernst equation* [34]:

$$E = E^0 + \frac{RT}{nF} ln \frac{C_O^\sigma}{C_R^\sigma} \tag{2.2}$$

where E^0 is the standard potential of the redox couple reaction, R is the gas constant, T is the temperature, F is Faraday's constant, and C_O^σ and C_R^σ are the concentrations of O and R at the electrode surface.

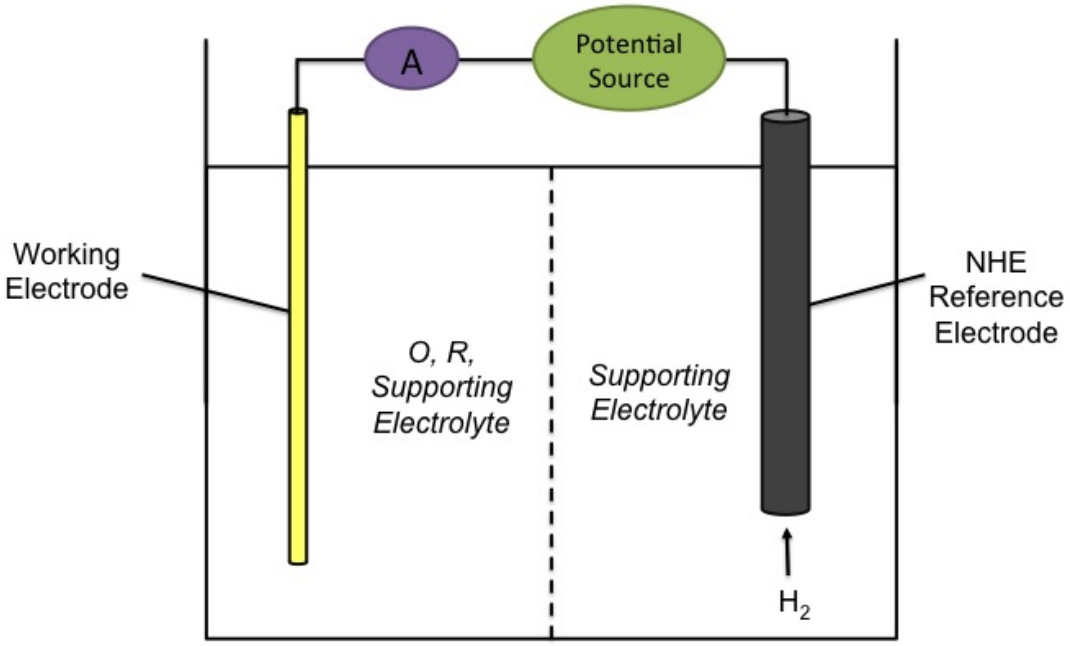

Figure 2.5: Schematic representation of an electrochemical cell.

When a potential is applied to the working electrode, in order to re-establish equilibrium, the system must push the redox reaction to occur to increase either C_O^σ or C_R^σ, and this will require a current to flow.

There are several factors which influence such an electrochemical system. For a start, not all reaction are as simple as the one described, and many involve several electron transfer steps and side reactions. Adsorption plays a role in these processes, since for the reactions to take place it might be necessary for reactants or intermediates to be adsorbed on the surface of the electrode. The products or side reaction products may end up depositing on the electrode surface, causing fouling and changing the electrochemical properties of the surface. A supporting electrolyte solution of low ionic conductivity will present a large electrical resistance between the electrodes, causing an ohmic potential drop proportional to the current flowing. Polarization of the reference electrode can also be an issue, since it is necessary to maintain the reference potential constant even when a current is passed through it for the determination of the working electrode's potential.

The differences between the surface and bulk concentrations of the redox species are also important factors that determine the electrode potential, as can be understood from the equation. In experimental conditions, the redox reaction is

composed by a series of steps that depend on both mass transport and electron transfer. For example, for the case of O reducing to R, as discussed above, O must first reach the electrode surface from the bulk solution, a process which is limited by mass transport. Once at the surface, the reaction takes place within the limits of electron transfer between the electrode and O. The product R must finally be taken away from the electrode surface, again by mass transport.

The Electric Double Layer

Since the electrochemical reactions of importance to the sensor field happen at the interface between electrode and electrolyte, it is important to clearly define the region where these two phases come into contact, for example a solid metal electrode with a liquid electrolyte solution (n.b. not all electrodes are necessarily solid, just like not all electrolytes are liquid solutions). At this interface, the properties of each component differ from those of the bulk of either phase. A transition region is formed, and this is where all the relevant redox reactions take place. It is the particularities of this transition region, called the *electric double layer* (EDL), that govern the overall electrochemical behavior of the electrode/electrolyte interface.

So how close to an electrode does an electrolyte ion have to be before being considered "at the electrode surface"? Since the intermolecular forces causing the existence of the EDL are only applicable over a short range, this zone is usually less than 100 $\mathring{A}$ thick, with its critical part consisting of less than 10 $\mathring{A}$ out into the electrolyte solution [35].

The *Helmholtz model* for the EDL's structure takes into consideration an electrode/electrolyte interface that behaves like an electric capacitor. Hermann Ludwig Ferdinand von Helmholtz was a German phsysicist who constructured one of the earliest EDL models in the 1850s, by treating the interface mathematically as a single layer of ions adsorbed at the electrode surface. In this model, the excess charge on the electrode is present at its surface, with another single layer of oppositely charged ions on the electrolyte side. This parallel-plate capacitor is useful in understanding the basic principles between the electrode/electrolyte charge transfer, but it does not give a complete picture of what is really going on, since measurements of the EDL capacitance give precise confirmation of the non-linearity of the EDL charge with the potential. These capacitors are in fact "leaky", meaning that charge transfer can also take place because of other redox reactions occuring at the interface, for example by oxidation of the electrode material itself.

Louis Georges Gouy and David Chapman, French and English physicists respec-

tively, improved this model by taking into account other parameters that affect the EDL capacitance, mainly the nature and concentration of the electrolyte and its diffusion properties. The latter can be accounted for as the main cause for the exponential decrease of the electric potential away from the electrode surface. In the *Gouy-Chapman model*, the EDL is created as a result of the interaction between the electrons on the electrode surface and the random thermal motion of the ions in the electrolyte, with the electrolyte "plate" layer being represented by a Boltzmann-type distribution. This model therefore is useful in defining the potential on the electrode surface, which is a function of the surface charge density and the differential capacitance of the diffused EDL at the limit of the layer. However, this model is not entirely correct, since experimental measurements can find capacitances lower than those calculated from the model for very concentrated electrolyte solutions, therefore for solutions with high ionic strenghts. The answer to the discrepancy of the Gouy-Chapman model relies on the size of the ions, that were taken as point-charges until the creation of the *Stern model*.

Several other models exist as combinations of the previous ones with more precise explanations of the mystery of the double layer. The *Grahame model*, for example, views the electrode/electrolyte interface as a zone consisting of 3 regions, the 2 first of which are often referred to as the *Stern layer* which is divided in 2 areas in this model. The first region, the *inner Helmholtz plane* (IHP), consists of the spacing through the *adsorbed* ions onto the surface. The second region, the *outer Helmholtz plane* (OHP), consists of the hydrated ions attracted to the adsorbed ions of opposite charge in the IHP. The potential changes linearly between the IHP and the OHP. The third region, beyond the OHP, is the diffuse double layer or *Gouy-Chapman layer*, where the potential approaches the limit of the bulk electrolyte's potential.

Taking it a step further, the *Bockris-Devanathan-Muller model* combines all the models discussed above and additionally includes the covering of the electrode's surface with a layer of solvent molecules, picturing the electrode like an very large ion. A schematic of this model can be seen in Fig. 2.6. This model therefore includes areas where the solvent molecules are replaced by adsorbed ions, as in the case of the IHP in the *Grahame model*, but also takes into account areas where the solvent molecules are there and do not give space for other ions to be absorbed. The main concept in this model is that every ion rests in solution with a layer of primary solvation, which must be eliminated for the cost of chemical work before being adsorbed onto the electrode surface.

As discussed, the structure of electrode/electrolyte interface is quite complicated, but it is important to understand its complexity in order to gain respect for the powerful techniques that are used in the field.

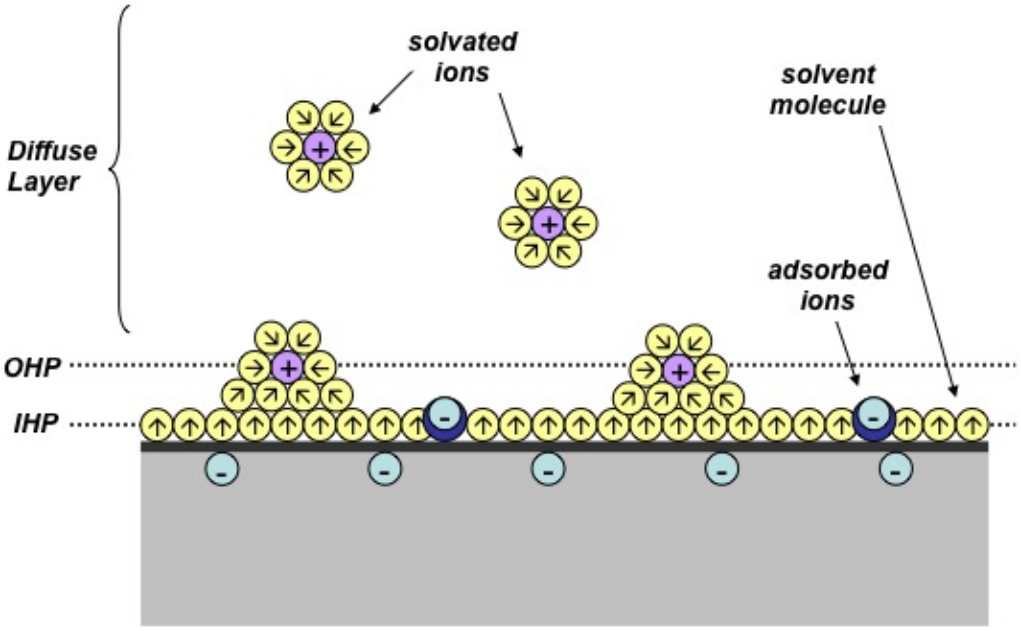

Figure 2.6: Schematic for the Bockris-Devanathan-Muller model for the structure of the EDL, showing positive and negative ions (+, -) and solvent molecules with dipole moments (arrow points towards negative dipole).

Faraday's Laws of Electrolysis

Michael Faraday, a British scientist, in 1834 published a series of articles explaining his findings in the field of electrochemistry related to electrolysis, an electrochemical redox reaction caused by an externally applied potential. The first of Faraday's Laws, also known as the *quantitative laws of electrolysis*, corresponds to a direct proportionality between the mass of any particular ion deposited onto an electrode surface (or undergoing a redox reaction) and the charge transported through the electrolyte, in other words the electrical current created during the process. The second Law of Electrolysis states that the weights of the deposited ions caused by the same quantity of electricity are proportional to their chemical equivalent weight, i.e. their molar mass divided by the number of electrons transferred per ion (valency number). According to these findings, the magnitude of the transferred electric charge per 1 mol of redox reactant is equivalent to 96,485.3365 C. This value is referred to as *Faraday's constant*, or more simply as a *faraday*.

The two Laws can be summerized in the following equation [34]:

$$m = \frac{Q}{F}\frac{M}{z} \tag{2.3}$$

where m is the mass of the redox reactant (deposited ion in Faraday's experiments), Q is the total electric charge transferred, F is Faraday's constant, M the molar mass of the substance and z is the number of transferred electrons per ion.

Redox reactions occurring at the electrode/electrolyte interface follow Faraday's Laws of Electrolysis, and the currents generated by them are therefore called *faradaic currents*. When a current flowing through the electrode is not a result of a redox reaction, but instead is caused by the charging or discharging of the double layer capacitance by accumulating charges at the interface, it is referred to as a *non-faradaic current*, or sometimes a *double layer current*. This is an important concept to be taken into consideration when evaluating the causes of resulting current traces obtained from an electrochemical reaction.

2.2.2 Electrochemical Techniques

Investigations of electrochemical reactions can be categorized into 3 different types [35]:

i) *Equilibrium techniques*, where a measurement of the electrode reaction is carried out at equilibrium or with a small perturbation. Examples of these methods are potentiometry, amperometry, differential capacitance, impedance or surface tension measurements.

ii) *Steady-state techniques*, where a measurement of the response to an applied perturbation is made after it has become independent of time. Some examples are voltammetry, polarography, coulometry and rotating electrodes measurements.

iii) *Transient techniques*, where the measurement is carried out throughout the perturbation from its equilibrium or steady-state, and important information is retrieved regarding the way that the system goes through relaxation to the new stady-state. These techniques include double potential step, chronoamperometry, chronocoulometry and chronopotentiometry.

All electrochemical experiments are based on the precise measurement and control of applied or generated potential, charge and current.

This section will discuss a typical setup used for an electrochemical investigation, as well as two techniques commonly used in the work carried out during the PhD project, mainly *Cyclic Voltammetry* and *Amperometry*.

3-Electrode Setup

A setup for electrochemical measurements usually includes the needed electrodes and the electrolyte, typically in a container of liquid. The most used setup consists of 3 electrodes: a *working electrode* (WE) used to define the electrode/electrolyte interface to investigate, a *reference electrode* (RE) to maintain a constant reference potential for the WE, and a *counter electrode* (CE) to supply the current needed for the measurements.

The WE is usually a conductive surface that preferably does not react chemically with the solvent or the components of the electrolyte. For this reason usually an inert material is preferred, such as gold or platinum. The geometry to be used is of course dependent on the experiment to be carried out, but typically it is designed so that all points on the WE's surface are at the same distance from the CE and RE, as well as from the injected analyte in the case of it's presence in the experiment.

The RE is used to give a fixed potential for reference to the WE. This potential should not change throughout the measurement, and therefore should be independent of current density. When connected to a potentiostat, the equipment makes sure that the RE's potential is fixed, so that any change in applied potential only affects the WE/electrolyte interface. Several typical REs are silver/silver chloride (Ag/AgCl), mercury/mercurous chloride (saturated calomel electrode, SCE), mercury/mercurous suplhate, and the normal hydrogen electrode (NHE), which is the international standard set at 0V.

The CE provides the current needed by the WE without altering the voltage difference between the WE and the RE. Without a CE, current will flow between the WE and the RE via the electrolyte solution, changing the reference potential by altering the concentration of ionic species on the RE. Using a CE avoids this phenomenon and ensures that the RE is in fact providing a stable reference potential. The CE should not change the measurement at the WE, and it should therefore have a large area compared to the WE. A CE with a relatively large surface area is required in order to maintain the potential of the WE independent of any reactions at the CE surface.

Cyclic Voltammetry

Cyclic voltammetry (CV) is probably the most widely used electrochemical technique for the study of electrode/electrolyte interface redox reactions and for electrode behavior characterization. CV is a potential sweep technique, and is based on the measurement of the WE current upon an applied triangular form potential sweep with a defined potential sweep rate (PSR) or scan rate. The sweep is typically carried out over a potential range relevant to the investigation at hand, e.g. in the potential range where the redox reaction occurs. The forward sweep produces currents representative of the oxidation reactions of the components of the electrolyte (*anodic current*), while a reverse sweep reduces the electrolyte components and produces a *cathodic current*. The curves obtained are called *cyclic voltammograms*, and an example can be seen in Fig. 2.7.

The current curves obtained follow the *Randles-Sevcik equation* [34]:

$$I_p = (2.69 \times 10^5) n^{3/2} C_o^{\infty} D^{1/2} \nu^{1/2} A \tag{2.4}$$

where I_p is the peak current (in A), n is the number of electrons involved in the reaction, C_o^{∞} is the concentration of analyte in the bulk solution (in mol cm^{-3}),

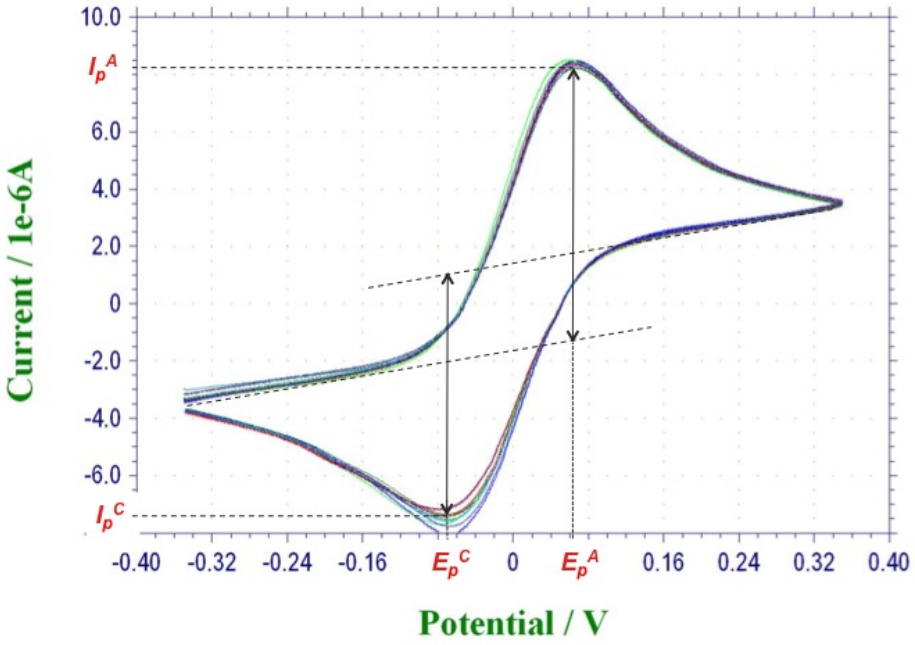

Figure 2.7: Cyclic voltammogram for a reversible process, showing the important parameters used for the technique.

D is the diffusion coefficient of the analyte (in $cm^2\ s^{-1}$), ν is the PSR (in V/s), and A is the electrode surface area (in cm^2).

The anodic and cathodic current peaks, I_p^A and I_p^C, together with the corresponding peak potentials, E_p^A and E_p^C, give important information about the redox species.

The diagnostics criteria for validation of the reversibility of the redox process are the following [35]:

1) $\Delta\ E_p = E_p^A$ - $E_p^C = 59/n$ mV ;

2) $\mid\ I_p^A\ /\ I_p^C\ \mid = 1$;

3) $I_p \propto \sqrt{\nu}$;

4) E_p is independent of ν

If the systems deviates from these criteria, it is thought of as irreversible, or pseudo-reversible in case of slight deviations from reversibility. For a redox reaction, the rate determining step can be the rate of mass transport of the electroactive

species, the rate of adsorption or de-sorption at the electrode surface, or the rate of the electron transfer between the electroactive species in solution. Therefore, a deviation from the reversibility criteria can be explained by either or all of these factors.

This powerful technique is used widely in the field both for electrode behavior characterization as well as investigations of electrolyte compounds, as can be seen further in this document. Each combination of electrode/electrolyte has its own distinct CV behavior, and thus this method can be used to study the behavior of an unknown solution and evaluate its composition.

Amperometry

Amperometry is an analytical technique typically used for electrochemical detection of present or added analytes in the electrolyte solution, or as in the case of this PhD project, for cellular exocytosis released analyte detection [36], where the cell exocytosis can be compared to an analyte addition. In Amperometry, a constant potential is applied to the WE, and the current trace over time is observed as analytes come in the vicinity of the WE. The current-time trace can then be related to information about the redox reactions happening at the electrode/electrolyte solution interface.

After the start of an amperometric experiment, the current trace quickly stabilizes to a constant value baseline. When an electroactive analyte is added on the electrode suface, either by manual pipetting, flow injection or cellular exocytosis, the current trace resembles a peak. The peak's shape during the rising gives information about how the analyte reaches the electrode. The molecules reaching the electrode can not in fact all arrive at the same time, as they are under the effect of diffusion limitations, therefore the peaks obtained are not sharp but resemble a shape as seen in Fig. 2.8. In the case of cellular exocytosis, for example, the rising of the peak reveals details about the neurotransmitter release mechanism from the cells. Eventually the current approaches a maximum value, which is related to the maximum flux of analytes added or released during an event [35]. The current trace then decreases and approaches a constant value, as redox molecules are consumed or diffused away from the electrode surface.

Integrating over the current-time trace yields the charge accumulated on the electrode, Q. This value is in fact much more important than the peak height, since by Faraday's Law (see previous section) it can be related to the amount of analytes reaching the electrode.

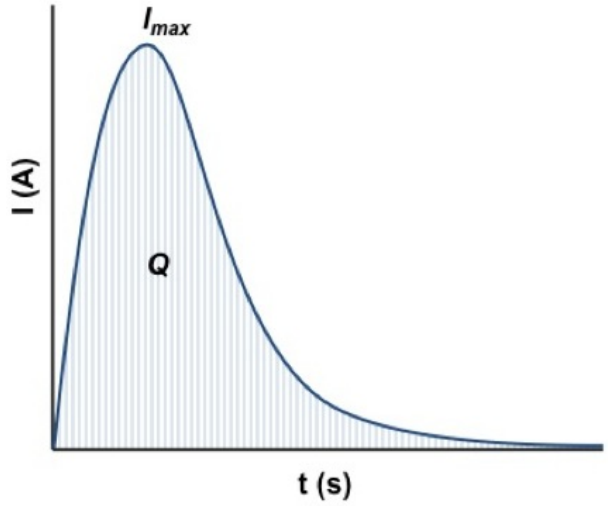

Figure 2.8: Typical current-time trace for the amperometric detection of an cellular analyte released via exocytosis.

2.2.3 Electrochemical Dopamine Detection

The detection of dopamine can be achieved by monitoring its redox reactions at the surface of an electrode using the afore mentioned electrochemical techniques: by cyclic voltammetry if it is present in an electrolyte solution or by amperometry when added to the solution or excreted from dopaminergic cells via an exocytosis event. CV was used in the context of this project when for example comparing the sensitivity of different electrode modifications, in order to choose the modification that yielded the highest current peak in the voltammograms. Amperometry was used instead when measuring dopamine release directly from a population of cells cultured on top of an electrode.

Dopamine Electrochemistry

The electrochemical oxidation of dopamine (DA) in aqueous solutions occurs with a one-step two-electron transfer reaction, the product of which is *o*-dopaminoquinone (*o*-DQ) [37]. In neutral or higher pH solutions, a chemical reaction can occur further producing leucodopaminochrome (LDC). The oxidation of DA into *o*-DQ is the reaction mainly used to detect the presence of the analyte, while the further chemical consumption of *o*-DQ is something secondary that relevant electrode

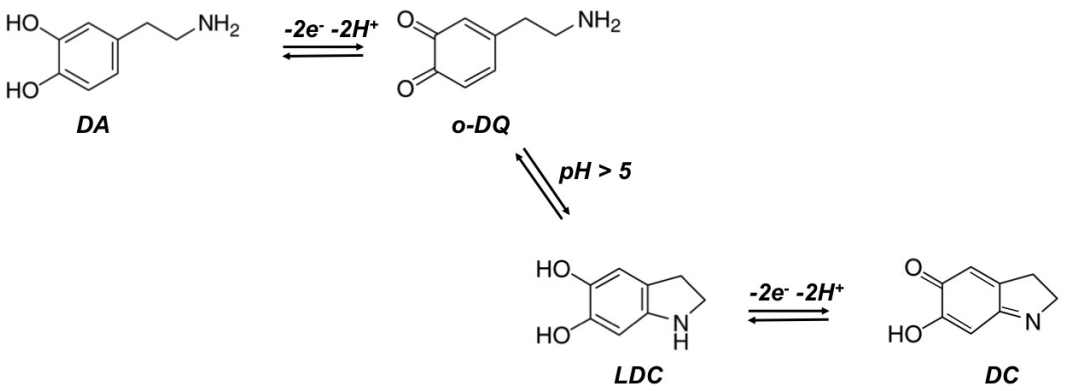

Figure 2.9: Schematic of dopamine electrochemistry, showing the oxidation of DA into *o*-DQ, the chemical reaction producing LDC and its oxidation into DC.

modifications can slow down or prevent, since LDC electrochemically oxidizes at nearby potentials to the one used for the DA detection and forms dopaminochrome (DC). DC is "dangerous" to the electrode surface because it polymerizes and causes electrode fouling and therefore the loss of electrode activity [38]. A schematic of these reactions can be seen in Fig. 2.9.

Chapter 3

Self-Assembled Peptide Nanostructures

This chapter is included as a mean to describe the work carried out throughout the doctoral project in regards to the use of self-assembled peptide nanostructures for cellular studies.

After a short introduction to the core principles of self-assembly, with focus on diphenylalanine as the specific peptide used and the nanowires synthesized from this molecule, the chapter continues by presenting the experimental work.

A section on the growth of vertical diphenylalanine peptide nanowires (PNWs) shows the optimized technique used to create such nanostructures. A section on the PNWs' functionalization describes several methods by which the PNWs can be decorated with biomolecules, metallic particles and chemical functional groups such as thiols.

What follows is a visual biocompatibility assessment of the PNWs using HeLa and PC12 cells, with *in vitro* investigations of cell growth, differentiation and behavior on PNW surfaces with and without an adhesion enhancement protein coating often used in cell culturing.

A soft-lithography technique for the patterning of PNWs in micrometer wide strips is also described, with a discussion on how the cellular behavior changes between plain and patterned PNW surfaces.

With the help of scientific partners at the NeuroNano Research Center at Lund University in Sweden, an *in vivo* study of the effect of the presence of PNWs onto implantable electrodes for brain-machine interface studies is presented, showing the advantages of including such type of structures onto implantable microelectrodes.

An intermediate conclusion at the end of the chapter reflects on the work carried out and the possible implications of the results.

3.1 Peptide Self-Assembly

Biological self-assembly is a scientific term utilized to describe a process based on the organization of structures or patterns from a system of disordered biological molecular components. This process relies on localized and specific intermolecular interactions between the building-blocks of the resulting structures or patterns, without the need for external direction.

The results of biological self-assembly can be 0-dimensional, as in the case of molecular dimers, 1-dimensional, like DNA double helices or other chains, 2-dimensional, e.g. lipid bilayers, or even full 3-dimensional solid state structures resulting from interactions in all dimensions, as is often the result of peptide self-assembly, e.g. peptide nanotubes, nanoparticles or nanowires. Understanding the forces that lead the self-assembly process can be of help in designing deliberate structures needed for a specific application.

Peptide self-assembly often starts with *nucleation*, or the formation of small compact molecular groups of 20 to 100 building-blocks already in the formation needed for the creation of solid state structures, after the formation of liquid-like clusters of molecules in a solvent. Nucleation happens via a rearrangement of these solute clusters into an ordered structure.

After nucleation, more building-block molecules attach themselves to the surface of the compact initial nucleus with growth directions dictated by the intermolecular interactions and the direction of the forces being created during this organization process.

Most peptide molecules interact with each other via strong or weak hydrogen bonds or interactions with the solvent used, emphasizing the importance of the solvent during the self-assembly process. Some building-block molecules hold aromatic rings, which often are the cause for ring-ring interactions such as stacking or the formation of aromatic pairs. Aside from providing the possibility for H-bonds, solvents are an important factor in the intermolecular organization because of the importance of solubility during the nucleation process, as well as some cases where solvent molecules are incorporated into the final 3-dimensional structures that are the outcome of the organization.

This manuscript will not dwell on self-assembly theory, as it is an independent and

complex subject which is not the focus of this PhD thesis. For more information on the topic of biological peptide self-assembly, the reader can refer to [39].

3.2 Diphenylalanine

The following section is reproduced from the article "Diphenylalanine: a short molecule with a big impact", published in the Swedish popular science journal Kemivärlden Biotech med Kemisk Tidskrift *(Publication XII):*

"Diphenylalanine (FF), the core recognition motif of Alzheimer's β-amyloid polypeptide, is a small aromatic dipeptide able to self-assemble into 3D nanostructures under very mild conditions (room temperature, aqueous conditions) without the need of specialized equipment. This self-assembled peptide plays a potential role in the formation of amyloid fibers involved in Alzheimer-s disease. However, despite this negative connection with neurological diseases, FF has found a long list of applications in different areas ranging from electrochemistry and biomedicine to applications in clean-room fabrication processes.

Around eight years ago Professor Ehud Gazit and Meital Reches at Tel-Aviv University described a simple method for obtaining peptide nanotubes by using FF [40]. This method proved to be fast, facile and low-cost compared with other methods used for the fabrication of more traditionally used nanostructures such as carbon nanotubes or silicon nanowires. Since then, an increasing number of scientific publications dedicated to the study, characterization and application of this short dipeptide have been reported [41, 42].

So why use FF? One of the more obvious answers to this question is the fact that, as mentioned before, this building block is able to self-organize into 3D nanostructures quickly and at room temperature. Gorbitz reported the visualization of peptide structures a few seconds after mixing a solution of the dissolved peptide in 1,1,1,3,3,3-hexafluoro-2-propanol [43]. Recently, the on-chip fabrication of nanotubes and nanoparticles was reported, which allows the synthesis of nanostructures with a more uniformly defined size [44]. A second advantage is that different types of structures can be obtained by changing the synthesis conditions. In this way, nanotubes, nanofibres or nanoparticles can be easily obtained.

Dyphenylalanine nanostructues have been structurally, electrically and chemically characterized [45, 46, 47, 48]. The fabricated nanostructures can be decorated with a variety of functional molecules such as enzymes, metallic or magnetic nanoparticles, fluorescent molecules or quantum dots, among others [49]. This gives researchers the opportunity to obtain functionalized biological nanostructures with

potential to be used in different applications like contrast imaging, photo thermal therapy, drug delivery or biosensor fabrication, to mention a few.

It was recently shown that FF nanotubes are extremely resistant to the bombardment of fluoride ions in a microfabrication process called reactive ion etching. This property was used for the fabrication of silicon nanowires using FF peptide tubes as etching mask [50]. This fabrication method was faster, cheaper and reduces the use of chemical reagents during the process. Preliminary biocompatibility studies involving the growth of cells in the presence of FF peptide nanostructures demonstrated that cells sush as PC12, HeLa or Chinese ovary cells can grow on top of nanowires (see Publications II, VI, VII, VIII) or hydrogels fabricated with the short peptide [51]. However, since these nanostructures have been suggested as candidates for the development of drug delivery systems and for tissue reparation experiments, a detailed study is necessary in order to obtain a more clear insight of the toxicity and immune response generated by these nanostructures. It is also necessary to mention that despite all these advantages, there are several challenges that need to be confronted when working with these nanostructures. These challenges involve their low conductivity, their manipulation, their solubility in liquid solutions and the intriguing different behaviors of nanotubes and nanowires, as reported in several publications [45, 52].

Applications

The development of electrochemical and optical biosensing platforms using FF structures has been described by several research groups. FF nanotubes have been immobilized on different metallic transducers for the electrochemical detection of compounds of biomedical relevance like glucose, ethanol or hydrogen peroxide [53, 54, 55]. In this case the FF nanostructures were functionalized with enzymes to introduce selectivity and sensitivity to the developed biosensor. In a different approach, FF nanowires were functionalized with a conductive polymer in order to improve their conductivity and used for the electrochemical detection of dopamine (see Publication II).

The decoration of FF nanostructures with photo luminescent compounds lead to the development of optical biosensors based on changes in light intensity [56]. A chinese group reported the use of a hydrogel created with entangled Fmoc-diphenylalanine nanowires that encapsulated quantum dots [57]. The formed hydrogel improved the stability of the quantum dots by protecting them from oxidation. Using a similar approach, glucose oxidase and horseradish peroxidase were encapsulated together with quantum dots inside a 9-fluorenylmethoxycarbonyl-diphenylalanine (Fmoc-FF) hydrogel. The functionalized hydrogel was used to

detect glucose and toxic phenolic compounds. Paraoxon, a neurotoxin that inhibits the activity of acetylcholine esterase in the brain affecting the synaptic transmission, was detected using FF nanotubes functionalized with lanthanide ions [58].

A drug delivery system using FF nanostructures is under development in order to selectively destroy the parasite responsible for a neglected disease known as Leishmaniasis. The idea here is to functionalize the biological nanostructure with compounds that will trick the infected cell, allowing the internalization of the nanostructure decorated with particles that will create a lethal toxic effect on the parasite.

FF nanostructures have also been used in micro- and nanofabrication processes. A very clever application was described in 2003 for the simple fabrication of silver nanowires [40]. By using the internal cavity of FF nanotubes as a mold, silver ions were reduced inside the peptide nanostructure, resulting in the formation of metallic nanowires with diameters below 100 nm. The same approach was later used for the fabrication of coaxial nanowires: in this case metal ions were deposited both inside the internal cavity and the external surface of FF nanotubes [59]. Nanofluidic channels were created in a polymer structure using FF nanotubes; the fabricated channels were used to connect two liquid reservoirs [60]. Finally, silicon micro- and nanowires were fabricated using FF nanotubes as etching mask material. These processes proved to be faster, cheaper and used less reagents compared with the traditional method for silicon nanowires fabrication [50].

One of the most recent applications involved the use of FF/Pd hybrid nanowires assembled inside a microfluidic system for micro mechanical hydrogenation and Suzuki coupling reactions. The developed micro reactor offers new applications in the development of new heterogeneous catalytic reactions [61].

As indicated above, FF and its analogues constitute a group of interesting molecules with a high number of applications. To keep exploiting their potentials, the combined efforts of researchers in disciplines such as chemistry, physics and engineering is necessary in order to unveil information that will allow understanding of how these molecules assemble under different conditions, how their properties change and how they will behave in different environments. Such efforts could lead to new and interesting applications in tissue reparation, electronics and drug delivery."

3.2.1 Vertical Diphenylalanine Nanowires

The initial work carried out in the project was focused on the creation of a reliable protocol for the reproducible growth of vertical diphenylalanine nanowires for use in the development of sensors for cellular analytes. Although many different self-assembling peptides have been shown to have excellent properties as cell-interactive scaffolds or generally as building blocks for nanodevices [62, 63, 64], these specific nanostructures were chosen because of the nature of their self-assembly process. Vertical structures solidly attached to the substrate give the advantage of better control over the position of the modification. Because of a surface nucleation-based growth mechanism, localized areas of modification with such structures were easier to achieve than with solution-based self-assembly techniques, which require additional manipulation and placement onto the sensor surfaces. Additionally, vertically grown bionanostructures adhere better to the surface and therefore render the overall sensor system more stable. A 3-dimensional bionanoscaffold also resembles better a physiological surface, giving an *in vivo*-like substrate for cellular studies [65, 66].

3.2.2 Experimental: Growth of Vertical Diphenylalanine Nanowires

The growth method involves the self-assembly of diphenylalanine nanowires with the use of a high-temperature aniline vapour treatment [67]. The schematic for such growth process can be seen in Fig. 3.1. The procedure starts with the preparation of a diphenylalanine monomer solution in 1,1,1,3,3,3-hexafluoro-2-propanol (HFP) with a desired concentration (typically in the range 1-100 mg/mL). A small drop of the solution is then placed on a sample substrate such as silicon or gold, allowing the drop to expand and dry in a desiccator to eliminate the effects of ambient water vapor pressure, creating an amorphous peptide film.

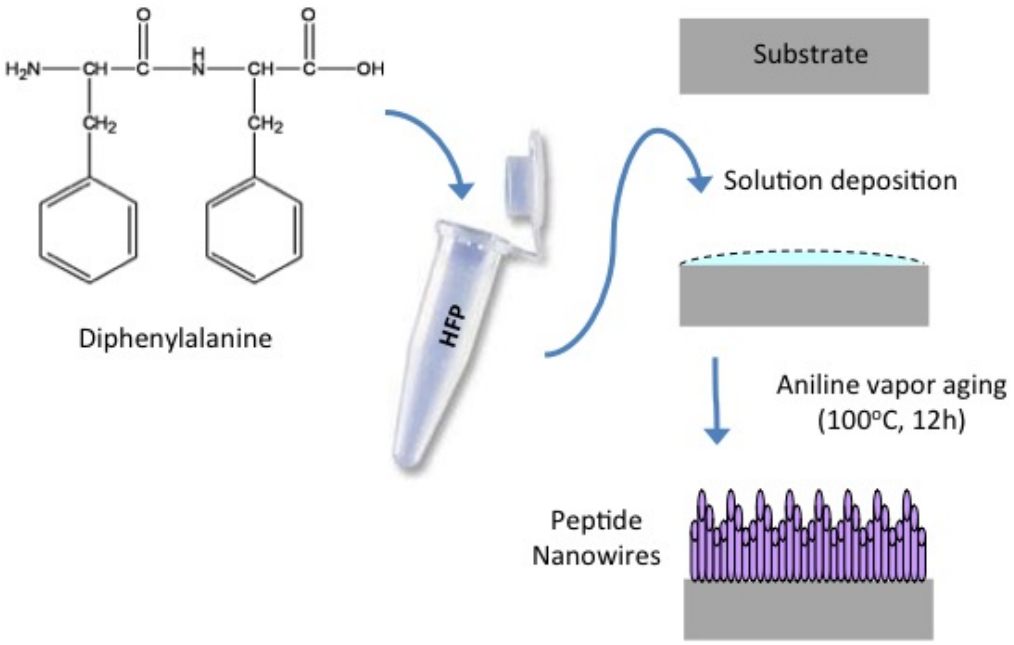

Figure 3.1: Schematic of steps involved in the growth of Diphenylalanine PNWs.

The sample is then placed in a home-made vapor aging system setup (see Fig. 3.2). The setup includes a closed vessel created with two large glass *Petri* dishes positioned in such a way so that the smaller top beaker acts as a lid to the larger bottom one. Two smaller glass containers are placed inside the closed system, one containing aniline liquid and the other containing the substrate sample. This setup ensures that the aniline vapor reaches the sample without letting the liquid come in contact with it. Silica beads are placed all around the closing fissures to obtain a saturated aniline vapor concentration inside the system and to eliminate water vapor coming from outside the system. The setup is then enclosed in aluminum foil and placed in an oven at 120 degrees C for at least 12 hours (typically overnight). It is important that the oven be hot when placing the sample. After 12 hours of aniline vapor aging, the system is taken out of the oven and placed in a fume hood for cooling by immediately opening the lids before the cooling. This is done to prevent the aniline vapor to condensate on the top lid of the system and potentially dripping down onto the PNW sample.

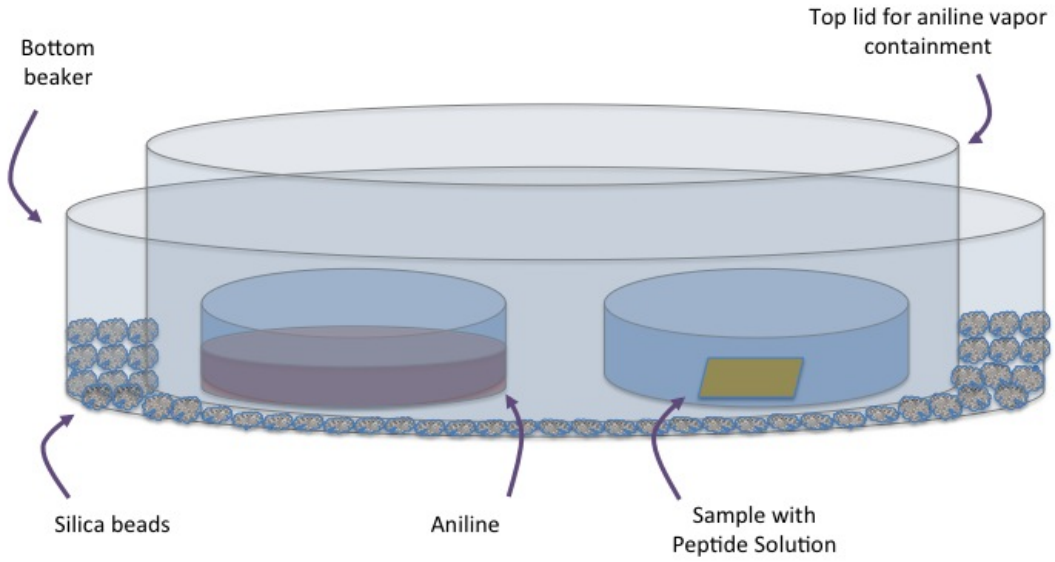

Figure 3.2: Laboratory setup for the growth of Diphenylalanine PNWs.

Typical results of such a growth process can be seen in Fig. 3.3, with peptide structures firmly attached to the substrate and vertically grown in a fashion resembling that of nano-sized grass, with typical diameters of 200-300 nm and heights in the range of 3-8 μm.

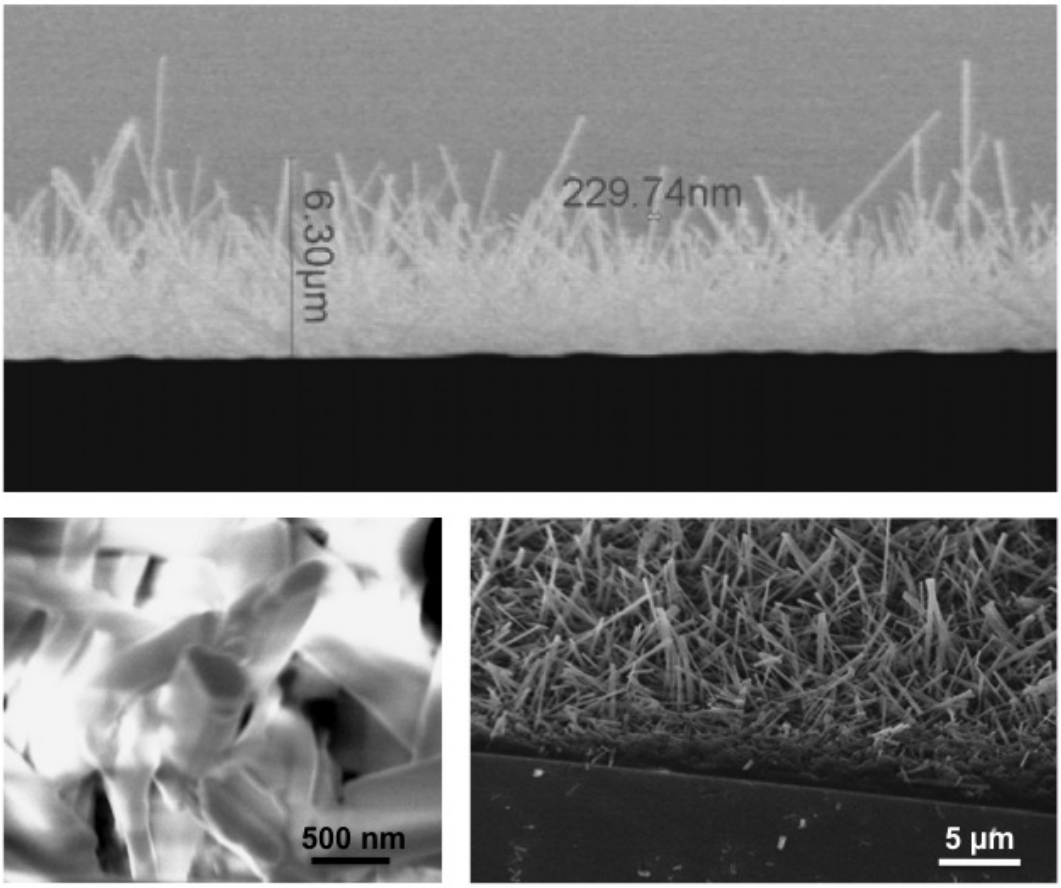

Figure 3.3: Low-vacuum SEM images of diphenylalanine PNWs grown on silicon substrates. The substrate was cut prior to the SEM characterization for better visualization of the structures.

3.2.3 Experimental: PNW Functionalization

In order to fully take advantage of the PNWs as a biological material for cellular studies, the structures' flexibility of functionalization has been investigated. This section hence presents various functionalization techniques which have been utilized to adorn the PNWs with different functional groups.

Biotin/Streptavidin Conjugates Attachment

Biotin/Streptavidin conjugates are one of the most commonly used biochemical linking molecules in biotechnology. Biotin is a water soluble vitamin (B_7), present in many physiological processes as a coenzyme, and plays a key role in the formation of fatty acids and the body's metabolism. Streptavidin is a protein expressed by bacteria, and it is known for binding very tightly to biotin in one of the strongest protein-ligand bonds known. The interaction of this biochemical conjugate is often used in biotechnology as a means to attach biomolecules, such as fluorophores, enzymes or other chemical tags used for protein purification or detection, onto a solid support substrate.

Being able to use this widely known and studied interaction in conjunction with PNWs opens up many possibilities for the functionalization of these bionanostructures, since a myriad of molecules and chemical groups can be attached to streptavidin, and therefore as a whole to the PNWs.

The proposed method for attaching Biotin to PNWs is illustrated in Fig. 3.4. PNWs grown onto 0.5 x 0.5 cm^2 gold squares with initial diphenylalanine concentration of 50 mg/mL were used for this work. First, biotin is attached to the surface of the nanostructures by incubating the PNWs in contact with a biotin solution at a concentration of 16.4 mM for 1 hour. This first step anchors the biotin molecules to the free amine groups present in the diphenylalanine molecules on the surface of the PNWs. The biotin used was EZ-link sulfo-NHS-biotin, a compound often used for similar functionalization protocols (Thermo Scientific). After the biotin attachment to the PNWs, streptavidin is introduced by direct contact of the samples with a fluorophore (Atto 610) labelled streptavidin solution in varying concentrations for 30 min (referred to as streptavidin*). All incubations were done in dark conditions at room temperature.

The result of this procedure was characterized by measuring the fluorescence intensity of the samples under an optical microscope with a relevant filter (Texas Red). Fig. 3.5 shows the increased fluorescence intensity of the fluorophore labelled streptavidin, with respect to streptavidin concentration in the last step of

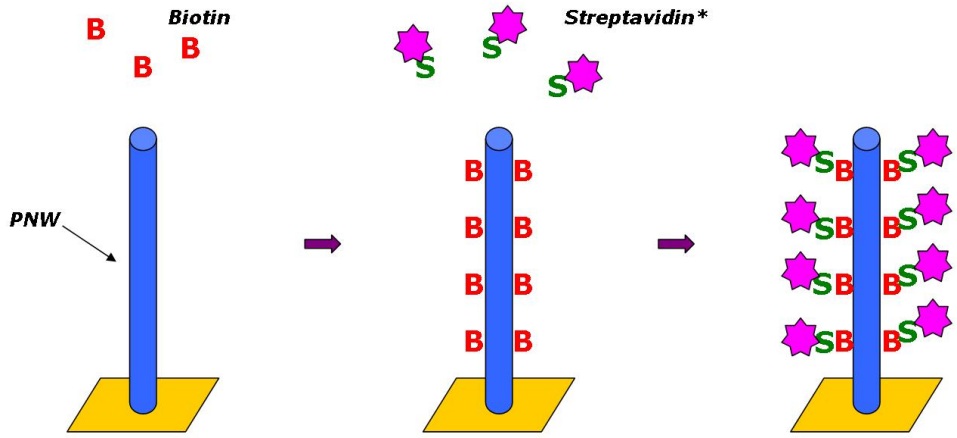

Figure 3.4: Schematic representation of the Biotin-Streptavidin* functionalization of PNWs. Here, B denotes biotin and S streptavidin.

the functionalization procedure (blue curve). The 0 point reflects the background fluorescence signal present in control samples of PNW/Biotin, where no streptavidin was added (after only the 1st step of the procedure). As expected, the absolute fluorescence intensity increases with respect to streptavidin* concentration until it reaches a saturation plateau, i.e. when all biotin sites are occupied (saturated) by straptavidin*. The plot in Fig. 3.5 also shows a curve for the same functionalization protocol but omitting the biotin attachment (red curve). This specific data reflects the unspecific binding present between the PNWs and streptavidin*. This unspecific binding could be due to adsorption of the fluorophore onto the PNW surface, adsorption of the streptavidin onto the peptide surface, or perhaps even a chemical linking between the streptavidin and the carboxylic group present in the diphenylalanine molecule, resulting in a similar chemical binding as in the case of the biotin-streptavidin interaction. Varying the concentration of the biotin solution and keeping the streptavidin* solution at 0.4 mg/mL yields in a functionalization with the same behavior (see Fig. 3.6).

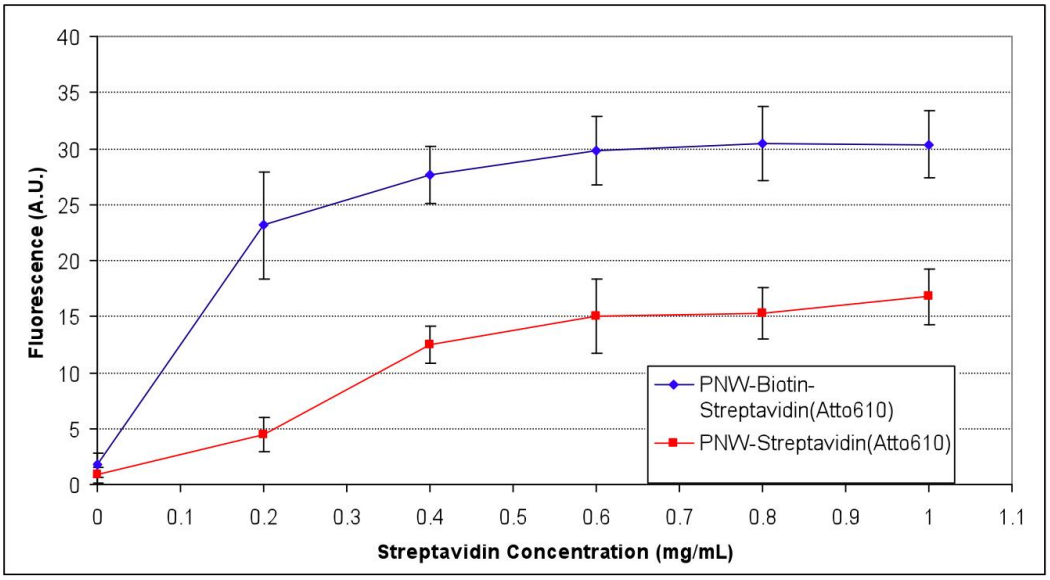

Figure 3.5: Fluorescence intensity plots of the PNW/Biotin-Streptavidin* functionalization (blue curve), and for the sampe protocol without the first biotin attachment step (red curve, non-specific interactions). Error bars represent standard deviations of measurement over 3 different samples for each plotted data point.

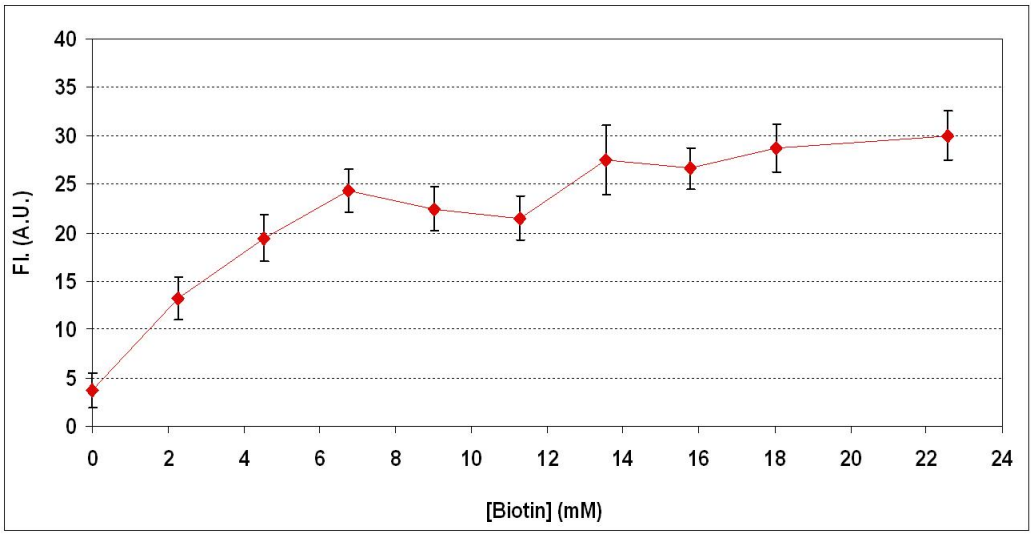

Figure 3.6: Fluorescence intensity plots of the PNW/Biotin-Streptavidin* functionalization, with varying biotin solution concentration and keeping the streptavidin* concentration at 0.4 mg/mL. Error bars represent standard deviations of measurement over 3 different samples for each plotted data point.

The same procedure for functionalizing the PNWs with the biotin-streptavidin conjugate can be used to attach metal nanoparticles to the surface of the PNWs. Using the same protocols and concentrations as discussed above, but exchanging the fluorophore labelled streptavidin for streptavidin molecules attached to gold nanoparticles (streptavidin-Au). The results for Au nanoparticle anchoring to the PNWs are shown in Fig. 3.7. Fig. 3.7A shows the results from the complete functionalization protocol, while Fig. 3.7B shows the same results but for an incomplete protocol, where the biotin attachment step was omitted, therefore reflecting a streptavidin-Au functionalization caused only by the unspecific binding, as discussed previously. Comparing these two images, one can notice a uniform layer of Au nanoparticles attached to the top surface of the PNWs for the case of a complete functionalization protocol (Fig. 3.7A), while the unspecific binding results in patches of Au nanoparticles uniformly attached to the PNW's surface (Fig. 3.7B). This is by all means an incomplete work, since by closer SEM inspection the gold particles seemed to attach only to the topmost surface of the PNWs, and not around their whole surface area. A more thorough optimization of the functionalization protocol, paying special attention to PNW packing density, Au nanoparticle diameter and biotin/streptavidin concentrations could yield a more homogeneous coverage of the PNWs' surface with a layer of gold.

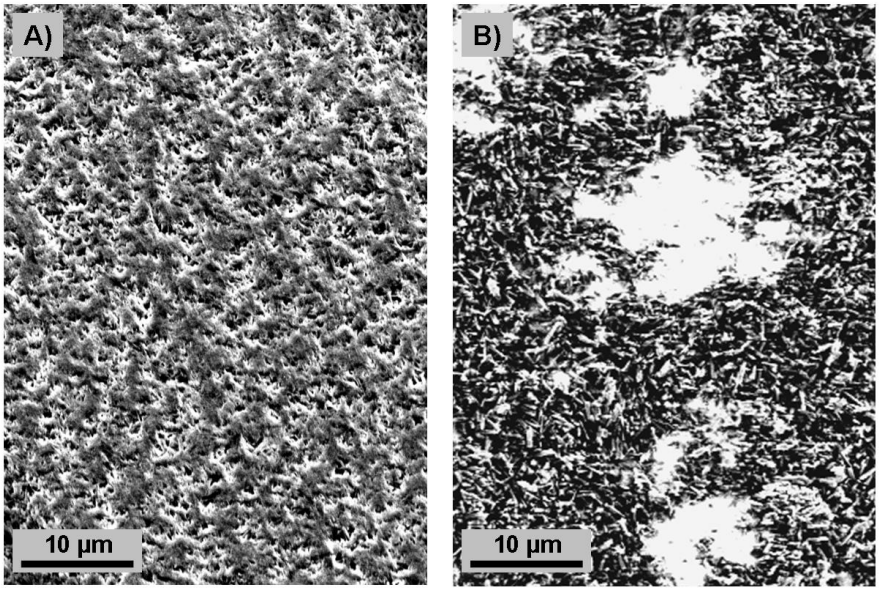

Figure 3.7: SEM images of PNWs functionalized with biotin/streptavidin-Au (top view of the functionalized PNW surface), with A) a complete functionalization protocol and B) unspecific binding caused by omitting the biotin attachment step.

Thiolation

Another kind of functionalization which is of interest for biological nanostructured materials is their decoration with thiol groups [68]. Thiols, or mercaptans, are defined as chemical groups containing a sulfhydryl group (-SH), which are widely used in biotechnology and chemistry as an anchoring chemical group for metallic compounds. The word "mercaptan", although deemed outdated in modern chemical nomenclature, derives from the Latin *mercurium captans*, meaning "mercury capturing", as this compound was originally used for the capturing of mercury salts. Having discussed the thiol affinity for metals, one application for such a modification is to provide another technique for the coverage of the peptide nanostructures with a gold layer, in order to add a conductive functionality to the structures and open up the possibilities for their application in the sensor field.

A method for the thiolation of other kinds of peptide nanostructures self-assembled from the same diphenylalanine monomer has previously been developed [54], but it has only been applied to diphenylalanine nanotubes.

The thiolation of the amine groups present on the surface of the PNWs was achieved by reaction with what is known as Traut's Reagent, a cyclic compound commonly used for the sulfhydryl addition to primary amine-terminated molecules [69]. This well known reaction (see Fig. 3.8) links the Traut's Reagent molecule to a primary amine, in this case amine groups from the diphenylalanine monomers present on the surface of the peptide nanostructures, to leave a free -SH group on the surface.

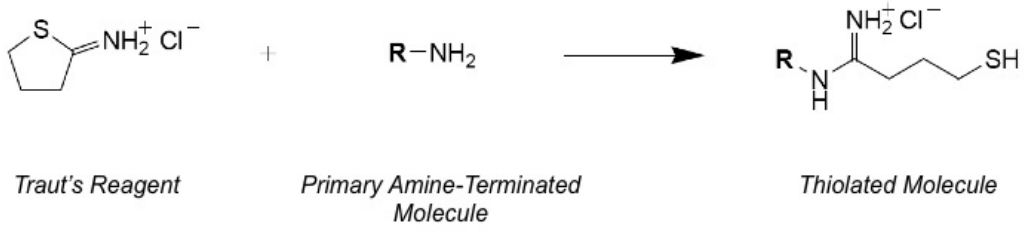

Figure 3.8: Schematic of reaction used for the thiolation by Traut's Reagent of an amine-terminated molecule at the surface of the PNWs.

PNWs were grown on plain silicon surfaces with diphenylalanine concentration of 100 mg/mL following the standard protocol described previously. Thiolation of the PNWs' surfaces was achieved by overnight incubation in a Traut's Reagent aqueous solution (56 mM) at room temperature.

The result of the functionalization was first characterized by Energy Dispersive X-ray (EDX) analysis. As seen in Fig. 3.9A, a sulfur peak is present, while in the case of non-functionalized PNWs (Fig. 3.9B) only carbon, oxygen and nitrogen peaks are shown, representative of the atomic composition of diphenylalanine. A chlorine peak also appears after the functionalization, since Traut's Reagent was given in form of a salt, and silicon peaks are present in both samples, because of the surface underneath the structures. To optimize this characterization, EDX was performed using a Scanning Electron Microscope (SEM) and one individual PNW surface was chosen for each analysis.

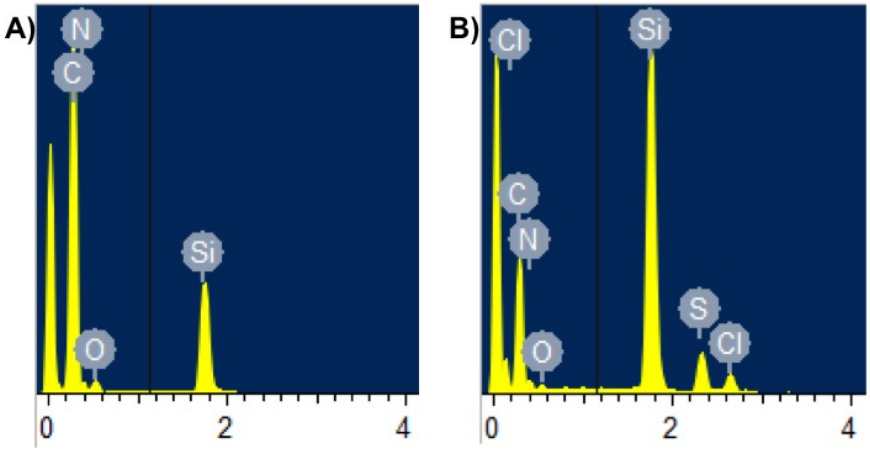

Figure 3.9: EDX analyses of A) Plain PNWs on a Si surface, and B) Thiolated PNWs on a Si surface (horizontal axis is in keV). The two plots are shown with different scale of the vertical axes for better visualization.

We can conclude from this experiments that the thiolation of PNWs was achieved, although further work must be done in this specific functionalization protocol to fully validate the completion of the Traut's reaction presented in Fig. 3.8, and not just check for the presence of Traut's Reagent molecules on the surface.

Furthermore, thiolating the PNWs opens up new possibilities for the metallization of the structures' surfaces, a tool which can be used to produce biological/metallic nanowires.

3.3 Peptide Nanowires for *In Vitro* Studies

3.3.1 Experimental: Biocompatibility Assessment

This experimental section presents an initial biocompatibility assessment of the PNWs as cell culturing and sensing substrates, based on visual inspection of the cell growth, differentiation and adhesion properties. Some of the work presented in this section resulted in Publication II and VIII. Details about the experimental protocols used can be found in Appendices C.2 and C.8.

Cell Growth

As an initial assessment of PC12 cell growth on a PNW surface, a cell growth curve was constructed by observing the evolution of a cell population seeded with known concentration over time, in terms of cell counts per surface area.

The samples used were 0.5 x 0.5 cm^2 gold squares obtained from depositing 100 nm of gold metal on a silicon wafer by e-beam evaporation. A specific dicing size of the square samples was chosen to be constant throughout the experiments for a better comparative study. Additionally, the small square samples were designed to fit into a multiwell plate which is of common use in cell culturing laboratories, to increase the facility in sample handling during cell seeding, counting and incubation. This way, several samples could also be cultured at the same time in individual cell culturing wells, providing the relevant data needed for the statistical analysis.

Peptide nanograss with relevant packing density was grown onto the square samples by pipetting 2.5 μL drops of a 50 mg/mL diphenylalanine solution in HFP onto each sample. The PNW growth was achieved via the usual protocol of aniline vapor aging in the house-build chamber setup.

The surface samples, both bare gold (Au) and gold with PNWs (Au/PNWs) were sterilized in ethanol and afterwards coated with a surface enhancement protein (laminin), by direct contact with a laminin solution in PBS (20 μg/mL) for at least 2 hours. The samples were then placed in multiwell plates for individual seedings with 1 mL of PC12 cell-containing medium at concentrations of 10000 cells/mL. After 48, 96 and 168 hours from seeding, 3 of each type of surface (Au and Au/PNWs) were removed from the multiwell plate and observed under an optical microscope. Cell counting was carried out by counting the number of cells present on defined surface areas in several locations of each sample (3 counts per sample, 2 on opposite corners and 1 in the center of the square), in order to obtain data with units of cells/cm^2.

As shown in Fig. 3.10, the cell growth for PC12 on Au/PNWs-laminin surfaces is comparable to that on bare Au-laminin surfaces, meaning that the presence of the PNWs did not hinder cell growth. Something must be said about the error bars present in this plot, showing the standard deviation in cell counts. As shown, the standard deviation increases drastically the longer the cells are left on the surfaces. This can be explained by keeping in mind that a cell count of a higher value is more difficult to count than when only a few cells are present in a specific area of the sample, since these data points were obtained by eye counts from optical microscopy images.

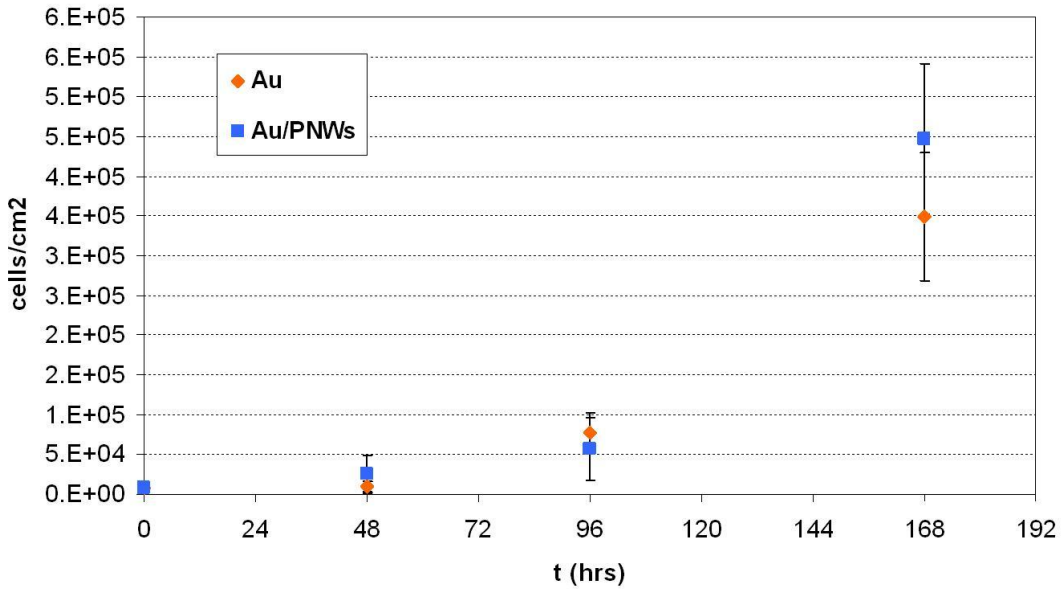

Figure 3.10: Growth curve of PC12 cells on bare gold surfaces coated with laminin (Au) and on PNWs grown on gold surfaces and coated with laminin (Au/PNWs), showing cell density counts after 48, 96 and 168 hours after seeding. Error bars show standard deviations of measurement for each data point.

PC12 Cell Differentiation

Another comparison was made between Au and Au/PNWs surfaces, in order to study whether the presence of the peptide nanostructure hindered the differentiation of PC12 cells. The same sample designs were used for these experiments (the 0.5 x 0.5 cm^2 Au samples), with the same protocols for PNW growth and cell seeding. Differentiation was initiated by introducing differentiation medium to the cell culture for several days, starting 24 hours after initial seeding. Rather

than observing the results by optical microscopy, the cells were fixed onto the substrates by glutaraldehyde based fixative and then analyzed by SEM. Fig. 3.11 is a typical SEM image resulting from these experiments, showing that the morphology and shape obtained from differentiated PC12 cells onto Au/PNWs surfaces is as expected, with the differentiated cells exhibiting their characterstic axon-like outgrowths connecting each cell to its neighbors. We can conclude from this that the presence of PNWs on the cell culturing substrate does not hinder their differentiation into the expected cell morphology.

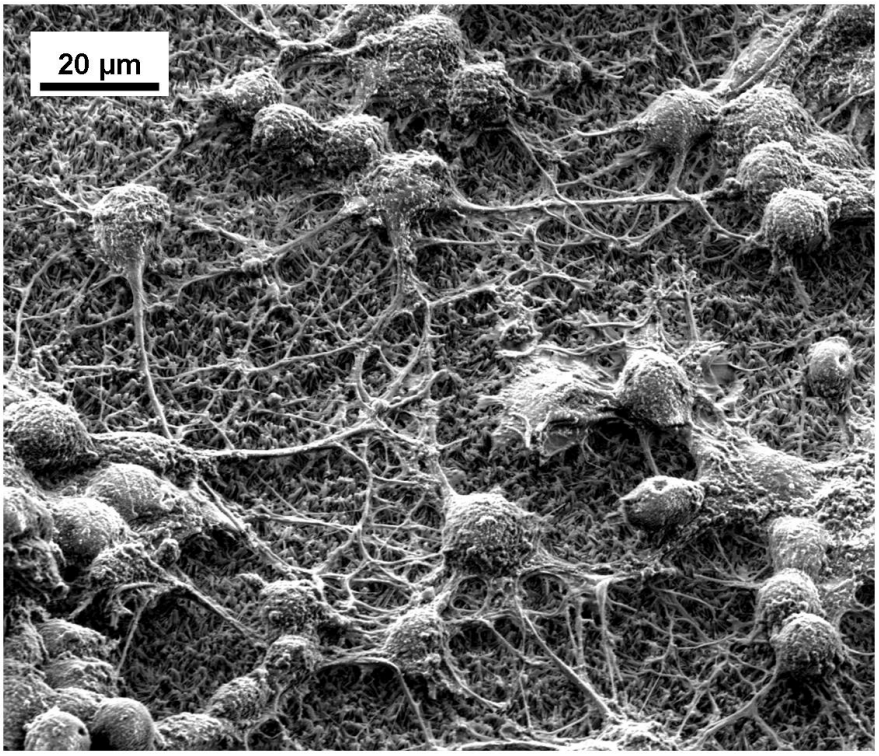

Figure 3.11: SEM image of PC12 cells grown and differentiated onto a surface of Au/PNWs.

Cell Adhesion to PNW Surfaces

Intuitively, we can expect a rough biological surface such as a patch of PNWs to mimick the 3-dimensional biological surfaces present in phisiological environments. In order to further explore this hypothesis, HeLa cells were cultured onto PNW surfaces (on an Au substrate) and used low-vacuum SEM to closely investigate the cell-surface interactions. HeLa cells are one of the most widely used human cell line in research, and originated from cervical cancer cells obtained in 1951 from

the cancer patient Henrietta Lacks [70]. HeLa cells were used in this project for quick assessments of surface properties, since they are easy to culture and handle in a laboratory environment.

As expected, the rough surface created by the PNWs offers the cells plenty of adhesion sites. The cells can then extend their finger-like cell membrane projections to "grasp" the PNWs, seemingly holding on to the nanostructures as they would to for example biological tissue or other cells. This phenomenon is clearly viewed in Fig. 3.12, showing the close interactions between HeLa cells and a PNW surface.

PNWs as Adherence Enhancers

Once the PNWs proved to be a suitable cell culturing substrate for PC12 cells, the research moved towards an investigation of wether the PNWs could replace the more commonly used protein adherence enhancers, such as laminin, used in cell culturing to increase the adherence and therefore survival of stem cells and other cell cultures. Laminin (LAM) was chosen for this comparative study because of its wide use in our laboratories and its compatibility with PC12 cells, specifically.

Similar sample sizes and experimental protocols were used as in the previous sections, although for this specific study 4 different type of surface culturing samples were studied: i) bare gold (Au), ii) laminin coated gold (Au/LAM), iii) PNWs on gold (Au/PNW), and iv) laminin coated PNWs on gold (Au/PNWs/LAM). PC12 cells were seeded onto the square 0.5 x 0.5 cm^2 samples with equal initial seeding densities throughout the 4 kinds of surface, using individual wells for each sample in a multiwell plate. After 48 and 96 hours of cell culturing, samples were taken out and the cell counting was done similarly to the previous cell growth studies, by counting cells on at least 3 different areas of known dimension of each sample. After counting, samples were discarded, meaning for example that the 96 hour samples were different than the 48 hours ones but seeded at the same time (so that 24 samples were used all together in this study). 3 samples per surface type, and 3 counts on each sample, were used to collect each data point in the study.

The results of this study are illustrated in Fig. 3.13. The cell counts plotted at 0 hrs reflect the seeding cell density (per surface area). After 48 hours, a difference can start to be seen between the bare gold and the surfaces that were coated with LAM, PNWs, and PNWs/LAM, showing how the presence of the PNWs seems to increase the cell count. Here we can already conclude that the presence of the PNWs has a positive effect on the cell adhesion properties and their viability. After 96 hours, the differences between the surfaces are clearer. The cells have difficulty when growing on bare Au surfaces, but adding a LAM

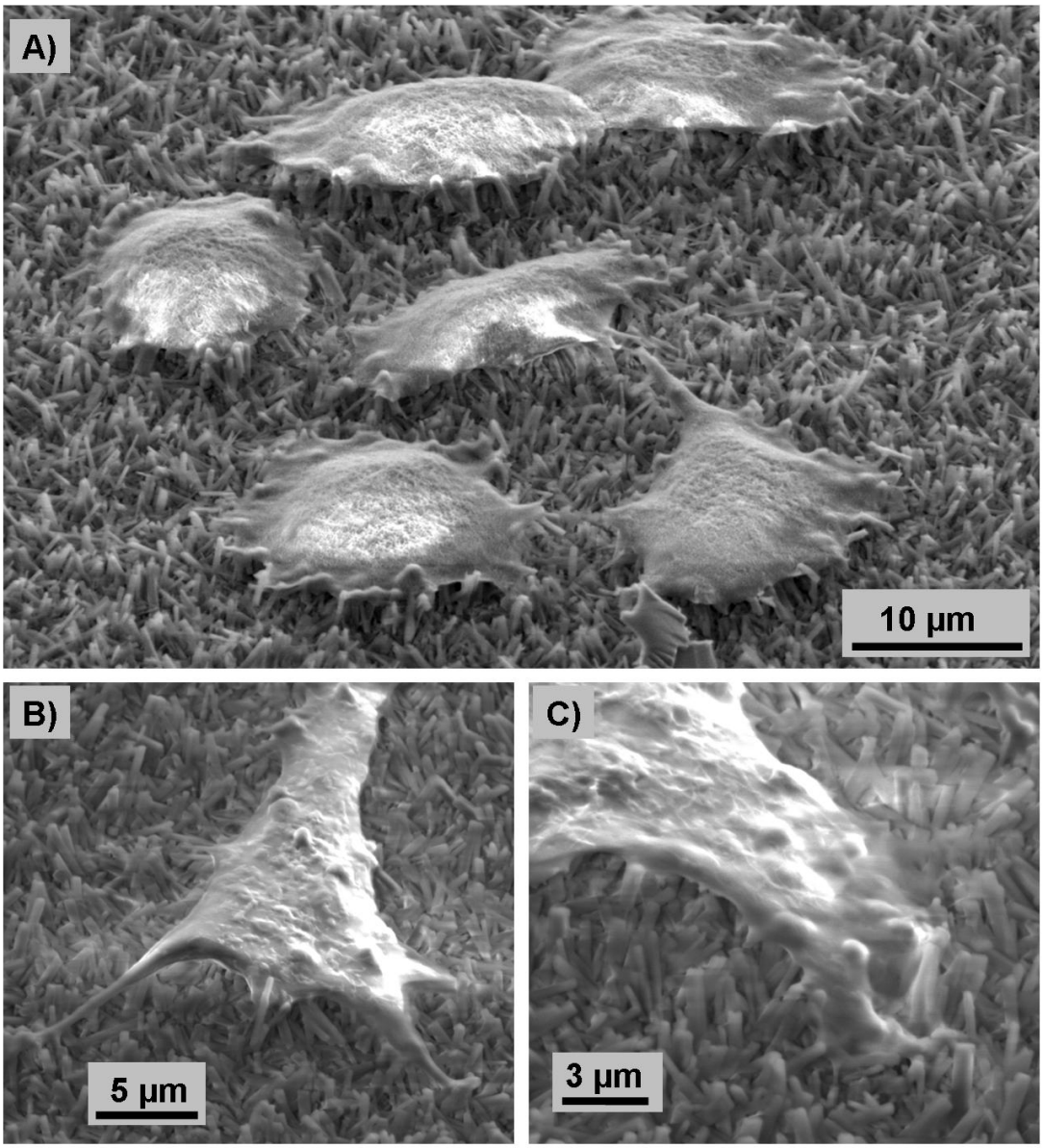

Figure 3.12: A) SEM image of HeLa cells grown onto a PNW surface (no laminin), B) and C) show zoomed in views of cellular adhesion pads onto the PNWs.

coating or PNWs increases the cell count drastically, showing a clear advantage in cell growth when having any sort of biological material onto the surface. The cell growth on Au/PNWs is comparable to their growth on Au/LAM. From these results we can see how PNWs could be used as an alternative biological material for increasing the adherence properties of the PC12 cells. The last data point

in the graph, reflecting the cell count on Au/PNWs surfaces additionally coated with laminin (Au/PNWs/LAM), suggests that an ever better cell adhesion can be achieved by combining the peptide nanostructures with a laminin coating, yielding the highest cell count between all the surface modifications investigated.

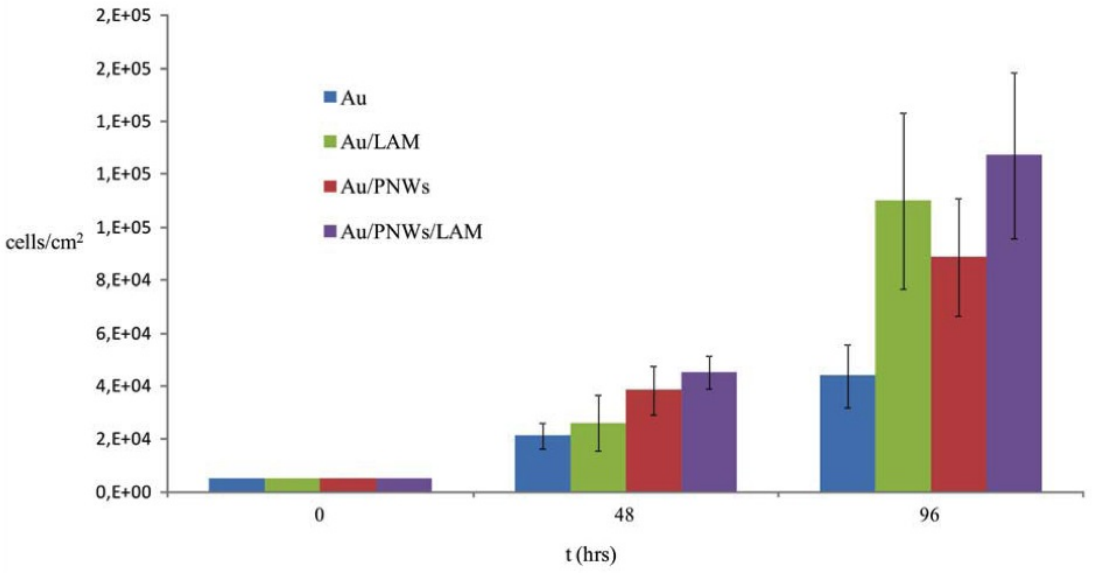

Figure 3.13: PC12 cell growth comparative study for various surface conditions, showing cells present on samples with surfaces of: i) bare gold (Au), ii) laminin coated gold (Au/LAM), iii) PNWs on gold (Au/PNW), and iv) laminin coated PNWs on gold (Au/PNWs/LAM). Error bars reflect standard deviations of measurements (Figure is reproduced from Publication VIII).

3.3.2 Experimental: PNW Patterning

Patterning of PNWs by Soft Lithography

This section describes a method for the patterning of PNWs in micron wide strips, and an visual investigation of cellular behavior onto such patterned surfaces. The results of this experimental work appear in Publication VIII, and further details about the experimental conditions can be found in Appendix C.8.

A soft-lithography technique was used to confine the growth of the PNWs to specific areas. A PDMS mold containing 10-40 μm wide microchannels was made from a previous stamp etched in silicon. The mold was placed into contact with a silicon surface, and the peptide solution (50 mg/mL in HFP) was placed on the entrance of the channels, so as to let the solution fill up the microchannels by capillary force (see Fig. 3.14).

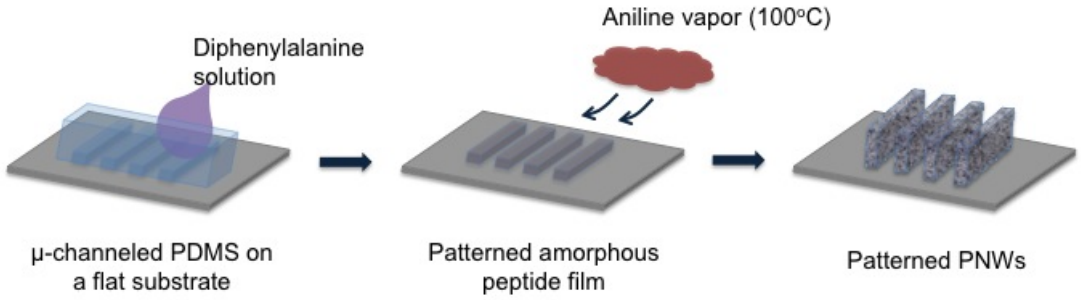

Figure 3.14: A schematic illustration for the micro-patterned growth of vertically well-aligned peptide PNWs (Figure is reproduced from Publication VIII).

The resulting patterned peptide nanograss, grown in organized μm wide stripes, can be seen in Fig. 3.15. It is interesting to note that the edge at the end of the stripes resembles that of a capillary velocity flow profile, used to fill in the PDMS channels with the diphenylalanine solution.

Cell Growth and Behavior on Patterned PNWs

PC12 cells were seeded onto surfaces of patterned PNWs on gold microfabricated chips at concentrations of 330000 cells/mL, in order to study the cell growth and behavior onto these patterned surfaces. Samples with LAM coating and without were used, to check wether the adhesion enhancer protein was required in the case of patterned PNWs. Prior to SEM inspection, the cells were fixed with a 2% glutaraldehyde solution in 0.1 M PBS, then rinsed with PBS and sterile water

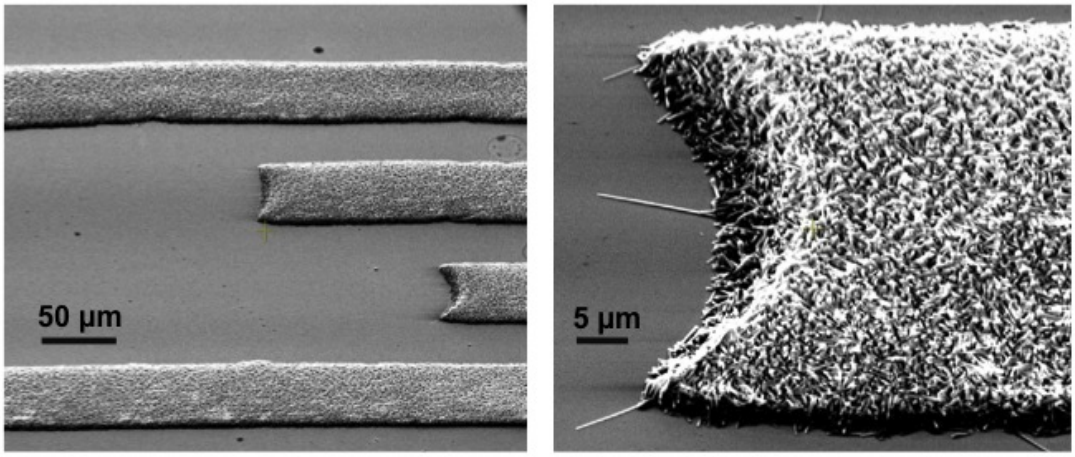

Figure 3.15: SEM images of 40 μm wide stripes of peptide nanograss.

before successive dehydration in ethanol solutions of 60, 70, 80, 90 and 100%. The slow increase in ethanol concentration was used in order not to damage the cell membranes during the drying.

The results of these experiments showed that without the use of laminin, the patterned PNWs did not offer an environment suitable enough for cell growth. Only few cells were seen on those samples, indicating that even if the cells could adhere and survive, they did not proliferate. This could be explained by relating the width of the PNWs strips to the dimension of a PC12 cell, meaning that a more thorough study of different widths of patterned PNW strips, as well as different packing densities of the nanostructures, could produce different cell behavior.

The cell growth on patterned PNWs with a LAM coating, however, yielded cells of similar shape and morphology as for unpatterned surfaces, as can be seen in Fig. 3.16. The cells seem to use the PNW strips as anchoring grounds. Future work can be focused on functionalizing the PNW surfaces with useful biomolecules for cellular studies, e.g. nutrients, growth factors or drugs.

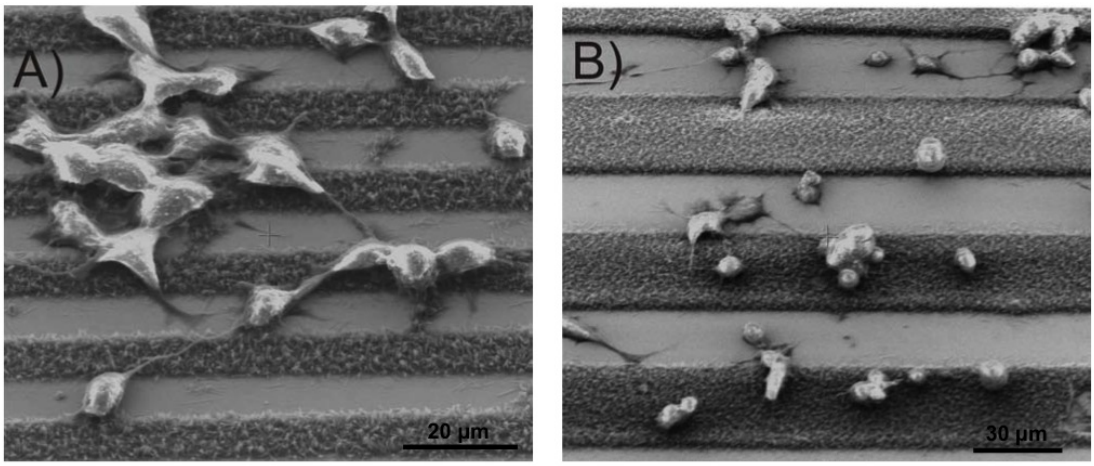

Figure 3.16: SEM images of PC12 cells cultured on patterned PNW gold surfaces coated with LAM, with patterning widths of A) 10 μm and B) 20 μm (Figure is reproduced from Publication VIII).

3.4 Peptide Nanowires for *In Vivo* Studies

The biocompabitility enhancement properties investigated with *in vitro* cell culturing techniques can be applied to implantable sensors and other devices in live animals. This section presents the work carried out in regards to the modification of the surface of implantable microelectrodes with PNWs.

3.4.1 Experimental: Peptide Nanowires on Implantable Microelectrodes

This work was carried out in collaboration with the Neuronano Research Center (NRC) at Lund University. Implantable electrodes were fabricated in Lund, modified with PNW grass at DTU and then brought back to Lund for the *in vivo* experiments.

An important aspect of neurological research is the development of new tools and techniques for a long term physiological characterization *in vivo*, in order to achieve a more in-depth study of neurological processes and mechanisms. Many electrode array designs have arisen in the past decade, most of which are composed of hard materials that are not suitable to long-term implantation due to the damage they create in live tissue [71, 72, 73].

Collaborators from the NRC at Lund University have developed a polymer based 3-dimensional microelectrode array for *in-vivo* impedance recordings in the cerebellum. The electrode arrays, designed as 8 to 12 μm thick needles containing gold electrodes created with a passivation layer of SU-8, are used for electrophysiological recordings from live animals [74].

A joint project was started to enhance the biocompatibility of the NRC implantable electrodes, by providing a biological-like PNW modified electrode surface to decrease the damages done onto the neuronal tissue during and after implantation.

PNW Growth on NRC Electrodes

The decoration of the NRC implantable electrodes with peptide nanograss was achieved by treating the electrodes as growth surfaces during the aniline-assisted PNW synthesis.

In order to obtain complete coverage of the electrodes on both sides of the tip, the deposition of the diphenylalanine HFP solution was achieved not by pipet-

ting the solution onto the electrode, but instead by dipping the electrode tip into the peptide solution. The results of this process showed uniform coverage of the electrodes' surfaces with PNWs, as shown in Fig. 3.17.

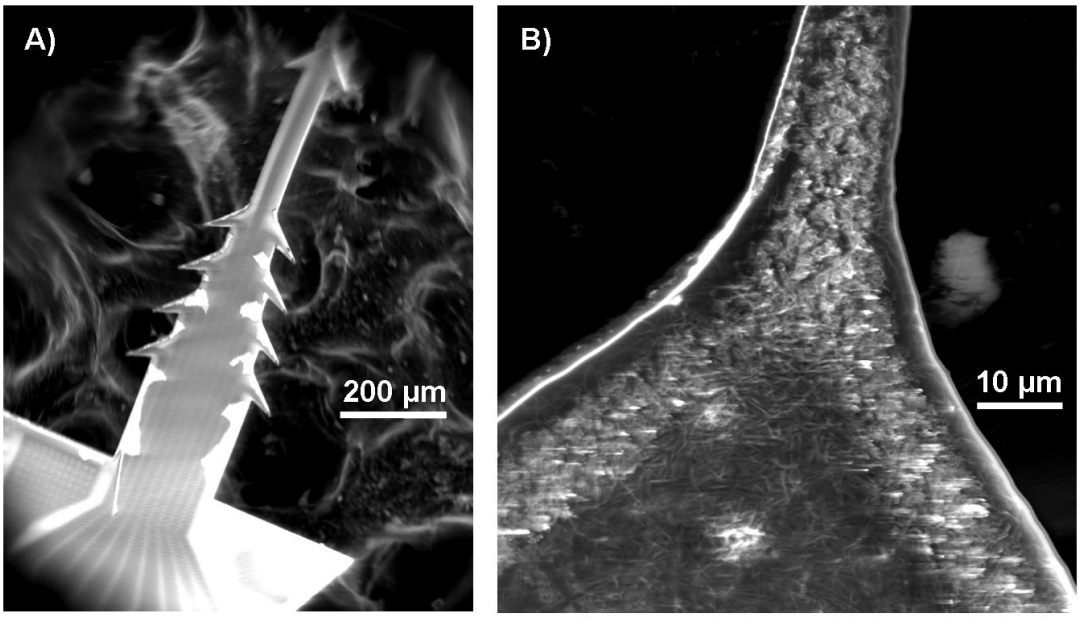

Figure 3.17: A) SEM image of an NRC implantable electrode; B) Zoomed-in image of an electrode tip covered with PNWs.

Curling of the electrode tip was observed for several trials of the PNW growth, a phenomenon possibly due to a difference in surface tension forces between the two sides of the electrode tip created during the growth process. Because of this curling effect, modified electrodes were implanted with the aid of a stiff(er) wire attached along the device.

Implantation and Evaluation of Tissue Response

Rats were implanted with a PNW modified NRC electrode at the animal facilities at Lund University. After 12 weeks of implantation, the animal was sacrificed and the implanted electrode carefully removed from the organ (see Fig. 3.18).

Histological studies on the brain tissue removed were carried out by our research collaborators. The organ was sliced and a stained with ED1, GFAP, DAPI and NeuN. The ED1 stain targets microglial cells, and it reflects the immune response in the tissue. Microglia are a type of macrophages typical of the central and

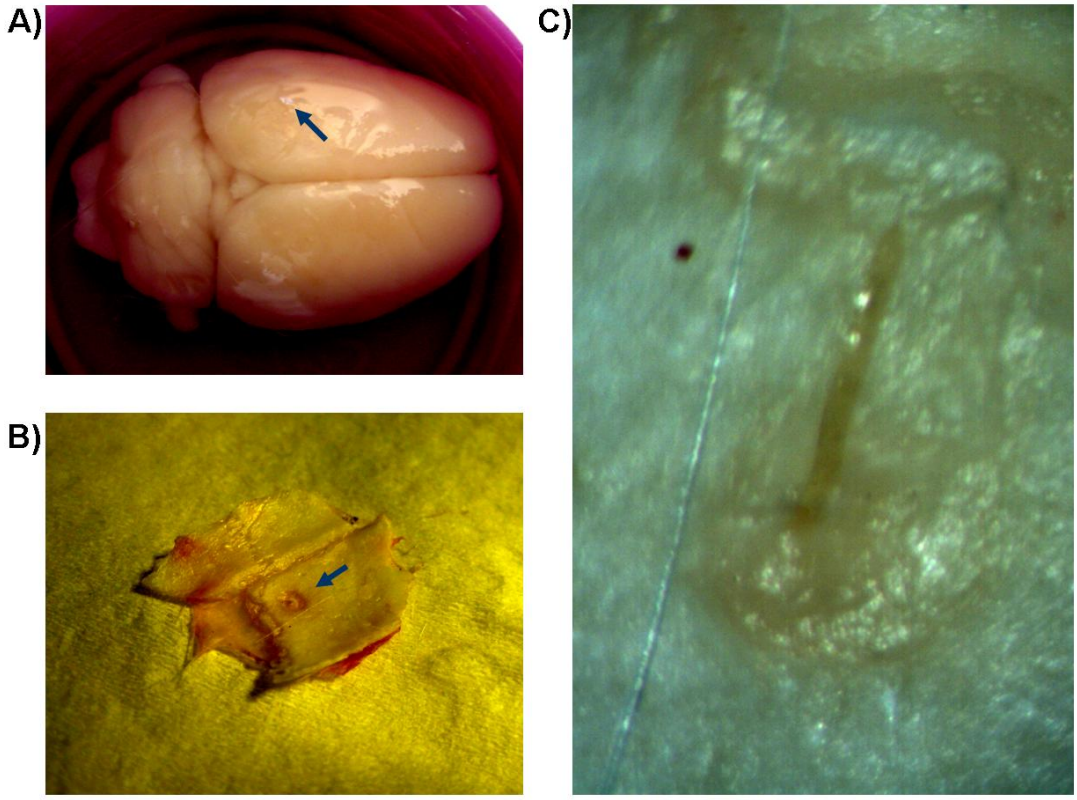

Figure 3.18: Images of a rat's brain after implantation of PNW modified electrode: A) Intact rat brain after animal sacrifice, arrow points to the location of implantation; B) Upper skull with arrow pointing to hole made during implantation, C) Microscopic image of an intact electrode inside the brain tissue.

peripheral nervous system that constitute the main form of active immune defense in the tissue. The GFAP stain targets astroglial cells, characteristic glial cells present in the brain whose main function is to repair damaged tissue. DAPI is an extensively used fluorescent staining technique in cell biology that passes through the cell membrane and stains the DNA present in the nucleus. NeuN is a neuron specific stain used mainly to identify this cell type versus other cells present in the tissue, in order to give information about the neuron to glial cell ratios.

Various sections of the tissue at different depths of the implanted electrode were studied via confocal microscopy. Fig. 3.19 shows an example of the histological study performed. As can be seen in the figure, the ED1 stain (green) shows a clear immune response from the tissue to the foreign implanted electrode at the interface between the device and the biological tissue. This, together with an increase of

glial cells in the implantation zone seen by the GFAP staining, suggests a clear scarring and repairing of the tissue by the brain's physiological mechanisms.

The presence of a thick insulating layer of scarring tissue around the implanted electrode formed by the glial cells could interfere with the electrical measurements, and it is therefore advisable to design implantable devices that minimize this effect. The hypothesis behind this experiment was based on the idea that the PNWs would create rougher and more "bio-like" surface that could lead the brain tissue to recognize it and minimize the glial layer around the electrode. Further experiments at the Lund University will allow to compare these results to implanted devices without PNWs, in order to validate or exclude this hypothesis. In the case of a validation of the advantages of the PNW modification, further tissue response evaluations and possible *in vivo* measurements will be carried out in the collaboration.

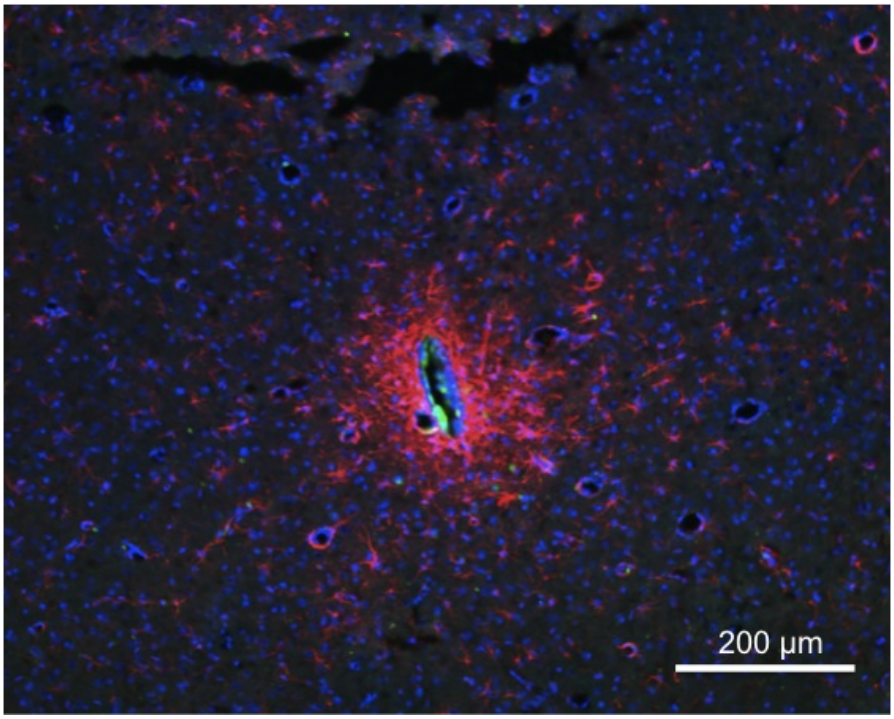

Figure 3.19: Typical example of a histological study of a brain tissue after implantation of the PNW modified NRC electrodes via confocal microscopy, showing ED1 (green), GFAP (red), DAPI (blue) and NeuN (blue) stainings.

3.5 Summary

This chapter presented the work carried out during the PhD project with respect to Self-Assembled Peptide Nanowires.

The experimental sections focused on the optimization of the growth of vertical diphenylalanine PNWs and their functionalization with biomolecules, metallic nanoparticles and chemical functional groups. *In vitro* studies resulted in a preliminary biocompatibility assessment of the biological nanostructures using PC12 and HeLa cells, including a cell growth investigation as well as comparison of the PNWs with an adhesion enhancement protein often used in cell culturing. A method for the patterning of PNWs in micron wide strips via a soft-lithography technique was presented, and the cell behavior onto such patterned surfaces was investigated. An *in vivo* study using PNW coated implantable electrodes was carried out in collaboration with Lund University, and the effects of implantation of such electrodes were studied.

Each presented section offers ideas for the continuation of the specific work, and some possible applications in the field of biology, focusing on cellular and tissue studies.

Chapter 4

Conducting Polymers

The worldwide scientific community started focusing its attention on intrinsically conducting polymers (ICPs) since the discovery of the electrical conductive properties of polyacetylene in 1977 [75]. In the year 2000, the Nobel Prize in Chemistry was awarded jointly to Alan J. Heeger, Alan G. MacDiarmid and Hideki Shirakawa "for the discovery and development of electrically conductive polymers", perhaps symbolizing the importance of the discovery of these materials in the past century [76]. Of course, as usually happens in science, the discovery of ICPs by the aforementioned Nobel Laureates was only a climactic point in a research field that actually sets its roots in the middle of the 1800s, when polyaniline and polypyrrole were already being prepared by electrochemical oxidation in the earliest years of fuel cells research. Indeed, it was not until the acceptance of the existence of macromolecules in the 1920s that the word "polymer" was coined and chemists started being interested in such materials.

ICPs are defined as organic polymers that possess the electrical properties of metals while preserving the mechanical properties of conventional polymers [77]. It must be noted that these materials, often referred to as "synthetic metals" in the original phases of their discovery, technically differ from "conducting polymers", which are basically mixtures of non-conductive polymers with conductive elements, e.g. carbon or metal particles distributed throughout the organic material, and therefore acquire their conductivity solely from the conductive dopant present in the insulating bulk material [77]. Throughout this thesis, though, the term "conducting polymer" is used also for ICPs.

Scientific interest in ICPs has primarly come to light because of a general worldwide interest in polymers in the late 20th century. The "age of plastic" seemed to want to completely swipe away metals from modern day technology by replac-

ing them with carbon-based materials, and although this has happened in many technological fields, especially where production and manufacturing play a key role in materials engineering (plastics shape our world simply because plastic can be shaped, some say), electronics technology was revolutionized by the advent of silicon-based microfabrication, and it is still struggling to climb up a row in the 14th column of the periodic table. However, many successful attempts have been made trying to replace metals and semiconductors with carbon-based materials, and the scientific world is finally starting to understand the advantages of uniting the powers of modern nanotechnology with the 6th element [78].

For the purpose of this thesis, though, we will focus on the application of ICPs as enhancement to metal electrodes, and not as replacement, therefore taking advantage of the true strenghts of these materials, eliminating their weakness of low conductivity and concentrating on their superiority over metals when it comes to flexibility of synthesis and functionality.

Polypyrrole (PPy) and polyaniline (PAni) have particularly attracted interest among the wide variety of ICPs available due to their historical importance in the past century as well as their application of their intrinsic conductive behavior as chemical sensors [80], their ability to be chemically functionalized [81], and their biocompatibility [82]. They have been utilized in research over the past three decades and have turned out to be exceptionally applicable in the field of microelectronics [83] and electrochemical sensing [84, 85], in the latter case especially due to their ability to immobilize electrochemically active biomolecules such as enzymes into their matrix when deposited onto an electrode surface [86]. Additionally, these electropolymerizable ICPs have proven to provide protection against electrode fouling [87, 88] and corrosion [89].

ICPs can be synthesized chemically [90] or electrochemically [91]. We will now deepen our understanding of these materials by separately elucidating each method of synthesis and giving practical experimental examples of how ICPs created in each fashion can be used in cellular micro- and nanosensors.

4.1 Chemical Polymerization

4.1.1 Theory of Chemical Polymerization

Chemical polymerization is based on the oxidative chain formation of the monomer with the use of chemical oxidants, and can occur in both aqueous or non-aqueous solvents. The main advantage in using a chemical polymerization is that this polymerization method does not require an underlaying conductive layer to catalyze the chain polymerization of the monomer in the solution. Furthermore, there is no need for electrical equipment to produce a voltage (i.e. a potentiostat) as in the case of electropolymerization. This method of synthesis is extremely facile and fast, and can yield bulk quantities of ICPs as fine powders of conductive composites or as dispersed particles in solution, or as thin films if the polymer is allowed to accumulate onto a surface.

Perhaps the most important parameters for good polymerization yield is solubility in the solvent used, since a requirement is that oligomers formed in the beginning of the polymerization process be reactive and soluble enough to further link up to other monomers. If the oligomers precipitate in the solution, the process ends unsuccessfully leaving an unstable coating on the walls of the polymerization container (e.g. a beaker or tube). The choice of oxidant is also important, as the cation radicals must be formed at a specific location in the monomer. This latter parameter is usually very specific to the polymer to be produced.

Mechanism for the Chemical Polymerization of Polypyrrole

We will look closely at the mechanism for the synthesis of PPy as an example of how such a chemical polymerization takes place. Even though PAni was also used in parallel with PPy during the initial period of the research, this section focuses on PPy only as it is the material that was eventually chosen for the remaining of the project.

For the chemical polymerization of pyrrole, water has been found to be the optimal solvent with respect to oligomer solubility, and iron (III) chloride the optimal chemical oxidant with relevance to the conductivity of the polymer formed [92]. The mechanism accepted by the modern scientific community by which this polymerization process takes place was first proposed in [93]. The process starts with the oxidation of a pyrrole monomer by electron transfer with an iron (III) oxidant ion present in the solution (see Fig. 4.1, step 1). The radical cations created by the first step react with each other to form dimers, or bipyrroles (Fig. 4.1, step 2), re-

leasing two protons as a biproduct. The pyrrole dimerization has been found to be the slowest step in the process, and therefore the rate-determining step [91]. The bipyrroles are further oxidized by the iron (III) ions to form dimer radicals (Fig. 4.1, step 3), which then react with radical monomers to start the oligomer chain formation (Fig. 4.1, step 4). The process continues in a simliar way to create long polymeric chains that constitute what is known as polypyrrole, with its backbone being sequential five-membered aromatic rings with incorporated nitrogen atoms.

The intrinsic conductivity of PPy relyes on an electrophilic aromatic substitution and its ability to stabilize the partial positive charge on any of the atoms present in the aromatic ring. In this fashion, charges are allowed to be carried around the rings and from one ring to another. From a bulk prospective, charges can then move around in the PPy polymeric chains, resulting in conductive behavior.

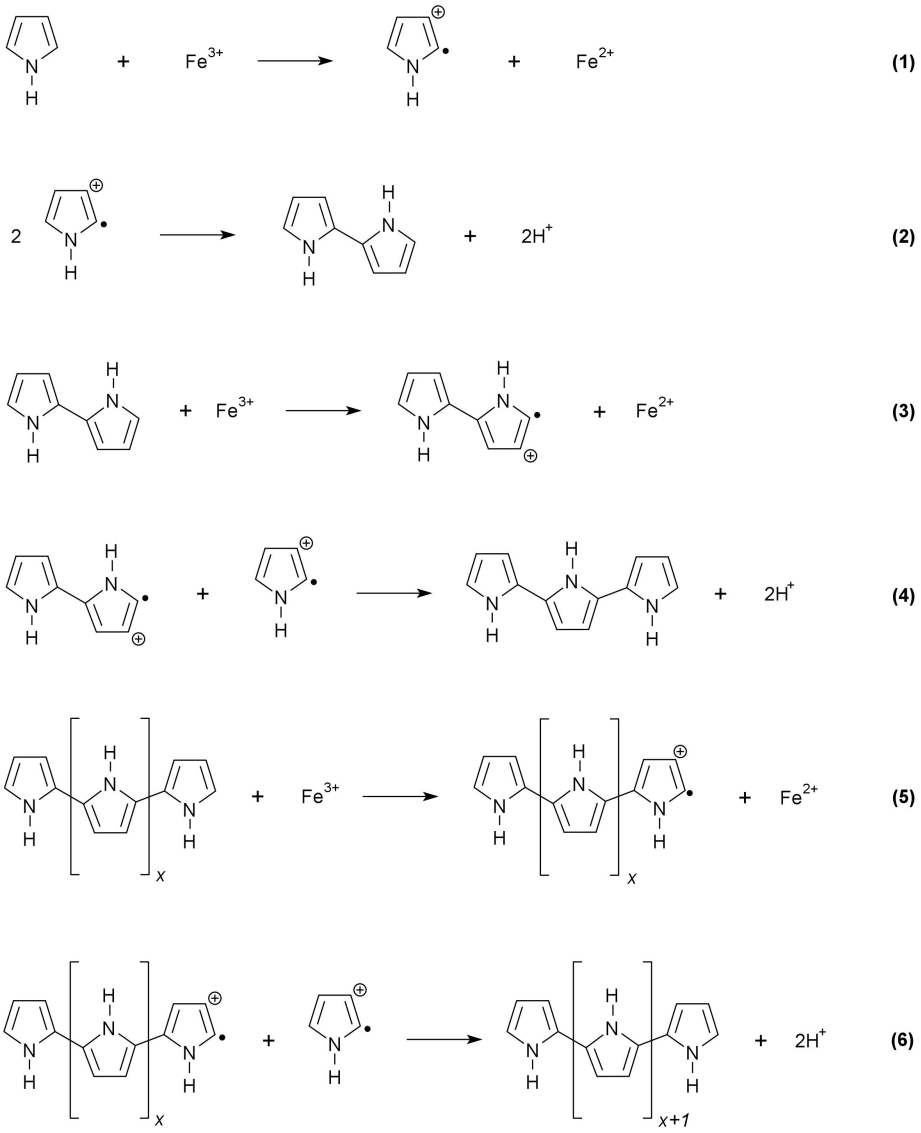

Figure 4.1: Scheme of the mechanism for the chemical polymerization of pyrrole in an iron (III) chloride aqueous solvent, divided in steps: (1) Oxidation of pyrrole monomer and formation of radical intermediate; (2) Dimerization; (3) Oxidation of the dimer; (4) Linking of a pyrrole radical intermediate to oxidized dimer. Steps (5) and (6) show the same mechanisms as steps (3) and (4) for oligomeric chains of polypyrrole.

4.1.2 Experimental: Chemical Polymerization on 3D Microelectrodes

The work presented in this section, about the use of chemical polymerization on 3D microelectrodes to enhance their conductive behavior, resulted in Publication I (see Appendix A). Details about the materials and methods for this work can be found in Appendix C.1.

Microelectrodes can be used to measure electrical signals generated by the action potentials from neurons, yielding a technique that can be used to investigate closely neuronal behavior, both as a single cells or as neuronal networks [94, 95]. Advances in micro- and nanofabrication technologies have helped in bringing this field from a tissue-network response to the single cell level [96, 97, 98]. Over the past 40 years, this technique has focused on utilizing arrays of planar microelectrodes for the detection of bioelectronic activity from *in vitro* neuron and neuron-like cell cultures.

A clear limitation so far has been the low amplitude of the signals acquired from the planar extracellular electrodes, in the range of a few mV, while it is known that intracellular electronic activity exists in the range of 60 to 100 mV [99]. The physical distance between the interior of the cell and the planar electrode outside of the cellular membrane hinders the detection of these signals, increasing the signal-to-noise ratio of the measurements. Because of these limitations, the technology has pushed for the creation of 3-dimensional needle electrodes, capable of penetrate the cellular membrane and detect intracellular bioelectrical activity [100]. Although this new approach has expanded from the vision of intracellular measurements, the use of 3D microelectrodes has also its advantages when it comes to extracellular signal recordings. The higher surface area achieved by the 3-dimensionality of these structures in fact reduces the overall electrical impedance, meaning a higher signal amplitude and therefore a better signal-to-noise ratio [101]. Furthermore, the use of 3D structures can be advantageous in measurements from neuronal tissue, since the out-of-plane structures are able to pierce the first layer of dead cells formed on the outskirts of the brain slice and come closer to the active neuronal network residing inside the tissue [102].

One of the main limitations to the use of 3D electrodes for measurements of bioelectrical activity from neuronal tissue is the reliable fabricaton of the electrode structures. Aside from the high costs and difficulties associated with cleanroom-based microfabrication, a particular draw-back to this technology is the metallization of out-of-plane structures with high aspect ratios. Although silicon fabrication is advanced enough to allow for the creation of the 3D structures, the difficulties in their metallization makes these structures inactive and useless as electrical or

electrochemical sensors. Common methods used in silicon-based microfabrication processes rely on e-beam evaporation and sputtering of metals onto surfaces for creating a thin conductive layer. Whereas this metallization works wonderfully on planar or tilted surfaces, it lacks the ability of producing a uniform metallic layer onto tall vertical structures of 70 μm or more (see Fig. 4.2), since the angle of incedence of the metallic ions during sputtering is not high enough to reach the base of the vertical structures [103].

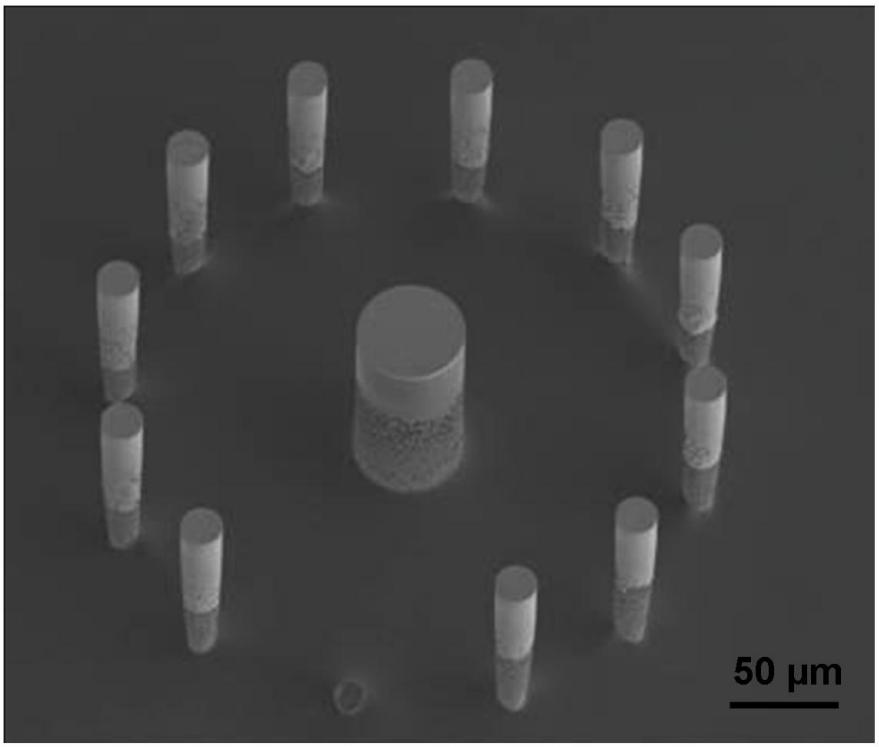

Figure 4.2: SEM image of electrodes partially metallized by sputtering. The image illustrates an example of a bad metallization where the pillar structures' bases are not reached by the incident sputtering angles of the metal ions, leaving gaps of non-conductivity on the structures (Figure is reproduced from Publication I).

A way to "bridge the gap" between the non- or badly metallized sections of the vertical pillars' surface is by depositing a thin layer of conductive material that will enhance the electrical properties of the electrode while maintaining the biocompatibility needed for the application at hand. Chemically synthesized ICPs offer a solution of this problem, since chemical polymerizaton does not require an underlying conductive substrate and has been shown to have the ability to be integrated into standard microfabrication processes (Publication I).

The work presented in this section aims at illustrating how the chemical polymerization of ICPs onto 3-dimensional electrodes can enhance the conductive performance of such structures and facilitate their fabrication.

Fabrication of 3D Microelectrodes

The 3D pillar structures were created via standard microfabrication techniques. A more detailed description of the cleanroom process can be found in [103], and a schematic of it can be seen in Fig. 4.3. The process starts with the spin-coating of a 4.5 μm layer of AZ5214E photoresist onto a silicon wafer, followed by a UV-lithography patterning step and a deep reactive ion etching to shape the micropillars, the latter step tuned to achieve structures with resulting heights of 70 μm and diameters ranging from 30 to 70 μm. A 200 nm passivation layer of silicon nitride was deposited by plasma enhanced chemical vapor deposition for isolating the individual electrode structures and passivate the wiring on the chip.

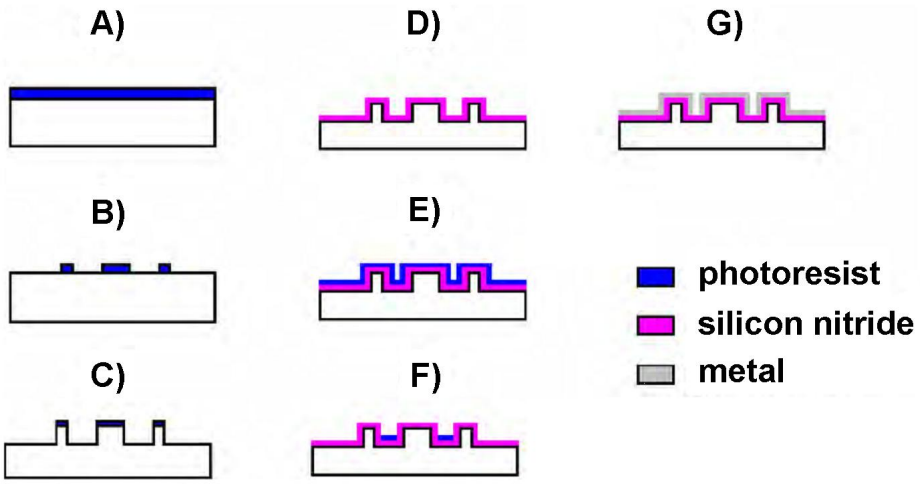

Figure 4.3: Fabrication procedure for 3D electrodes: A) and B) Typical steps for pholithography-assisted patterning on a silicon wafer; C) Creation of the pillars by dry Si etching; D) Isolation of electrode structures by silicon nitride deposition; E) and F) Second photolithography step to define wiring and electrodes areas G) Metallization of electrodes. [103].

At this point in the fabrication process-flow a metallization step is carried out, depositing 200 nm of gold onto the structures. For out-of-plane structures of high aspect ratios, the metal coverage does not cover the entire surface area of the pillars as well as their tops, as discussed before, therefore resulting in a non-uniform metal layer typically resembling that shown in Fig. 4.2.

Patterning of Chemically Synthesized ICPs

A novel method for patterning ICPs onto a substrate was developed during the duration of the project, combining a chemical oxidative polymerization technique with standard cleanroom microfabrication, and was applied for the creation of polyaniline and polypyrrole layers onto on-chip 3D electrode structures.

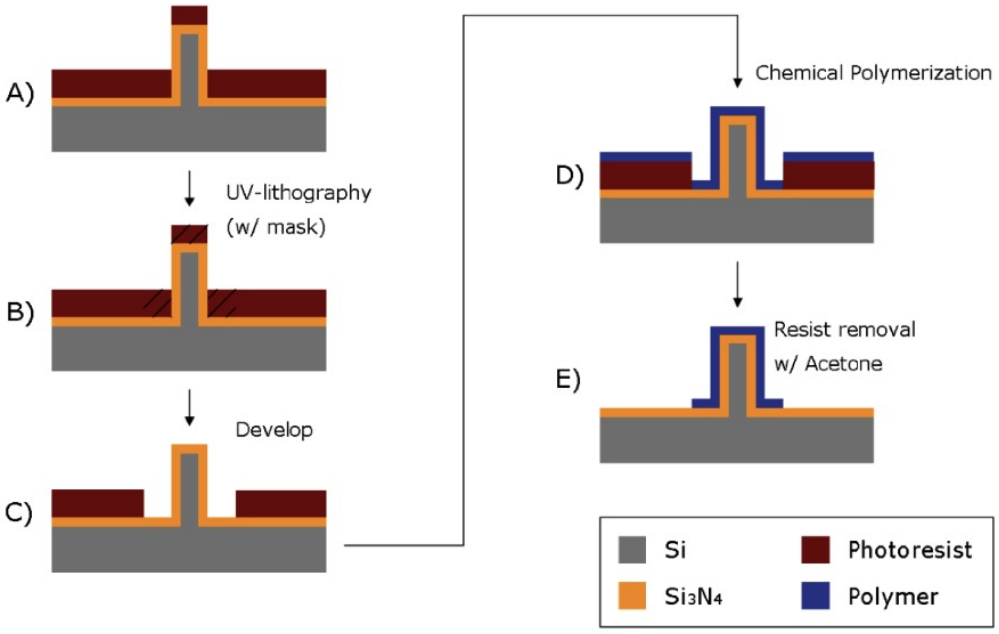

Figure 4.4: Schematic illustration of patterning of a chemically synthesized polymer film. A) Spin-coating of photoresist onto a silicon nitride surface previously deposited on a silicon wafer (containing the pillar structures); B) Mask assisted UV-lithography; C) Photoresist development; D) Chemical synthesis of polymer film on the surface; E) Sacrificial resist removal with acetone (Figure is reproduced from Publication I).

After the fabrication process and the creation of a chip containing the badly metallized electrode structures, a mask-assisted lithography step was carried out in order to define the locations on the chip for the deposition of the polymer layer. Immersing the chip into a polymerization solution for a defined time, depending on the polymer used and wanted thickness, resulted in the formation of a layer of ICP onto the whole surface of the chip (details in Appendix C.1, Publication I). After removal from the polymerization solution, the remaining photoresist was removed by lift-off in acetone, leaving behind a polymer layer only on the areas of the chips defined by the lithographic step.

An example of the result of such ICP patterning onto a chip can be seen in Fig. 4.5, showing the patterning of an ICP layer. Three major areas can be seen present on the chip in Fig. 4.5A: the 3D microstructures to be used as electrodes in the center of the chip (see Fig. 4.5C), the rectangular pads used for connection to electrical equipment (see Fig. 4.5B) and the wiring strips connecting the pillars to the pads.

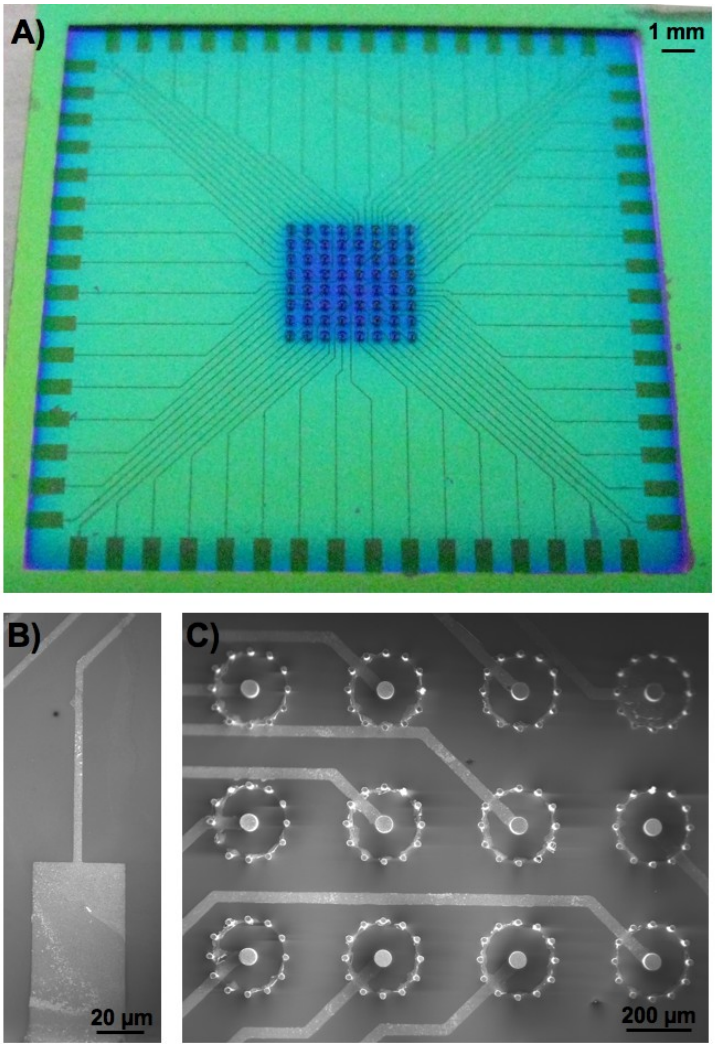

Figure 4.5: A) Patterned polymer film on a silicon nitride surface (dark areas). The microchip included pads for electrical connections, conductive paths, and areas with 3D pillar electrode structures; B) SEM top-view image of one of the pads; C) SEM top-view image of areas with 3D microstructures (Figure is reproduced from Publication I).

Aside from SEM imaging showing clear patterned layers of ICP onto all areas

of the chips, the validation of the polymer deposition was carried out via EDX analysis. For all areas containing the lithographically defined polymer layer, a clear elemental carbon peak can be identified in the spectra obtained. The peak is however not present in the areas that were covered by the photoresist during the polymer deposition. A clear illustration of the excellent quality of these results is shown in Fig. 4.6. The polymer coverage was uniform everywhere on the patterned areas, including the surface along the height of the pillar structures. A surface profiler revealed thicknesses of about 90 nm for PAni films and 50 for PPy films.

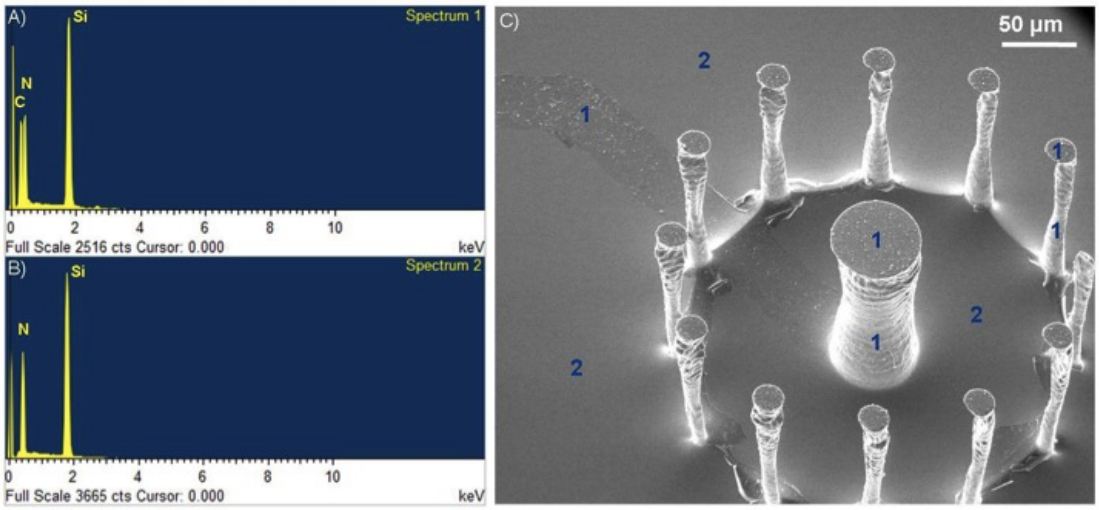

Figure 4.6: Validation of the presence of ICP films by EDX analysis: A) EDX spectrum of a polyaniline covered surface; B) EDX spectrum of the area of a surface without polyaniline film; C) SEM image corresponding to one of the 3D electrode structures with 1) areas where the film is present (spectrum 1) and 2) areas where the film is not present (spectrum 2) (Figure is reproduced from Publication I).

Electrochemical Characterization

An electrochemical characterization of variants of PPy and PAni modified electrode chips was carried out. A comparison was made between i) PPy electrode chips (no metal underneath), ii) PPy on badly metallized Au (Au/PPy) and iii) bare Au electrode chips, resembling structures like those in Fig. 4.2. PAni covered electrode chips were excluded from further characterization because of the material's lack of high conductivity at pHs higher than about 4 [77], rendering these electrochemical

sensors' functionality unsatisfactory at the neutral pH needed for tissue and cellular culturing.

With the use of a in-house fabricated poly(methyl methacrylate) (PMMA) holder, the electrodes' electrochemical behavior was studied by cyclic voltammetry in a 10 mM ferrocyanide solution in PBS (pH 7.4), utilizing single 3D pillars as working electrodes and external reference (Ag/AgCl) and counter (Pt) electrodes. The potential was swept from -0.2 to 1.0 V and cycled with different potential sweep rates.

Comparing the voltammograms resulting from such a characterization from type i), ii) and iii) electrodes clearly shows the enhancement of the electrochemical behavior brought upon by the presence of the ICP (see Fig. 4.7A). The anodic and cathodic peaks shown refer to the ferrocyanide oxidation and the reduction of its product, respectively. In case i), the polypyrrole alone was not conductive enough to ensure good electron transport between the electrode surface and the electrical equipment, therefore resulting in poor electrochemical activity. Comparing ii), a "badly" metallized Au electrode and iii), the same with a PPy coating, we can deduct correct the initial hypothesis concerning the use of the intrinsic conducting properties of PPy to bridge the non-conducting gaps present in the badly metallized pillar electrodes' walls. As seen in the figure, the Au/PPy electrodes showed higher current responses, due to the higher current passing through the PPy coated badly metallized electrodes. The Au/PPy electrodes showed quasi-reversible electrochemical behavior with a linear increase in peak current amplitude proportional to the square root of the potential sweep rate (see Fig. 4.7B).

A further voltammetric investigation in a KCl solution reveals the still present electrochemical activity of the ICP layer, showing the redox behavior of the PPy layer rather than that of the electrolyte in solution as in the previous cases (see Fig. 4.7C). Again, because of the relationship between the current peaks and the potential sweet rate and the nonexistence of a potential shift, the behavior shows quasi-reversibility. The latter discussed voltammograms are typical of a PPy film onto Au metal electrodes, showing the oxidation and reduction peaks of PPy, reflecting the predominant redox reactions of PPy. The peaks obtained are at higher potentials that otherwise expected [93], but this can be explained by the formation of PPy-Au(I) complexes with the "badly deposited" gold material underneath and the sequent Au(I)-Au(III) transformation of these complexes [104].

4.1.3 Summary

The presentation of this work was used to illustrate a manner in which chemically polymerized ICPs can be applied as solutions to problems related to cleanroom processing. Via a novel combination of chemical polymerization and microfabrication techniques, out-of-plane metal electrodes were coated with a thin film of ICP. Good deposition coverage was made certain via electron microscopy methods, and an electrochemical characterization was used to show the enhancements in sensor performance caused by the presence of the ICP.

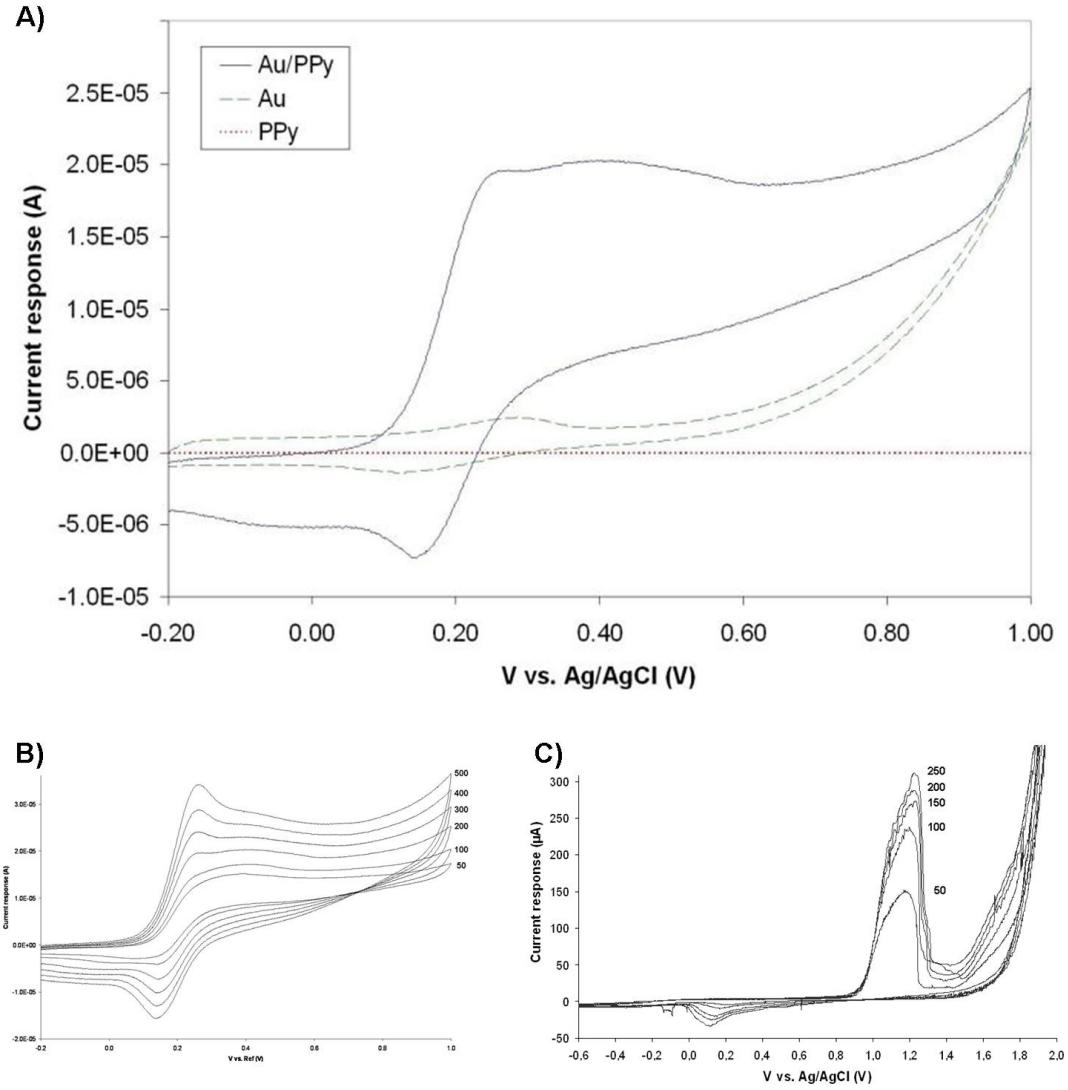

Figure 4.7: A) Cyclic voltammograms of single 3D microelectrodes in Au, PPy, and Au/PPy combination, obtained in a 10 mM Ferrocyanide aqueous solution in PBS (pH 7.4), using a Ag/AgCl (3M KCl) reference electrode and a Pt wire counter electrode. Voltage is cycled from -0.2 to 1.0 V with a potential sweep rate of 200 mV/s. B) and C) Typical cyclic voltammetric behavior of a single 3D Au/PPy microelectrode, using a Ag/AgCl (3M KCl) reference electrode and a Pt wire counter electrode, obtained in B) a 10 mM Ferrocyanide aqueous solution in PBS (pH 7.4) where the voltage is cycled from -0.2 to 1.0 V for several potential sweep rates between 50 and 500 mV/s and C) a 0.1 M KCl solution in double distilled water with potential sweep rates of 50, 100, 150, 200 and 250 mV/s in a potential window between -0.6 and 2.0 V (Figure is reproduced from Publication I).

4.2 Electropolymerization

4.2.1 Theory of Electropolymerization

Electropolymerization is based on the formation of polymer chains from the monomer in solution under the influence of an electrical potential. This process leads to the easy and reproducible creation of conductive organic films over conductive surfaces, regardless of their shape and size. This method for ICP film formation has found its use in many applications, from biotechnology to automobile manufacturing. The reason for the success of electropolymerization lies in its versatility of monomer design as well as processibility of the polymer itself, meaning that this technique can be tailored to the specific application in mind by changing the film's conductive, electromagnetic, mechanical or optical properties. Similarly to the case of molecular self-assembly, electropolymerized films can be tuned to specific properties by either changing the monomer building blocks or the parameters during the polymer formation and deposition. Furthermore, the polymer matrix structure created upon electropolymerization can be used for the entrapment of specific ions or organic molecules onto an electrode surface, making this technique a very useful tool in the modification of electrodes for electrochemical sensing.

The kinetics behind electropolymerization rely heavily on several parameters, including the potential used at the electrode [105], solvent [105, 106], counterion used [107, 108] and temperature [109]. The electrode materials used also have an effect on the turn-out of the electropolymerization process [110].

Mechanism for the Electropolymerization of Polypyrrole

We will look closely at the mechanism for the electrosynthesis of PPy as an example of how such a process takes place. PAni has also been used throughout the work, but PPy has shown to have better conductive properties in the pH ranges relevant to cell culturing (neutral pHs), therefore the mechanism for the electropolymerization of PAni is not described, even though it resembles that of PPy [111].

The electropolymerization of pyrrole resembles the mechanism for the chemical synthesis of polypyrrole, as discussed previously. This is quite expected, since the monomer and the resulting polymer are the same. Several mechanisms with slight changes have been proposed since the first investigation of these electropolymerization reactions, but here we present the most aknowledged and accepted mechanism, referred to as the *Diaz mechanism* [112].

Pyrrole monomers can be present in an aqueous solution as several resonating structures (see Fig. 4.8), although structures (III) and (V) are more stable, because they hold positive and negative charges near each other [113].

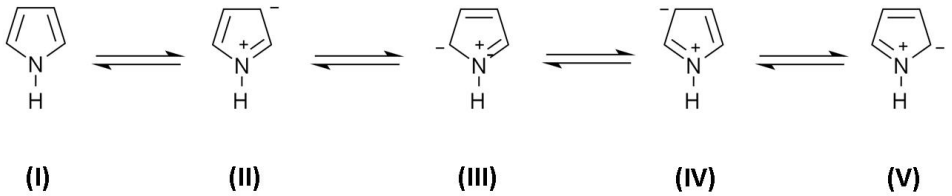

Figure 4.8: Possible resonating structures of a pyrrole monomer.

An *initiation step* is required to start the polymer formation and linking the monomers together. Pyrrole monomers are oxidized in this step, i.e. they lose an electron, and radical cations are formed, similarly to the case of chemical polymerization (see Fig. 4.9).

The next *propagation step* refers to the interaction between the radical cations formed in the initiation step. The reaction between the two produces dimer radical cations, which then stabilize into an aromatic dimer by loss of 2 protons, as shown in Fig. 4.10C. The aromatic dimers then becomes oxidized under the influence of a potential and forms a dimer radical cation, the most stable resonance of which can be seen as a product of this reaction in Fig. 4.10D. It is important to note here that the oxidation potential of the dimer in this step is lower than the oxidation potential of the monomer, meaning that the monomer is more difficult to oxidize, making the monomer oxidation the rate determining step in the electropolymerization reactions [114].

The dimer radical cation product of the preceding reaction then reacts with a monomer radical. After several stabilization steps not shown in the figure, the product of this reaction is the trimer shown in Fig. 4.10E. Similarly to the formation of the trimer from the dimer, more and more monomer radicals get linked up at the end of the chain, to finally produce polypyrrole as the final product of the sequence of reactions (see Fig. 4.11).

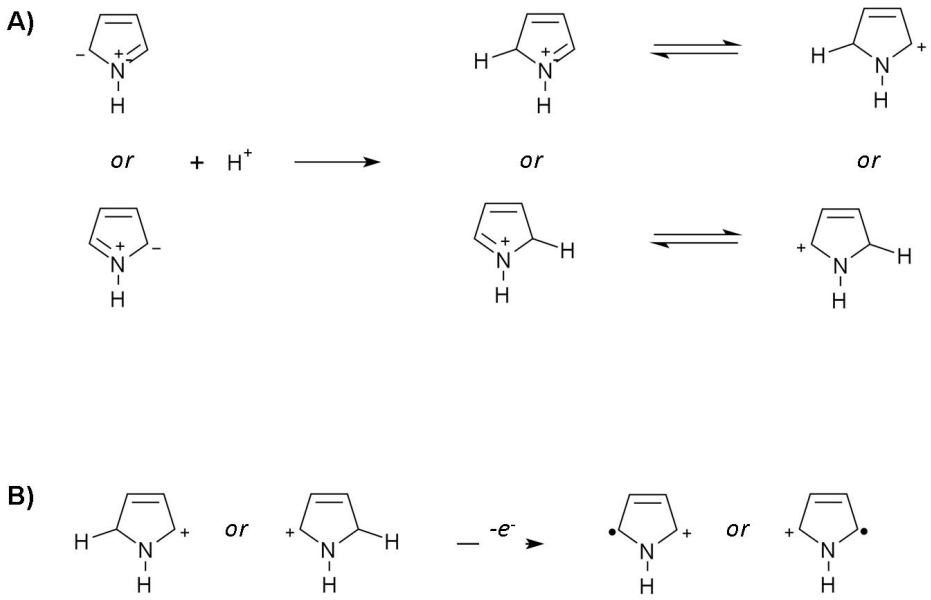

Figure 4.9: Initiation step during pyrrole electropolymerization showing A) reaction for the oxidation of pyrrole monomers and formation of intermediates and B) reaction for the formation of radical cations.

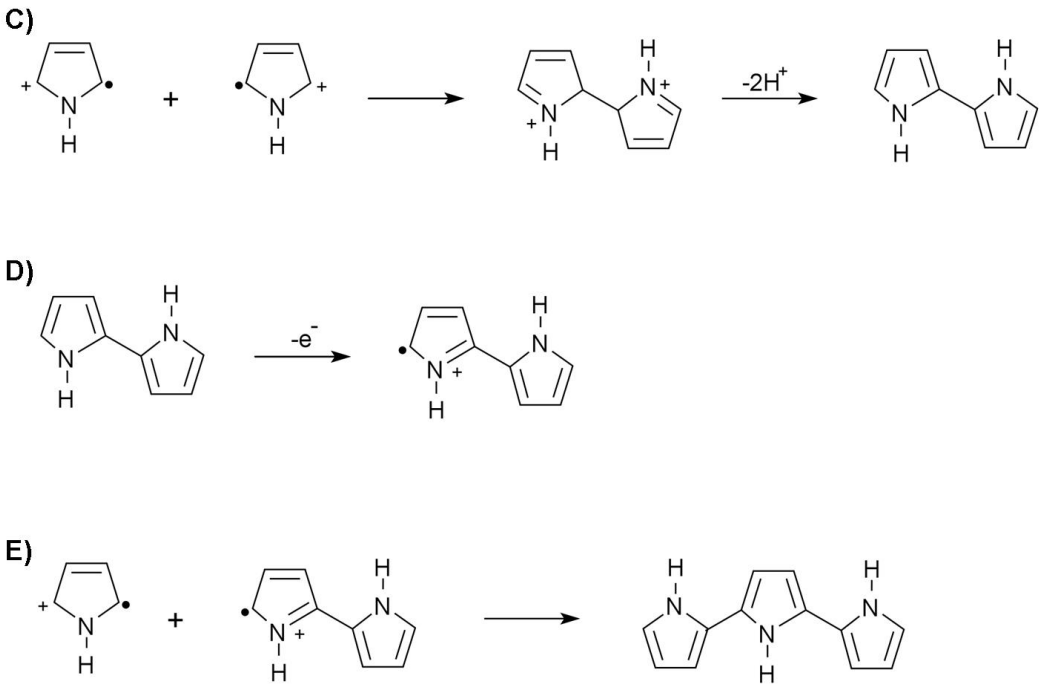

Figure 4.10: C) Propagation step during pyrrole electropolymerization and stabilization of the dimer radical cations into aromatic dimers, D) The formation of cation radicals by oxidation and E) the formation of a polypyrrole trimer.

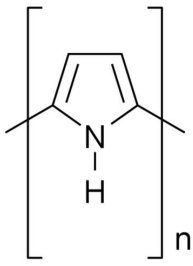

Figure 4.11: Chemical structure of polypyrrole.

4.2.2 Experimental: Electropolymerization on 3D Nanoelectrodes

This section describes yet another way in which ICPs, and in this case specifically ones synthesized via electropolymerization, can aid in designing microfabricated sensor devices for cellular studies. In addition to pillar microelectrodes dedicated to tissue studies, attempts have been made in the research group to develop nano sized structures that offer the possibility of intracellular measurement and therefore single cell analysis (Publications IV, V, VI, VII). In the course of this work, electropolymerization has been useful throughout the development process for the achievement of nanoelectrodes, and the results have been published in Publication IV. Further details about the experimental procedures can be found in Appendix C.4.

Fabrication of 3D Nanoelectrodes

3D nanoelectrodes (see Fig. 4.12) were fabricated using cleanroom technology starting from a single polished silicon wafer. After a 500 nm of silicon oxide growth, photolithography was used to pattern the structures, with a special alignment mask as described in Publication IV. A combinatorial wet and dry etching technique allows for the creation of 3D structures with sharp tips smaller than 1 μm in diameter.

The electrodes are then electrically isolated from each other with the deposition of 500 nm of silicon dioxide, deposited by plasma-enhanced chemical vapor deposition (PECVD), before metallization of the 3D electrode structures as well as the wiring and pads for electrical connection. The metallization for these electrodes was achieved by deposition of platinum instead of gold, because of availability of metals during the time of fabrication.

A final passivation layer of silicon nitride is deposited by PECVD, and then etched to expose the electrode structures with the use of mask-assisted photolithography.

Electropolymerization of Polyaniline as Validation of Microfabrication Process

After an electrical impedance characterization of the electrode structures showed poor conductivity (a relatively large impedance), a possible hypothesis explaining this behavior was formulated, relating the poor electrode conductivity to a residual layer of silicon nitride present on the surface of the 3D nanopillar. Although

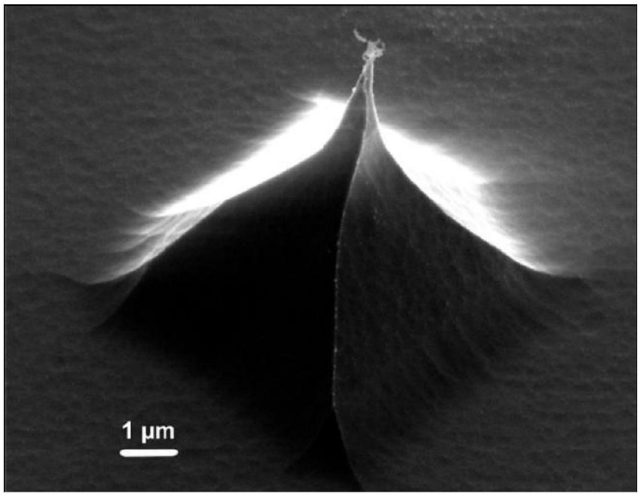

Figure 4.12: SEM image of nanoelectrode structure with sharp tip, before metallization and passivation steps which enlarge the tip size (Figure is reproduced from Publication IV).

the silicon nitride used for passivation was supposed to be etched away in the lithographically patterned areas, therefore exposing the electrodes and electrical pads, the etching rate obtained in the microfabrication process could have differed from the calculated one due to the structures' geometry and size.

In order to be sure that this was, or was not, the case, electropolymerization was carried out on the nanoelectrodes. The idea behind this validation was rather simplistic: if the metal tips of the electrodes were exposed, applying a potential onto them in the presence of a ICP monomer solution would catalyze polymer formation onto the structures.

Polyaniline was chosen for this experimental work because of the ease in polymerization parameters as well as know-how present in the research group at the time. Electropolymerization was achieved by cycling the potential from 0 to 1 V and back vs. Ag/AgCl (1.0 KCl) at a potential sweep rate of 100 mV/s for 25 cycles in a 1.0 M HCl solution with an aniline concentration of 1.0 M.

The validation of the presence of the polymer onto the electrodes was achieved by cyclic voltammetry, showing a clear electrochemical response of the PAni layer. From the voltammograms obtained (see Fig. 4.13) we can see two irreversible anodic peaks, reflecting the two shifts in oxidation states of PAni, from the fully reduced leucoemeraldine to the partially oxidized emeraldine, and from the latter to the fully oxidized form, pernigraniline [77]. These results are typical for PAni films synthesized on different conductive substrates [115]. The irreversibility is

explained by the lack of reduction peaks and by the peak potential shift obtained with increasing potential sweep rates. Nevertheless, the electrochemical activity of the electrodes is good evidence that the nitride layer was indeed removed during the microfabrication process etching step.

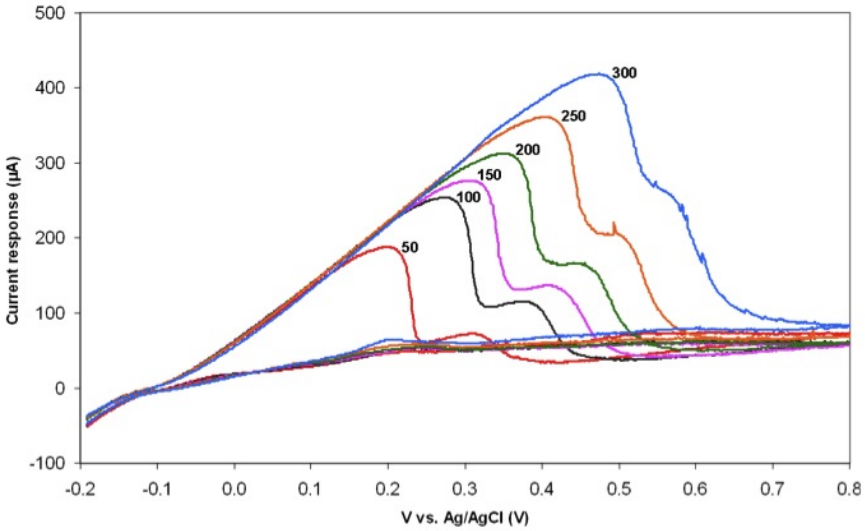

Figure 4.13: Cyclic voltammograms from nanoelectrodes after the electrodeposition of a polyaniline film in a 1.0 M HCl solution using an Ag/AgCl reference electrode, for potential sweep rates of 50, 100, 150, 200, 250 and 300 mV/s (Figure is reproduced from Publication IV).

A further validation of the presence of the electropolymerized PAni layer was carried out by EDX analysis, and the spectra can be seen in Fig. 4.14. A comparison of the 3D platinum nanoelectrodes after the nitride removal by etching (Fig. 4.14A) and before the nitride removal (Fig. 4.14C) show that in fact an energy peak corresponding to atomic nitrogen is present in the latter case but not in the first. Additionally, a Pt nanoelectrode after PAni electropolymerization shows a clear atomic carbon peak (Fig. 4.14B), further validating the presence of the polymer film on the structure and its localization on the active areas of the electrodes.

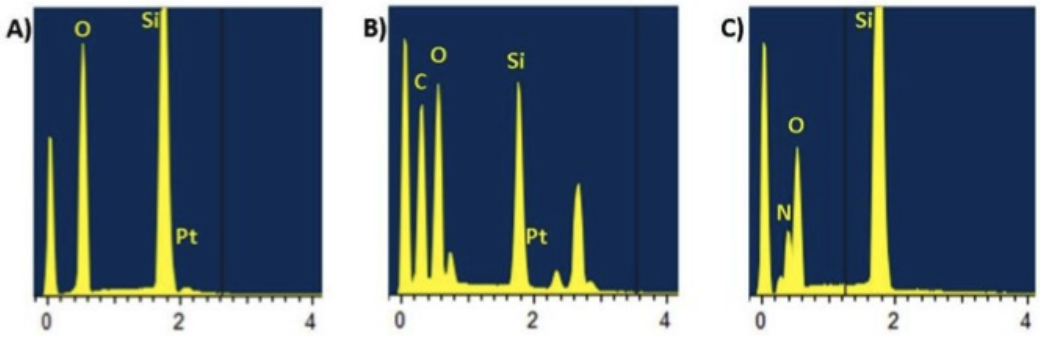

Figure 4.14: EDX analysis spectra of (A) a nanoelectrode at the end of the fabrication process after the nitride etching step, (B) a small electrode after electrochemical polymerization of aniline, (C) a nanoelectrode structure present in the wafer but that has not undergone a nitride etching step. Spectra were taken at 15 kV, units on the horizontal axis are keV, units on the y axis are arbitrary units reflecting the amount of the material present (Figure is reproduced from Publication IV).

4.2.3 Experimental: Electropolymerimerization on Interdigitated Microelectrodes

This section is presented to show an example of how the electropolymerization of ICPs can be used to increase the sensitivity of an electrode towards a specific analyte, in this case dopamine. The following section is a collection of excerpts taken from the article "Doped Overoxidized Polypyrrole Microelectrodes as Sensors for Detection of Cellular Dopamine Release", submitted to the peer-reviewed journal Biosensors and Bioelectronics *by the author (Publication III). Details about the materials and methods for this article can be found in Appendix C.3.*

"A surface modification of interdigitated gold microelectrodes (IDEs) with a doped polypyrrole (PPy) film for detection of dopamine released from populations of differentiated PC12 cells is presented. A thin PPy layer was potentiostatically electropolymerized from an aqueous pyrrole solution onto electrode surfaces. The conducting polymer film was doped during electropolymerization by introducing counter ions in the monomer solution. Several counter ions were tested and the resulting electrode modifications were characterized electrochemically to find the optimal dopant that increases sensitivity in dopamine detection. Overoxidation of the PPy films was shown to contribute to a significant enhancement in sensitivity to dopamine. The changes caused by overoxidation in the film morphology and electrochemical behaviour were investigated by SEM and AFM as well as cyclic voltammetry, respectively. The optimal dopant for dopamine detection was found to be polystyrenesulfonate anion (PSS-). Rat pheochromocytoma (PC12) cells, a suitable model to study exocytotic dopamine release, were differentiated on IDEs functionalized with an overoxidized PSS- doped PPy film. The modified electrodes were used to amperometrically detect dopamine released by populations of cells upon triggering cellular exocytosis with an elevated K+ concentration. A comparison between the generated current on bare gold electrodes and gold electrodes modified with overoxidized doped PPy illustrates the clear advantage of the modification, yielding 2.6-fold signal amplification. The results also illustrate how to use cell population based dopamine exocytosis measurements to obtain biologically significant information that can be relevant in, for instance, the study of neural stem cell differentiation into dopaminergic neurons.

IDE Microfabrication

The microchips having 12 electrode sets, each comprising an interdigitated electrode (IDE), a counter electrode (CE) and a reference electrode (RE) (see Fig. 4.15), were fabricated using standard cleanroom-based micromachining techniques.

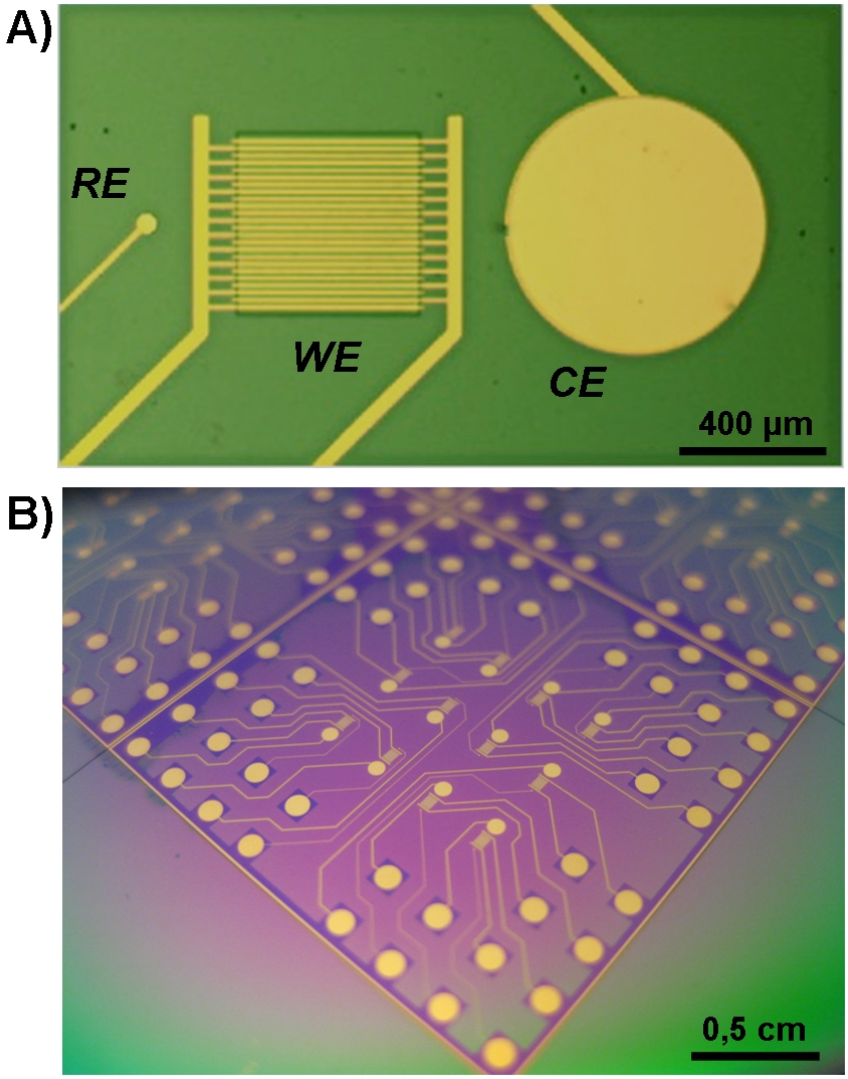

Figure 4.15: A) An individual set of reference electrode (RE), working IDEs (WE) and counter electrode (CE); B) a microfabricated chip containing 12 sets of electrodes with individual contact pads on the outskirts of the chip for electrical connections (Figure is reproduced from Publication III).

A 670 nm layer of thermal oxide (SiO2) was grown on a silicon wafer (one side polished) in a drive-in furnace at 1050 ^{o}C in the presence of water vapor (wet growth). The gold structures, i.e. electrodes, leads and contact pads, were photolithographically defined in positive photoresist using an image reversal process, followed by metal deposition (10 nm thick Ti adhesion layer and 150 nm thick

gold layer) through electron beam evaporation and lift-off in acetone. Prior to metal deposition, the SiO_2 was etched for 100 sec in the areas having opened resist using buffered HF solution to form ca. 150 nm deep isotropic undercuts [116] that eliminate the formation of lift-off ears at the edges of the metal structures. The non-active gold areas (the leads connecting the electrodes to the contact pads) were passivated with 500 nm thick silicon nitride deposited using plasma-enhanced chemical vapour deposition. A second photolithography step coupled with reactive ion etching of the silicon nitride was used to expose the active electrode areas and contact pads. Removal of the final photoresist was achieved by ultrasonication in acetone followed by intermediate rinsing with ethanol and final rinsing with deionized water.

Polypyrrole Electropolymerization and Overoxidation

For the electropolymerization and electrode characterization, the electrode chips were placed in a micromilled poly(methyl methacrylate) (PMMA) holder (see Fig. 4.16A). The holder formed a 500-L vial on top of the electrode chip to facilitate liquid handling during experiments. Interconnections between the electrode chip and the potentiostat (1010 eight-channel potentiostat from CH Instruments, Austin, USA) were obtained using a tailor-made PCB having gold plated spring loaded pins.

Before use, the electrode chips were cleaned for 10 minutes in a solution containing 50 mM KOH and 25 % H_2O_2, followed by a potential sweep on the IDE working electrodes (WE) from -200 mV to -1200 mV in 50 mM KOH at 50 mV/s to remove the gold oxides formed during the chemical cleaning [117]. The polypyrrole (PPy) electrode modification was achieved by electropolymerizing pyrrole monomers under potentiostatic conditions for 10 seconds at 700 mV with or without dopant counterions. The IDEs of the microchip were used as WEs together with the RE and CE from each respective electrode set. Overoxidation of the PPy layer was carried out by cyclic voltammetry in a 0.1 M NaOH solution by applying 50 cycles in a potential window from 0 to 1000 mV at the sweep rate of 100 mV/s. The electrochemical behaviour of the doped PPy-modified electrodes was characterized by cyclic voltammetry in a potential window from 0 to 700 mV at a potential sweep rate of 50 mV/s in solutions having various dopamine concentrations. A morphological comparison of the polymer layer was done by low-vacuum scanning electron microscopy (SEM) and Atomic Force Microscopy (AFM). The results showing the average thickness of the obtained PPy films are presented +/- standard error of mean (s.e.m.).

In potentiostatic polymerization, the formation of PPy is initiated by the creation

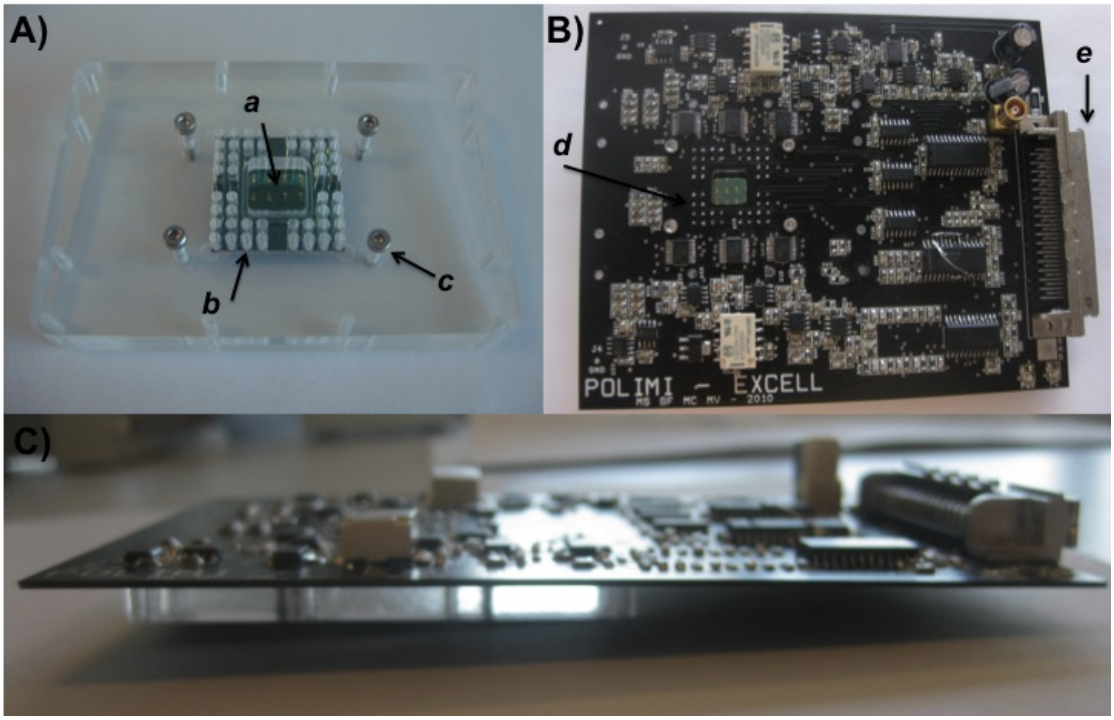

Figure 4.16: The complete analytical setup showing: A) the 2-piece PMMA holder fabricated using micromilling technology (a) open chamber with exposed IDE sets, b) holes to exposed contact pads for connections via spring-loaded pins and c) screws to ensure good contact between the top and bottom layer of the PMMA holder, to avoid leakage out of the open chamber); B) a top view of the potentiostat incorporated directly onto the PMMA holder (d) locations where the metallic pins extrude from the bottom of the potentiostat PCB to connect directly with the contact pads of the microchip underneath and e) connection to an external computer); C) a side-view of the complete mounted setup (Figure is reproduced from Publication III).

of pyrrole radical-cation intermediates and further on dimmers and oligomers that are adsorbed at the electrode surface, initiating the formation of polymer chains in different nucleation points [118]. Allowing this process to proceed for a certain time, PPy films with varying morphological and electrochemical properties are created on the electrode depending on the time exposed to the applied potential and the used counter ion. The nominal thickness of the obtained PPy films can be estimated based on Faradays law of electrolysis by integrating the amperometric current-time traces for the polymerization experiments, upon the assumption of 100% current efficiency, the average polymer density of 1.5 g/cm^3 and the involvement of 2 electrons in the polymerization reaction [119].

Subjecting PPy films to several potential cycles in the presence of oxygen, reach-

ing sufficiently high overpotentials (up to 1 V), results in irreversible overoxidation of the polymer film. In electropolymerized PPy, the conductivity of the polymer film is based on its ability to undergo partial oxidation of the polymer backbone, whereas overoxidation of the polymer blocks the electron transfer in the nitrogen-containing aromatic rings of the backbone, forming oxygen-containing functionalities, such as carbonyl [120] and carboxylic groups [121]. However, although the presence of oxygen in the polymer backbone reduces the conductivity of the PPy film, the resulting electronegativity attracts positively charged molecules to the surface of the film, therefore rendering the electrode more sensitive towards cations, such as dopamine, as well as more permselective, eliminating anionic interferents, e.g. ascorbate and dopamine metabolite dihydroxyphenylacetic acid [122].

In order to compare an electropolymerized PPy film (neutral state) with an otherwise similar but overoxidized polymer film, electropolymerization at a potential that does not result in overoxidation is necessary. Previous experiments have shown that the overoxidation takes places at around 900 mV (data not shown). An electropolymerization potential of 700 mV vs. gold RE was thus chosen to obtain a neutral state PPy film.

A characteristic increase in sensitivity to dopamine due to overoxidation of PPy can be seen in Fig. 4.17, which shows cyclic voltammograms of a PPy-modified gold IDE set (without any added counter-ion during electropolymerization) before and after overoxidation. The presence of dopant counter-ions results in very similar voltammograms for dopamine concentrations in the range from 10 nM to 1 mM for both overoxidized and neutral state PPy. In the case of the electrode modification with conducting PPy in its neutral state, which on virtue of its conductivity promotes the dopamine oxidation, the voltammograms show that the peaks corresponding to dopamine oxidation and reduction are hidden under currents generated by redox processes of the polymer and non-faradaic processes caused by an increased double layer capacitance, making the anodic current rise with an almost ohmic behaviour. In the case of the non-conducting overoxidized PPy film, dopamine electron transfer occurs directly to the underlying gold IDEs. The effects of the double layer capacitance are drastically decreased and clearly defined peaks can be seen, corresponding to the oxidation (top anodic peak) and reduction (bottom cathodic peak) of dopamine.

Counterion Doping

Depending on the counter-ion used as dopant and particularly on its size, the electropolymerized PPy film will exhibit different morphologies and electrochemical

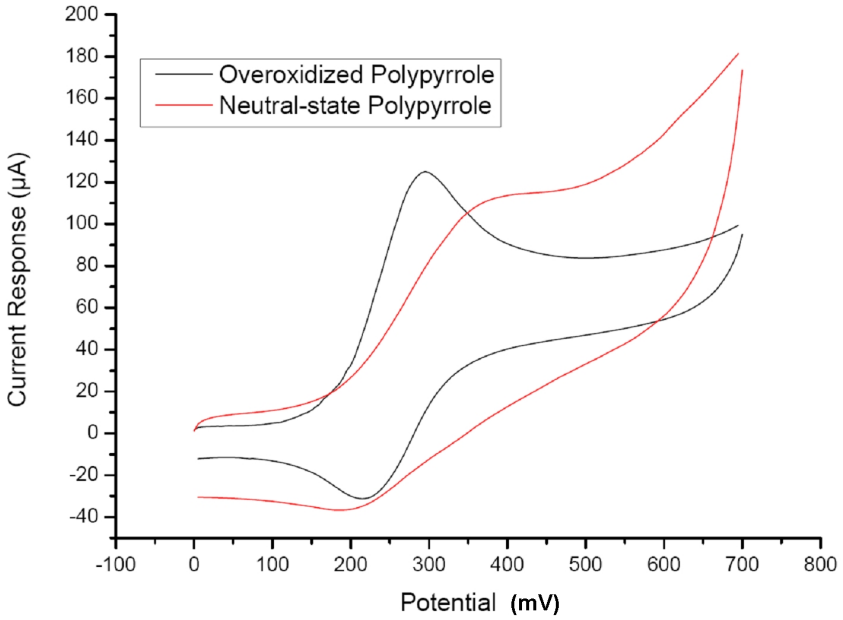

Figure 4.17: Cyclic voltammograms of a set of polypyrrole modified gold IDEs in 100 M dopamine (in PBS) before and after overoxidation. The integrated RE and CE for the IDE set were used to obtain the three-electrode configuration. The potentials were adjusted vs. gold RE and the potential sweep rate was 50 mV/s (Figure is reproduced from Publication III).

behaviour [123, 124, 125]. The presence of negative ions in the solution helps to stabilize the pyrrole radical-cation intermediate by interaction with the pyrrole rings during electropolymerization by maintaining local electroneutrality in the solvent environment [126]. Incorporating an anion in the polymer matrix therefore changes the obtained overall structure of the film; this effect increases in the case of large anions, such as DS- and polymeric PSS-. Hence, when evaluating the influence of counter ion doping on the morphology of electropolymerized PPy, two cases have to be considered: one where the dopant counter ion is a relatively small anion, as in the case of Cl-, SO_4^{2-} and PO_4^{3-}, and one where the dopant molecule is large enough to have an effect on the final polymer film morphology and thickness, as for the large anions PSS- and DS-. The calculated average thickness of the obtained PPy film in the presence of small counter-ions was 44 nm 1 nm (s.e.m.; n=24), while in the case of large counter-ions the estimated thickness was 82 nm 5 nm (s.e.m.; n=12). A larger variation in thickness was found for PPy films polymerized in the presence of large dopant counter-ions.

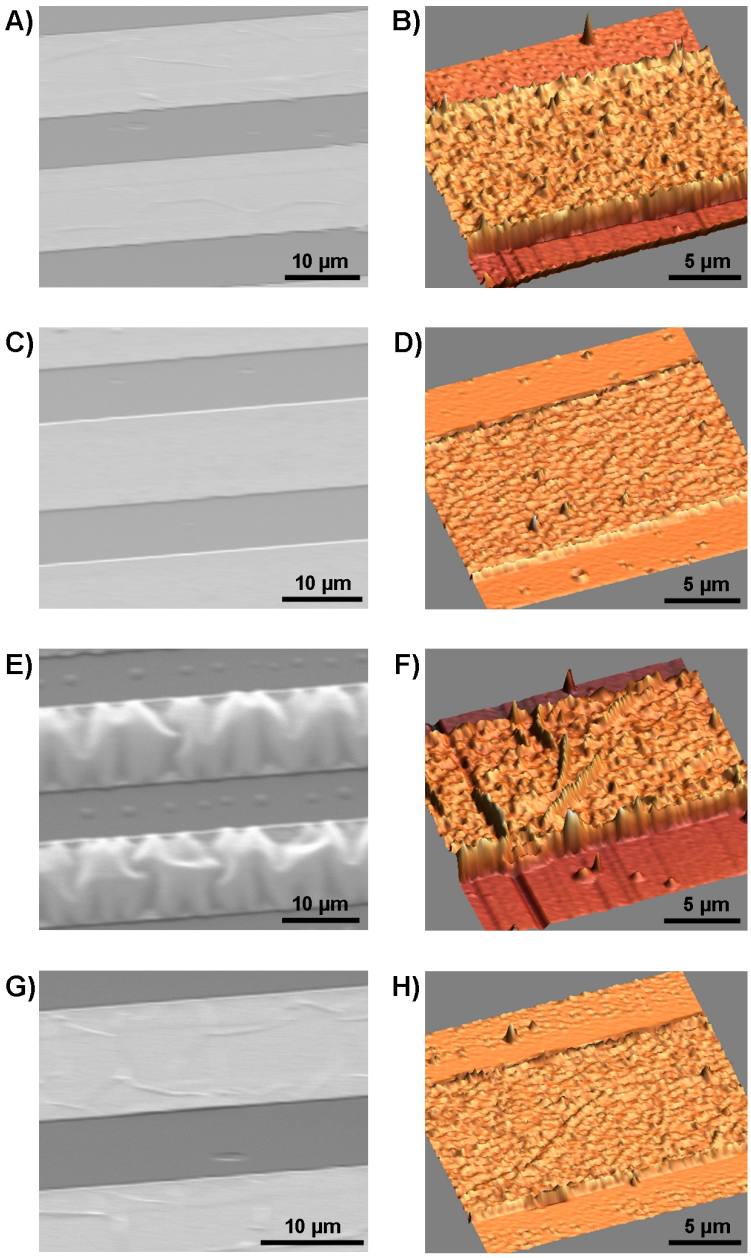

Figure 4.18: SEM (A, C, E, G) and AFM (B, D, F, H) images of electropolymerized PPy films on IDEs, showing typical morphologies for A, B) small-counter ion doped films (in this case Cl-); C, D) overoxidized small-counter ion (Cl-) doped films; E, F) large-counter ion (PSS-) doped films; G, H) overoxidized large-counter ion (PSS-) doped films (Figure is reproduced from Publication III).

The effect of overoxidation on the morphology of the polymer film created by electropolymerization can be visualized in the SEM and AFM images shown in Fig. 4.18. In the case of both small- and large counter ion doping, overoxidation of PPy results in a flattening of the film (compare Fig. 4.18A,B with 4.18C,D and Fig. 4.18E,F with 4.18G,H). The AFM images show that the flattening resulting from the overoxidation also reduces the roughness of the film, therefore affecting its porosity. Hence, even if the overoxidation yields a loss of conductivity in the film, the thinning of this film reduces the electron transfer distance between the electrochemically active analyte and the underlying gold electrode, which retains its conductive metallic properties.

Fig. 4.18 clearly illustrates the differences between the morphologies when using small and large counter ions. Small dopant ions make the resulting PPy film tightly packed onto the surface of the electrode (Fig. 4.18A,B), whereas large dopant ions render the PPy film relatively rough with a more amorphous surface (Fig. 4.18E,F). This visual investigation of the PPy surfaces can be related to differences in the calculated thickness of the PPy films doped with small and large counter ions.

The electrochemical response to dopamine of electrodes with doped overoxidized PPy films was investigated. Fig. 4.19 shows cyclic voltammograms of a 100 μM dopamine solution on gold IDEs modified with overoxidized PPy doped with the different counter ions. Evaluation of the obtained peak currents immediately leads to the conclusion that an electrode modified with a PPy film electropolymerized using large counter ions as dopants, such as DS- or PSS-, yields a significantly higher response than those having small counter ions, such as Cl-, SO_4^{2-} and PO_4^{3-}. In fact, an overoxidized PPy film doped with small counter ions has a response similar to that of a non-doped overoxidized PPy film, indicating that the small counter ions do not enhance the signal response and, therefore, neither the sensitivity of the electrodes. However, an overoxidized PPy film clearly enhances the response in comparison with the ones recorded using bare gold IDEs. This lack of difference between signals from a non-doped and a small counter ion doped PPy film can be explained by the overoxidation process, which, as mentioned above, introduces electronegative functionalities in the film. These can repel small negative counter ions entrapped in the polymer matrix, whereas large counter ions remain entrapped in the polymer film [123], further enhancing the attraction to positively charged analytes, such as dopamine.

The dopant counter ion that contributed to the highest electrode response and hence to the greatest sensitivity to dopamine in all experiments was PSS-; clear peaks could be observed in cyclic voltammograms down to dopamine concentrations in the nM range (see inset in Fig. 4.19). This electrode modification displayed

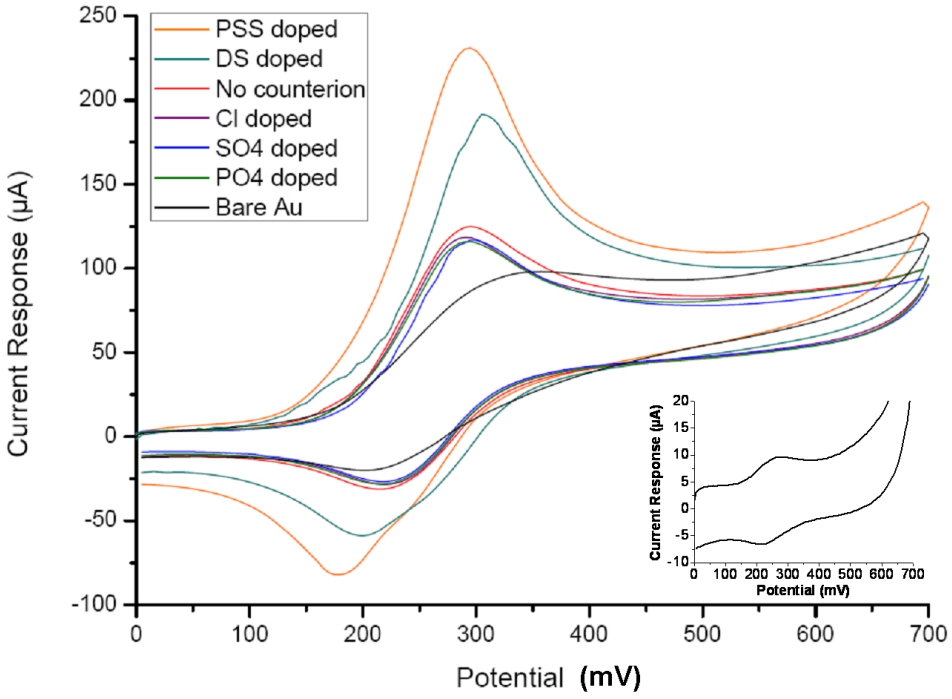

Figure 4.19: Cyclic voltammograms of 100 μM dopamine (in PBS) on sets of IDEs modified with overoxidized PPy doped with different counter ions. The integrated RE and CE for each IDE set were used to obtain the three-electrode configuration. The potentials were adjusted vs. gold RE and the potential sweep rate was 50 mV/s. Inset shows a voltammogram obtained from the overoxidized PPy/PSS modification as a response to 10 nM (Figure is reproduced from Publication III).

a sensitivity comparable to other approaches for the detection of dopamine and other chatecholamines, e.g. enzyme based modifications [127, 128, 129, 130, 131]. The observed increase in response to dopamine is related to the formation of carbonyl- and carboxylic acid functionalities, as previously pointed out [122]. The effect of these functionalities have been seen in an analogous manner in the case of thiol self-assembled monolayers (SAMs) as a modification to improve dopamine electrochemistry (thiol SAMs having a partially deprotonated carboxylic tail group, e.g., thioctic acid [132] and mercaptopropionic acid [133]. It is believed that the presence of carbonyl- and carboxylic acid functionalities orient the electroactive hydroxylic groups of dopamine molecules toward the electrode surface, in this way enhancing the oxidation of dopamine.

In the case of overoxidized PPy, an additional effect can be proposed to further

explain the observed current amplification during oxidation of dopamine. Despite the fact that the overoxized PPy film becomes morphologically flattened in comparison with the initial conducting PPy film, it is a 3-dimensional polymer network comprising carbonyl- and carboxylic acid functionalities as well as retained counter ions (PSS-) with dispersed negative charges. This structure can more effectively accommodate the diffusing dopamine in the vicinity of the electrode surface, increasing the fraction of oxidized dopamine.

Aside from simply orienting the hydroxylic groups of dopamine molecules toward the electrode surface or accommodating more dopamine molecules in the vicinity of the electrode surface, the 3-dimensional structure with dispersed negative charges can also decrease the freedom of movement of the tail of dopamine molecules with the protonated positively charged amino group. This can be seen as a combined steric and electrostatic hindrance, limiting the possibility of intramolecular cyclization, which is the prerequisite for polymerization of dopamine on an electrode surface [134]. Hence, overoxidized PPy can serve as a protection against electrode fouling that otherwise could decrease current response. However, since steric hindrance in the packing of the PPy matrix leaves uncovered areas on the electrode surface, there is, nevertheless, a possibility for electrode fouling as observed, for instance, during continued cyclic voltammetric experiments (results not shown).

Cell Culturing and Exocytosis Measurements

The cell-based experiments were conducted using rat pheochromocytoma (PC12) cells. Initially, PC12 cells were grown for 48 hours in PEI-coated (2-hour coating at room temperature using sterile filtered 50 g/mL PEI diluted in PBS followed by rinsing twice with PBS) T25 culture flasks using growth medium. 24 hours prior to seeding the cells onto an electrode chip, the growth medium was changed for the differentiation medium to initiate the cellular response to NGF. Sterilization of all microfabricated cell culture substrates and materials was done by immersing them in 0.5 M NaOH for 30 minutes followed by rinsing with PBS trice. Electrode chips were coated with laminin (20 g/mL laminin diluted in PBS) in a *Petri* dish for 2 hours to ensure cellular adhesion. Adsorption of laminin, and hence adhesion of cells, only in the central part of an electrode chip where the electrode sets are located was achieved using a hydrophobic pen. The pre-differentiated PC12 cells were rinsed with PBS and trypsinized for 5 minutes followed by 5-minute centrifugation at 850 rpm at 20 ^{o}C. The cell pellet was resuspended in the differentiation medium and the cells were seeded onto the coated electrode chips with a surface density of 105 cells/cm^2. All cell culturing and differentiation was done in an incubator at 37 ^{o}C in a humidified atmosphere of 5% CO_2/95% air. SEM

imaging of the differentiated cells was done after fixation with 2% glutaraldehyde solution diluted in PBS for 1 hour followed by rinsing with PBS (twice for 15 min) and cell culture tested water (twice for 5 min). Cell counting on microchips was done using an optical microscope equipped with a computer controlled CCD camera.

After 4 days of differentiation, the differentiation medium was replaced by the L-DOPA medium and the cells were kept in the incubator for one hour to increase the dopamine load in the vesicles [135]. Before conducting the exocytosis measurements, each electrode chip with the differentiated PC12 cells was placed in a micromilled PMMA holder to facilitate contact between the individual electrode sets and the 24-channel potentiostat with a tailor-made acquisition software [136] (see Fig. 4.16B and 4.16C). The open vial in the holder facilitated the addition of the necessary buffer solutions during exocytosis measurements. The medium was immediately replaced by 160 μL of the low K+ buffer to record a baseline for the measurements. Each array of interdigitated WEs was poised at 400 mV vs. the gold RE adjacent to the array. After a stable baseline had been recorded, exocytosis was triggered by pipetting 80 μL of the high K+ buffer directly into the vial of the PMMA holder to elevate the K+ concentration to 150 mM [137]. The current peaks corresponding to the oxidation of the dopamine released by the cells were obtained shortly after triggering the exocytosis. Recording of the exocytotic events was done simultaneously on each IDE array. Exocytosis experiments were carried out on 3 different electrode chips, each having non-modified IDE arrays and IDE arrays modified with overoxidized PSS–doped PPy. All the amperometric recordings were done at room temperatrure. All calculated results from cell-based measurements are presented +/- (s.e.m.).

100,000 cells/cm^2 was chosen as the cell density for seeding PC12 cells onto the electrode chip (seen in Fig. 4.15B) in order to facilitate differentiation for several days without reaching too high a confluency. This precaution is significant in order to allow proper formation of the characteristic axon-like outgrowths. As shown in Fig. 4.20A, the PPy electrode modification did not hinder proper cell differentiation. Since PC12 cells require an adhesion factor on a growth substrate, the PPy-modified electrodes were coated using physisorbed laminin, which has been shown to provide good differentiation for different cell types, including neurons and PC12 cells [138]. A PC12 cell population differentiating on one set of IDEs can be seen in Fig. 4.20B. The PC12 cells extended the axon-like outgrowths on the IDEs, seemingly preferring the modified electrode surface to the rest of the chip (see Fig. 4.20C). Cells on the laminin modified electrodes showed the typical cell adhesion, differentiation morphology and confluency expected for PC12 cells [18]. This electrode configuration is optimal for accommodating the axon-like out-

growths when monitoring release of neurotransmitters from a whole population of differentiating cells.

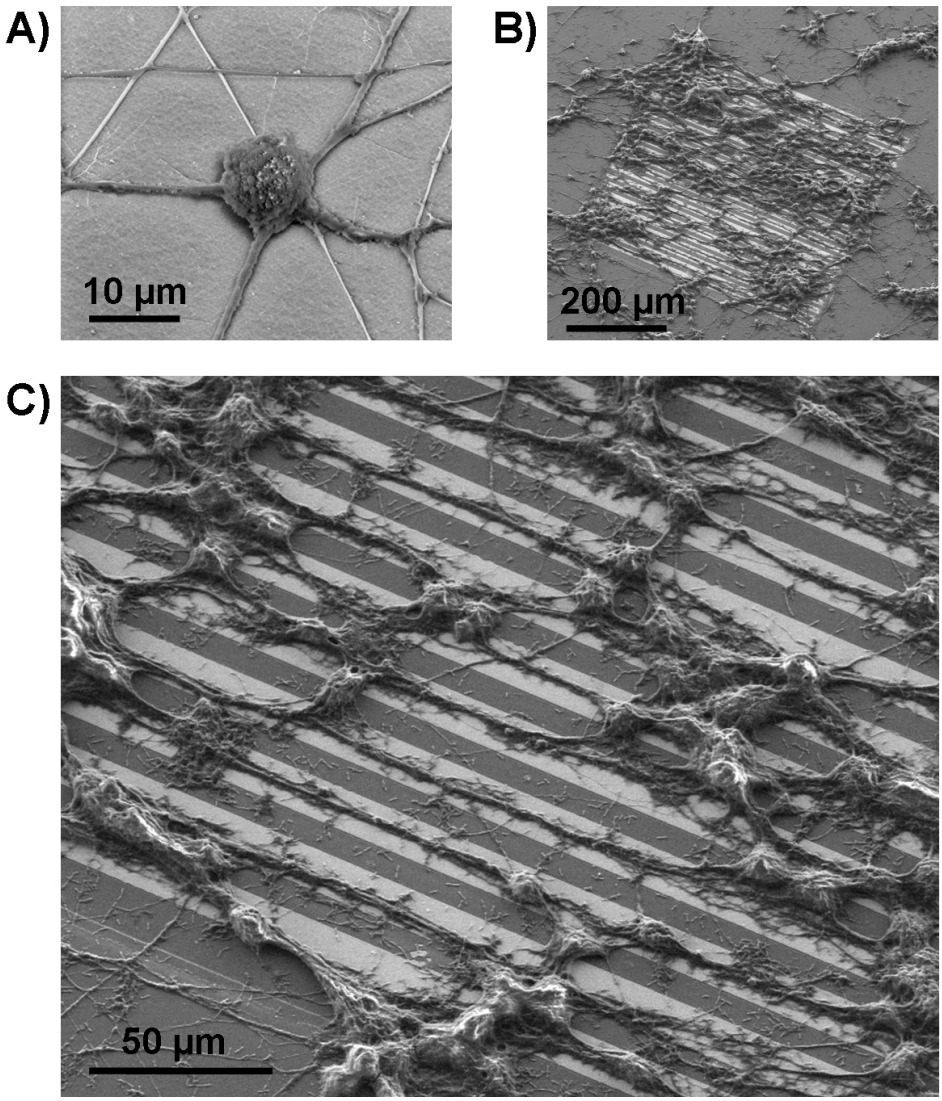

Figure 4.20: SEM images of differentiated PC12 cells on PPy-modified electrodes showing A) a single PC12 cell, B) a population of PC12 cells and C) a magnified view of the cell population in B (Figure is reproduced from Publication III).

Fig. 4.21 depicts amperometric current-time traces generated on IDEs during a measurement, as well as the baseline for a control measurement where no cells were present on the IDE. As expected, the amplitude of the recorded current generated

by dopamine oxidation on an IDE modified with overoxidized PSS- doped PPy (PPy/PSS) was significantly higher than that obtained on a bare gold IDE. In detection of single vesicle exocytotic events, various parameters can be extracted from recorded current-time traces (spikes), such as the integrated area of the current spikes (the charge Q yielding the amount of molecules released during each event), the maximum oxidation current, half-width, and the rise-time [139]. In measurements of dopamine release from a cell population, the recorded current-time traces are composed of a large number of superimposed single vesicle events. In this case, the most significant parameter is the total charge, which, in an analogous manner as in the case of single vesicle measurements, is proportional to the detected amount. The average generated charge on bare gold IDEs having an average cell population of 217 +/- 5 cells (s.e.m.; n=10) (based on visual counting under microscope) was 8.7 nC +/- 0.6 nC (s.e.m.; n=5), while on PPy/PSS modified IDEs, having cell populations of the same order as on bare gold IDEs, the average generated charge was 23 nC +/- 2 nC (s.e.m.; n=5).

The different charges generated on bare gold IDEs and PPy/PSS modified IDEs upon dopamine detection do not, however, mean that the cells residing on bare gold electrodes and PPy/PSS modified electrodes released different amounts of dopamine. Instead, the PPy/PSS modified IDEs show an increased sensitivity to dopamine, indicating 2.6-fold amplification. This is in accordance with the value previously published for PPy modified CFMEs [122]. It is significant to point out that measurements conducted on bare electrodes and PPy/PSS modified electrodes are not directly comparable since, for a cell population of the same dimension, different level of charge is being recorded. On the other hand, the increase in detection sensitivity makes the electrode modification highly suitable for monitoring dopamine release under conditions, where very small changes need to be detected, such as in vivo monitoring of the dynamics of dopamine release in the rat brain [122] and characterization of conditions leading to differentiation of neural stem cells to dopaminergic neurons [140, 141].

The results presented in this paper highlight the novelty of overoxidized PPy as an electrode modification for detection of cellular dopamine release. The modification is readily prepared, resulting in a reproducible electrode behaviour and improves the capability to monitor small amounts of released molecules. Furthermore, the modification is stable under cell culture conditions for long-term experiments and shows no adversary effects on the differentiated cells.

Although PSS- as the dopant clearly provided the highest amplification in dopamine detection, the results obtained in this work when using DS- as the dopant also indicated amplification. This is in accordance with the previously published findings [142]. However, the dimension of the DS- ion is very critical. Due to its size it

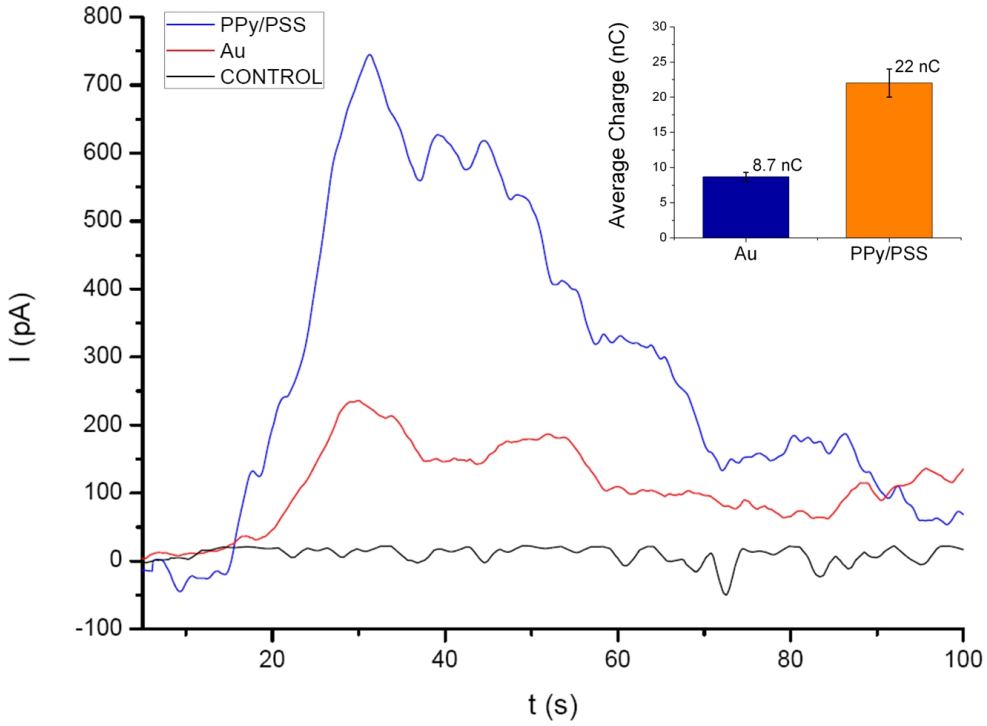

Figure 4.21: Typical amperometric current-time traces, corresponding to dopamine release from differentiating PC12 cells, obtained during an exocytosis measurement on a bare gold IDE (red line, Au) and on an IDE modified with PSS–doped overoxidized PPy (blue line, PPy/PSS). The black line (CONTROL) corresponds to the signal recorded on an IDE without PC12 cells. Inset shows the average charge accumulated during measurements on non-modified (Au) and modified IDEs (PPy/PSS). The error bars represent s.e.m. (n = 5) (Figure is reproduced from Publication III).

can be retained in the overoxidized PPy film but has an increased possibility to leak out during long-term experiments, which can cause harmful effects on the cultured/differentiated cells. This was indicated as decreased and irreproducible cellular dopamine release (results not shown). Hence, for reliable application of overoxidized PPy as an electrode modification for monitoring cellular dopamine release, PSS- is considered the optimal dopant of those tested in this work during PPy electropolymerization."

4.2.4 Summary

This section described the experimental work carried out regarding the electropolymerization of ICPs onto relevant structures and electrodes for cellular sensing platforms.

The electropolymerization of aniline was utilized as a mean to validate a specific step of the microfabrication process behind 3D nanostructures intended for tissue and cellular measuring of relevant analytes, particularly the removal of the silicon nitride passivation layer from the active parts of the electrodes. The PAni electrodeposition not only showed that the nitride etching step did indeed work as predicted, but it also illustrated how the electropolymerization of ICPs can be used on 3D nanostructures, opening up possibilities for selective, facile functionalizations of the pillars. As discussed previously, this technique can in fact be used to entrap relevant biosensing elements onto the 3D pillar (e.g. enzymes, antibodies), or even drugs that could in future works be delivered inside mammalian cells.

An electrode modification for dopamine detection based on an electropolymerized polypyrrole film onto planar electrodes was also presented. The study included an investigation of the consequences of overoxidation of the conducting polymer film, which proved to enhance the electrochemical behaviour of the sensor. A detailed survey of the effects brought about by counter ion doping on the overoxidized PPy film allowed for the selection of an optimal dopant for better sensitivity of the electrode towards dopamine. The optimized electrode modification, a potentiostatically electropolymerized PPy thin film doped with polystyrene sulfonate and subsequently overoxized, was utilized on microfabricated interdigitated electrodes to amperometrically detect dopamine released from populations of differentiated PC12 cells upon triggering exocytosis with an elevated K+ concentration. The modification presented in this work resulted in an amplification of the current signal by a factor of about 2.6 in comparison with non-modified gold electrodes. The optimized and characterized electrode modification presented in this work provides the basis for future biological studies on, for instance, characterization of neural stem cell differentiation to dopaminergic neurons.

Chapter 5

Peptide/Polymer Sensor Systems

This chapter is a discussion on how the two main material types investigated in this PhD work, i.e. PNWs and ICPs, can be combined for the development of dopamine detection in cellular sensing. The sensitivity towards dopamine achieved by the conducting polymer modifications can be applied in sensor platforms which include the advantages brought by self-assembled peptide nanostructures, opening up the electrochemical sensor to new functionalities and sensing possibilities.

This chapter is divided in two main sections, each related to a different polymerization method. The first experimental investigation discussed is based on the chemical polymerization of polypyrrole (see section 4.1) onto patches of peptide nanowires (see chapter 3). The second section of this chapter deals with a combination of doped polypyrrole electrode modification (see section 4.2) with electrode-aligned patterned strips of peptide nanowires (see section 3.3).

5.1 Experimental: Chemically Polymerized PPy on PNWs

This work is an investigation of a chemical polymerization method to coat the PNWs with a conductive material in order to use them in an electrochemical dopamine sensor. Polypyrrole was deposited onto peptide nanowires to create hybrid structures (PNW/PPy) onto gold electrodes that were characterized via cyclic voltammetry. Amperometric detections of dopamine give insights about the sensitivity of this electrode modification. This work is presented in Publication II, and the details about the materials and methods can be found in Appendix C.2.

PNWs were grown onto commercial gold electrodes with the protocols described in section 3.2.2, with diphenylalanine solution concentrations in the range of 0.05-25 mg/mL. Changing this concentration affects the packing density of the nanowires after the aniline vapor treatment. The electrochemical behavior of PNW modified Au electrodes was carried out via amperometric detection of hydrogen peroxide, in order to choose the peptide concentration which gives the highest current response. Subsequent additions of 30 % H_2O_2 resulted in stepwise current increases, which were then compared between peptide concentrations.

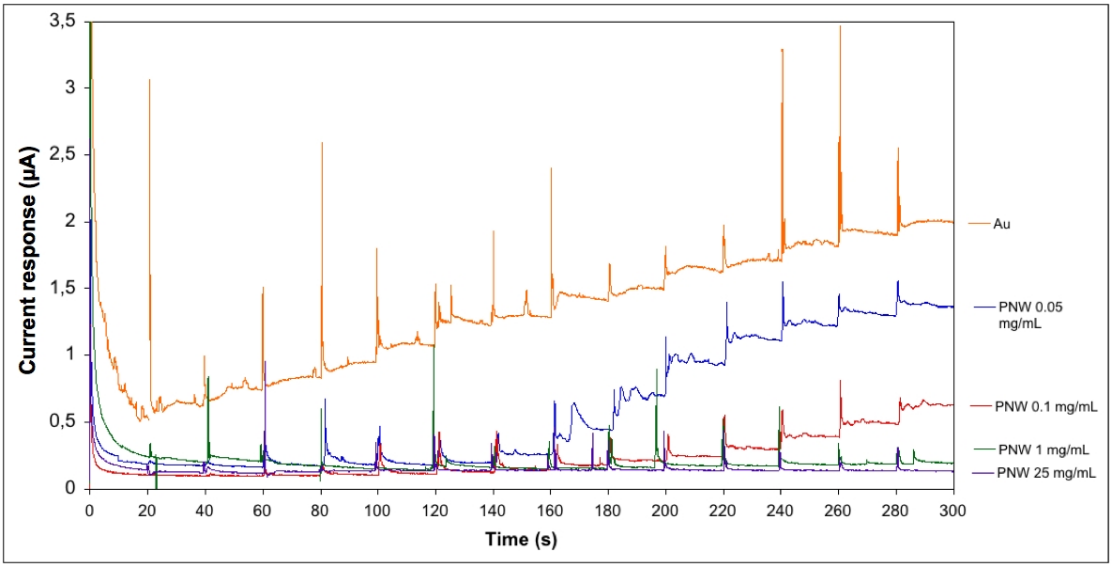

Figure 5.1: Amperometric measurements of the PNW modified gold electrodes at 600 mV versus Ag/AgCl in 0.1 M KCl with subsequent additions of hydrogen peroxide (30 wt %) every 20 seconds. The different curves correspond to different concentrations of diphenylalanine solution in HFP used for the modification. The spikes correspond to the addition points (Figure is reproduced from Publication II).

As can be seen from the amperometric current traces in Fig. 5.1, there is a clear decrease in current response with increasing packing density of the PNWs (dictated by the concentration of diphenylalanine solution). This was expected, since lower concentrations result in a lesser number of PNWs covering the conductive electrode surface, therefore leaving more electrode areas exposed for electron transfer, while a large number of PNWs blocks the active electrode surface.

Chemical polymerization of pyrrole that followed protocols similar to those discussed in section 4.1.2 was applied to the Au/PNW electrodes, to achieve a PPy film coating the PNWs. This combination was tested in hope of increasing the possibility of charge transfer in the electrode/electrolyte interface by taking advan-

tage of the intrinsic conductive properties of polypyrrole. An SEM investigation allowed to observe the morphology of the polymer film on the PNWs (see Fig. 5.2). A clear difference can be seen on the PNWs' side walls, with the PPy causing a rough surface marked by irregularities, e.g. polymer agglomerates, onto the otherwise smooth surface of the PNWs (compare to Fig. 3.3). These results can be compared to similar work on PNW coating with another conductive polymer, polyaniline, where the presence of the conducting polymer was used to make these otherwise insulating structures conductive [143].

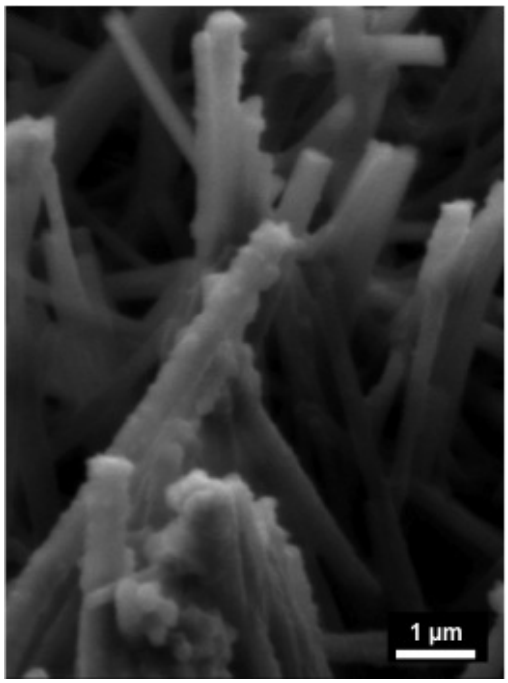

Figure 5.2: Low-vacuum SEM image of PNWs after the PPy film coating (Figure is reproduced from Publication II).

The electrochemical activity of the PPy coating on the Au/PNW electrodes was characterized by cyclic voltammetry in 0.1 M KCl. Fig. 5.3 shows voltammograms obtained for several potential sweep rates. The current peaks seen in the CVs reflect the oxidation and reduction of polypyrrole [104]. This is a case where only the gold electrode underneath is considered the working electrode, and the polypyrrole film coating with the KCl solution dissolved throughout its pores is considered the electrolyte. The current peak heights were found proportional to the square root of the potential sweep rates, showing signs of reversibility. The peak potential, though, shifts with increasing potential sweep rate, meaning that the electrode can be considered to have a pseudo-reversible behavior. The anodic and cathodic peaks are also not of the same amplitude, and this can be blamed on

the overoveroxidation of polypyrrole film (coated in its neutral state) that happens while conducting the experiments. After the anodic sweep, not all the oxidized PPy film is able of being reduced back, since overoxidation is not reversible. The inset in Fig. 5.3 shows a cyclic voltammogram of the Au electrode modified with PNWs alone (Au/PNW), reflecting the blocking behavior of the PNWs, as discussed previously.

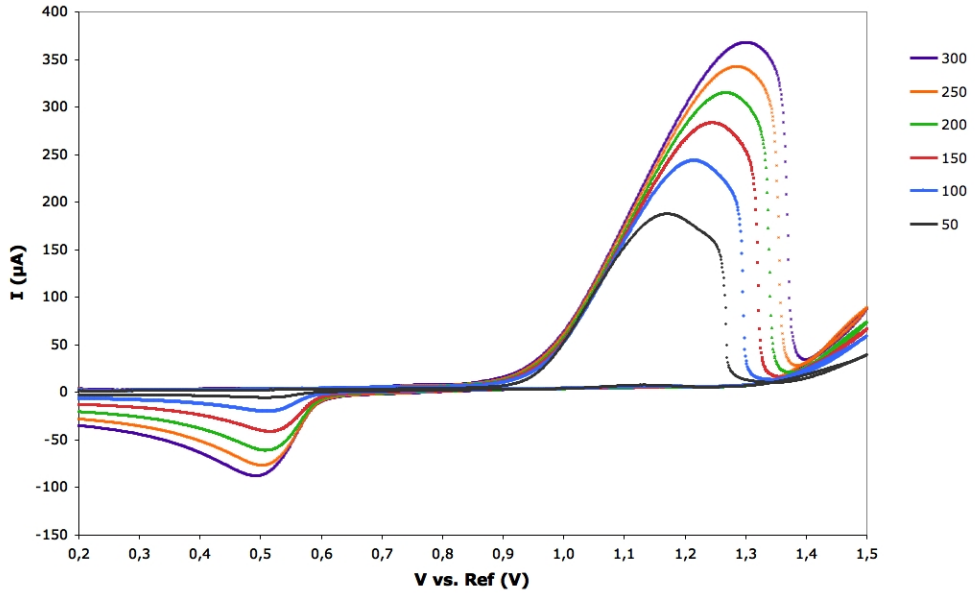

Figure 5.3: Cyclic voltammograms of PNW/PPy modified gold disk electrodes in 0.1 M KCl versus a Ag/AgCl (3 M KCl) reference electrode at potential scan rates of 50, 100, 150, 200, 250 and 300 mV/s. Inset: control CV of PNW modified gold disk electrode in 0.1 M KCl versus a Ag/AgCl (3 M KCl) reference electrode at 200 mV/s (Figure is reproduced from Publication II).

The Au/PNW/PPy electrodes were used in amperometric dopamine measurements. The electrodes were subjected to pipetted additions of dopamine and the current recorded was measured and plotted against dopamine concentration ranging between 2.4 and 4.1 μM see Fig. 5.4. Two main regions can be seen in the plot: a horizontal range where increasing the dopamine concentration does not results in a current increase, and a linear range where the current signal increases linearly with dopamine concentration. The detection limit was calculated using relevant statistical analysis, by defining it as the analyte concentration where the current signal is equal to the blank signal plus 3 times the standard deviation of the blank [144]. The detection limit obtained was 3.1 μM, reflecting the lowest concentration of dopamine that can be detected with this sensor system. This value is comparable to the that of dopamine detection systems using enzymes [145] or

CMOS detection [146], and is in the relevant concentration range present in other *in vivo* systems [147].

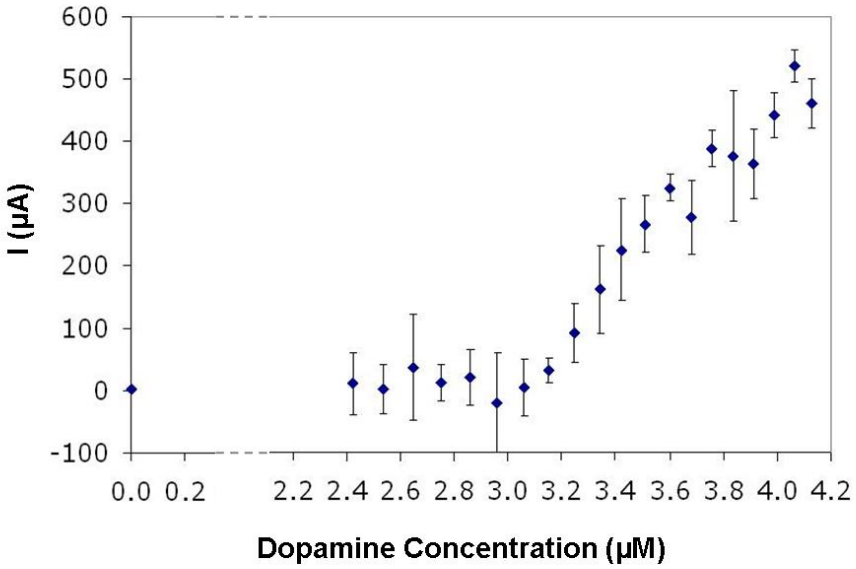

Figure 5.4: Plot of average current signals versus dopamine concentrations for amperometric responses of the Au/PNW/PPy at different dopamine concentrations. Error bars denote standard deviation of measurement.

5.2 Experimental: Electropolymerized Doped PPy on Patterned PNWs on Interdigitated Microelectrodes

This section presents the work carried out at the end of the project aiming at combining the patterning method for creating PNW strips onto microfabricated gold IDEs modified with overoxidized doped polypyrrole for the detection of dopamine from cellular release. The idea is to utilize the conducting polymer modification developed and the sensitivity that it provides towards dopamine in a platform that places the sensors in close vicinity of the peptide structures with the biocompatibility and functionalization potential that they provide to the system.

The soft-lithography technique described in section 3.3.2 was applied to the IDE chips used in section 4.2.3, resulting in PNW strips in between electrodes, in the non-active areas of the working electrode in the set (see Fig. 5.5). A careful alignment was done in an optical microscope to overlap the relevant areas of the electrode chip substrate and the PDMS mold used for the patterning of the diphenylalanine solution (again, see section 3.3.2).

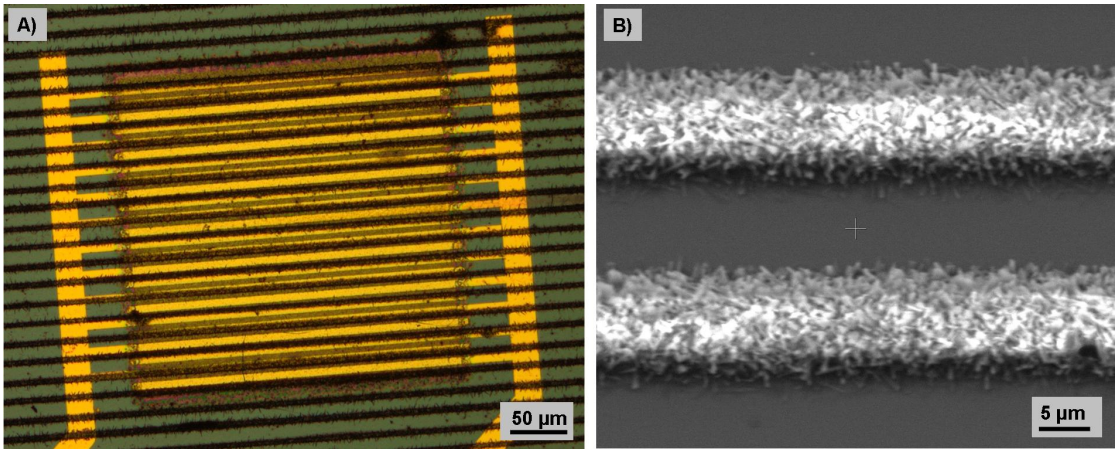

Figure 5.5: A) Optical image of PNW strips patterned onto an IDE, patterned to be in between the active electrodes. B) SEM image of pattrned PNW strips of the same dimensions.

After the patterned PNW growth, the PSS- doped polypyrrole modification developed during the project was applied to the active electrode areas, using the same protocols as described in section 4.2.3. The same PMMA holder was used to seed and culture differentiated PC12 cells on the PPy modified electrodes with PNW strips around them. A laminin coating was applied to the sensor platform due to

the findings from the cell growth and behavior studies on patterned PNWs (see section 3.3.2).

Once a differentiated PC12 population was present on the sensor platform, after incubation in L-Dopa medium (see protocols for cell culturing in Appendix C.3), exocytosis was triggered chemically and the dopamine release from cells was measured by amperometry. The experimental results showed typical amperometric current-time traces following the forms discussed in section 2.2.2, with a peak after the addition of the chemical triggering solution of high KCl concentration, reflecting the oxidation of dopamine coming from the cells upon chemical triggering (see Fig. 5.6).

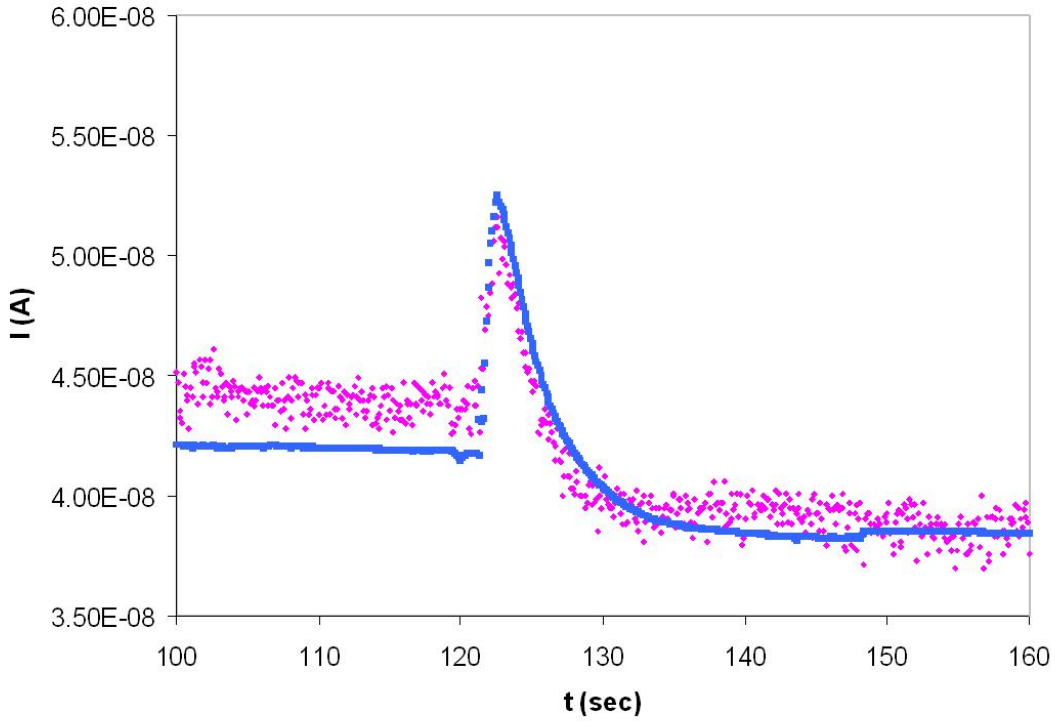

Figure 5.6: Amperometric current-time traces corresponding to dopamine release from a population of differentiated PC12 cells, obtained during an exocytosis measurement on PSS-doped overoxidized PPy sets of IDEs with patterned PNWs present in between the active electrodes. The two curves refer to two separate IDE sets used simultaneously in the same experiment.

When compared to the amperometric current traces obtained for the case of the PPy modification without the patterned PNWs (see section 4.2.3), these curves show a higher current peak amplitude denoted by a sharper rising of the peak

before reaching its maximum value. Speculations can be made about the PNWs' role in this electrochemical sensor system, particularly about the retainment of the dopamine molecules in vicinity of the electrode surface after the exocytosis event, resulting in a higher local dopamine concentration at the electrode surface. This would mean that the PNWs not only add functionalization possibilities and biocomparability properties to the sensor platform, but they also positively affect the sensitivity of the electrochemical sensor.

5.3 Summary

This chapter provided examples of how to combine the two main material types studied during the project: ICPs and PNWs.

The first section of this chapter has shown how PNWs can be coated with a conductive polymer film to increase their possibility for application in electrochemical sensors. The investigation of the Au/PNW/PPy electrodes' electrochemical behavior showed that this modification can be used for dopamine detection, reaching detection limits relevant to the application. This example of a sensor assembly can be used to tune the detection towards other relevant redox species such as other neurotransmitters.

The second section presented a method for microfabricated electrode surface modifications that combines the signal amplification resulting from the doped polypyrrole deposited via electropolymerization with the advantages of retaining peptide nanostructures in the vicinity of the electrodes, patterned by soft-lithography. With the functionalization techniques presented earlier in the thesis, the PNWs allow for the introduction of relevant biological molecules needed for the cell culturing or the sensing. For example, attaching nutrients or growth factors to the PNWs could yield a way to culture or differentiate the stem cells prior to the dopamine detection without the need for replacing the medium so often (although gas concentrations and acidification of the medium would need to be taken into account). This could give substantial advantages in microfluidic cell culturing platforms, where the medium replacement requires complicated microchannel designs and often results in the formation of air bubbles or other factors that affect the biological behavior of the system.

Chapter 6

Conclusions

The major aim of this project was to investigate novel materials for use in a cell culturing and sensing platform for the study of cellular dynamics upon interaction with nanostructures. The two main material types investigated were (1) biological nanostructures to provide a functionalizable and *in vivo*-like substrate for the cell culturing and (2) conducting polymers to improve the sensitivity of microelectrodes towards specific analytes relevant to the cellular dynamics studies, with focus on dopamine detection from differentiated neuronal stem cells.

Self-assembled peptide nanowires were grown vertically from flat surfaces to create a 3-dimensional biological substrate for the cell culturing. Various functionalization methods were developed for the attachment of key functional molecules and chemical groups to the surface of the PNWs. A biotin-streptavidin conjugate functionalization was achieved, opening up the possibility of decorating the PNWs with many components that could be linked *a priori* with the streptavidin, with an example of using this method for fluorescent molecules and gold nanoparticle attachment to the PNWs. A functionalization with thiol groups via *Traut's reaction* was also presented as yet another method for decorating the nanowires. *In vitro* studies of cell behavior upon culturing on a PNW surface and a comparison of the PNWs with an adhesion promoter protein coating showed that these nanostructures do not hinder cell growth, adhesion or differentiation of PC12 cells. A technique for patterning the PNWs into micron sized stripes via soft-lithography was developed, and an *in vitro* study of cell behavior on patterned PNW surfaces resulted in the development of suitable conditions for the growth. An *in vivo* investigation of the use of PNWs as a coating for implantable electrodes showed the effect of these structures on brain tissue after removal of the electrode after 12 weeks of implantation in a live animal.

Conducting polymers were used for developing a sensor modification to increase sensitivity towards dopamine. A chemical polymerization method was utilized to aid the microfabrication of out-of-plane structures, dismissing limitations of the metallization process of the 3-dimensional side walls and increasing the overall conductivity of the electrode structure, taking advantage of the intrinsic properties of the conducting polymer. Electrochemical polymerization was also used for electrode enhancement. After showing how this conducting polymer deposition technique can aid in the design of microfabrication processes, a thorough electrochemical investigation of the embedment of counter-ion dopants in an electropolymerized polypyrrole matrix showed the optimal parameters and dopant to be used for an increase in sensitivity towards dopamine, with detections down to a dopamine concentration of 10 nM. A modification of interdigitated microelectrodes with overoxidized PSS- doped polypyrrole yielded the highest electrochemical sensitivity towards dopamine. *In vitro* amperometric measurements of dopamine released from PC12 cells cultured on a microchip with the optimal electrode modification showed a signal amplification of 2.6 fold upon chemical exocytosis triggering of the cells.

The last chapter of this thesis discusses methods that can be used for combining the two main materials for surface modifications investigated in the project. A chemical polymerization coating on a PNW surface showed a signal response with a minimum detection limit of 3.1 μM, a value comparable to physiological dopamine concentrations. A second combination was also presented, showing the overoxidized PSS- doped polypyrrole modification on interdigitated electrodes with patterned stripes of PNWs around the electrochemical sensing areas, and *in vitro* dopamine detection upon PC12 exocytosis experiments was carried out to show how this combination can be used of cellular sensing.

6.1 Perspectives and Final Remarks

The work presented in this thesis shows an investigation of 2 main material types for the use in cellular nanosensors, but this study is by no means complete, as is the case of any research project, and more work can always be done to increase the value of the findings discussed in this document.

Any cell biologist reading this thesis will probably have issues with the way that *biocompatibility* has been referred to throughout the chapters. This is a very touchy subject for anyone working in this extremely interdisciplinary field, since when the ambiguous term *biocompatible* is used, it is often misused by scientists with a technical background and the concept behind the use of the term is misunderstood by biologists. In order to fully take use of this term and not treat it as a taboo, there is an international standard series of evaluations to truly validate the biocompatibility of a material, the *ISO 10993* set [148]. This standard set of evaluations gives a thorough and precise guideline for biocompatibility. These tests are expensive and require specific training in the field, and were behind the scope of this PhD work. As a first outlook for continuation of the work presented in this thesis, then, it would be important to run the necessary tests to "officially" call these materials *biocompatible* before continuing their use in cellular studies.

Aside from this, the topic discussed in this thesis that requires the most further in-depth investigation is the functionalization of the PNWs. I have shown how to attach various kinds of molecules and chemical groups to the surface of the peptide nanostructures, but no relevant complete functionalization was carried out that was immediately applicable to cellular studies. There are many paths that this research could take, especially when thinking of the last combination of materials presented, with the patterned PNWs in the vicinity of the conducting polymer modified IDEs for cellular exocytosis experiments. For example, a functionalization with an enzyme or some other kind of catalyst for the redox reactions of cellular analytes could further increase the sensitivity of the electrochemical sensor towards that specific analyte, since the PNWs, and therefore the functionalization, is present near the electrodes. Another option could be to attach nutrients or even growth factors that are usually present in the medium to the PNWs on the cell culturing substrate, in order to (i) limit the medium change which is often a problem in microfluidic platforms and (ii) to use the patterning advantages to obtain different kind of differentiations by the same stem cells on the same culturing substrate, therefore obtaining arrays of cellular studies in the same sample.

When it comes to the conducting polymer work, even though a reliable modification was developed for the detection of dopamine from *in vitro* exocytosis, the

stability of this sensor system needs to be investigated further and possibly improved. There are several effects that were observed during experiments but not further investigated, such as electrode fouling or polymer film stability, that could deserve a more in-depth study. A full amperometric calibration of this system could also be carried out, in order to gain comparable insights between the detected current signal (and therefore accumulated charge on the electrodes), which can be by Faraday's Law translated directly into the amount of dopamine detected, and the actual dopamine released from the cells. This sort of study can also give a deeper understanding of the mechanism behind the signal amplification given by this modification. A similar modification could additionally be developed to increase sensitivity towards other relevant cellular analytes than dopamine. This way, the localized deposition offered by the electropolymerization technique could be taken into consideration, to include several modifications onto the same microchip, for the creation of a multianalyte cellular sensing platform.

All in all, this thesis gives enough of a basis for continuing the work in the ways discussed as well as other research lines. Additionally, this document could also be taken as an example for a similar investigation of other material types, with the aim of producing standard material characterization methods for application in cellular sensing or similar fields.

References

[1] T. Haruyama. Micro- and nanobiotechnology for biosensing cellular responses. *Advanced Drug Delivery Review* **55**, 393-401 (2003).

[2] Kshitiz, D.-H. Kim, D.J. Beebe, A. Levchenko. Micro- and nanoengineering for stem cell biology: the promise with a caution *Trends in Biotechnology* **29**, 399-408 (2011).

[3] S. Kaur, B. Singhal. When nano meets stem: The impact of nanotechnology in stem cell biology. *Journal of Bioscience and Bioengineering* **113**, 1-4 (2012).

[4] S. Carrara. Nano-Bio-Technology and Sensing Chips: New Systems for Detection in Personalized Therapies and Cell Biology. *Sensors* **10**, 526-543 (2010).

[5] N. Rozlosnik. New directions in medical biosensors employing poly(3,4-ethylenedioxy thiophene) derivative-based electrodes. *Analytical and Bioanalytical Chemistry* **395**, 637-645 (2009).

[6] K.Ø. Andresen, M. Hansen, M. Matschuk, S.T. Jepsen, H.S. Sørensen, P. Utko, D. Selmeczi, T.S. Hansen, N.B. Larsen, N. Rozlosnik, R. Taboryski. Injection molded chips with integrated conducting polymer electrodes for electroporation of cells. *Journal of Micormechanics and Microengineering* **20**, 055010 (2010).

[7] K. Kiilerich-Pedersen, C.R. Poulsen, T. Jain, N. Rozlosnik. Polymer based biosensor for rapid electrochemical detection of virus infection of human cells. *Biosensors & Bioelectronics* 28, 386-392 (2011).

[8] R.M. Wightman, L.J. May, A.C. Michael. Detection of Dopamine Dynamics in the Brain. *Analytical Chemistry* **60**, 769A-779A (1998).

[9] C. Revenu, R. Athman, S. Robine. The co-workers of actin filaments: from cell structures to signals. *Nature Reviews Molecular Cell Biology* **5**, 1-11 (2004).

[10] A.E. Berman, N.I. Kozlova, G.E. Morozevich. Integrins: Structure and signaling. *Biochemistry* **68**, 1284-1299 (2003).

[11] A. Gossler, T.C. Doetschman, H. Eistattaer, M. Katz, W. Schmidt, R. Kemler. Transgenesis by means of Blastocyst Derived Embryonic Stem Cell Lines. *Proceedings of the National Academy of Science, USA* **83**, 9065-9069 (1986).

[12] J. McNeish. Embryonic Stem Cells in Drug Discovery. *Nature Reviews Drug Discovery* **3**, 70-80 (2004).

[13] Y. Tomozawa, N. Sueoka. In vitro segregation of different cell lines with neuronal and glial properties from a stem cell line of rat neurotumor RT4. *Proceedings of the National Academy of Science, USA* **75**, 6305-6309 (1978).

[14] A. Villa, J.F. Rubio, B. Navarro, C. Bueno, A. Martinez-Serrano. Human neural stem cells in vitro. A focus on their isolation and perpetuation. *Biomedicine & Pharmacotherapy* **55**, 1-5 (2001).

[15] A. Martinez-Serrano, F.J. Rubio, B. Navarro, C. Bueno, A. Villa. Human Neural Stem and Progenitor Cells: In vitro and in vivo properties, and potential for gene therapy and cell replacement in the CNS. *Current Gene Therapy* **1**, 279-299 (2001).

[16] A. Villa, A. Martinez-Serrano. Strategies for the generation of human dopaminergic neurons that could be used in the clinics: Scientific and bio-ethic implications. *Journal of the International Society of Bioethics (SIBI)* **8**, 71-82 (2002).

[17] R. Levi-Montalcini. The Nerve Growth Factor: thirty-five years later. *Nobel Lecture* 349-369 (1986).

[18] L.A. Greene, A.S. Tischler. Establishment of a noradrenergic clonal line of rat adrenal pheochromocytoma cells which respond to nerve growth factor. *Proceedings of the National Academy of Science, USA* **73**, 2424-2428 (1976).

[19] R.H.S. Westerink, A.G. Ewing. The PC12 cell as model for neurosecretion. *Acta Physiologica (Oxf.)* **192**, 273-284 (2008).

[20] F. Hefti, J. Hartikka, M. Schlumpf. Implantation of PC12 cells into the corpus striatum of rats with lesions of the dopaminergic nigrostriatal neurons. *Brain Research* **348**, 283-288 (1985).

[21] P. Aebischer, M. Goddard, A.P. Signore, R.L. Timpson. Functional Recovery in Hemiparkinsonian Primates Transplanted with Polymer-Encapsulated PC12 Cells. *Experimental Neurology* **126**, 151-158 (1994).

[22] D. Knight, P.F. Baker. Calcium-dependence of catecholamine release from bovine adrenal medullary cells after exposure to intense electric fields. *Journal of Membrane Biology* **68**, 107-140 (1982).

[23] B. Katz. On the quantal mechanism for neural transmitter release. *Nobel Lecture* 485-492 (1970).

[24] R.M. Wightman, C.L. Haynes. Synaptic vesicles really do kiss and run. *Nature Neuroscience* **7**, 321-322 (2004).

[25] J.M. Finnegan, K. Pihel, P.S. Cahill, L. Huang, S.E. Zerby, A.G. Ewing, R.T. Kennedy. Vesicular quantal size measured by amperometry at chromaffin, mast, pheochromacytoma, and pancreatic beta-cells. *Journal of Neurochemistry* **66**, 1914-1923 (1996).

[26] L.M. He, L.G. Wu, The debate on the kiss-and-run fusion at synapses. *Trends in Neuroscience* **30**, 447-455 (2007).

[27] T.L. Schwarz. Release of neurotransmitters, in: L. Squire, D. Berg, F.E. Bloom, S. du Lac, A. Ghosh, N.C. Spitzer (Eds.). *Fundamental neuroscience, 3rd edition.* Academic Press, San Diego, pp. 157-180 (2008).

[28] M. Velasco, A. Luchsinger. Dopamine: pharmacologic and therapeutic aspects. *American Journal of Therapeutics* **5**, 37-43 (1998).

[29] J. Jankovic. Parkinson's disease: clinical features and diagnosis. *Journal of Neurology, Neurosurgery & Psychiatry* **79**, 368-376 (2008).

[30] J.-M. Beaulieu, R.R. Gainetdinov. The physiology, signaling, and pharmacology of dopamine receptors. *Pharmcological Reviews* **63**, 182-217 (2011).

[31] E.N. Pothos, V. Davila, D. Sulzer. Presynaptic recording of quanta from midbrain dopamine neurons and modulation of the quantal size. *Journal of Neuroscience* **18**, 4106-4118 (1998).

[32] L.J. Wallace, R.M. Hughes. Computational analysis of stimulated dopaminergic synapses suggests release largely occurs from a single pool of vesicles. *Synapse* **62**, 909-919 (2008).

[33] International Union of Pure and Applied Chemistry (IUPAC), *http://www.iupac.org*.

[34] A.J. Bard, L.R. Faulkner. *Electrochemical Methods: Fundamentals and Applications* (2nd Ed.), Hoboken, NJ, USA, John Wiley & Sons (2001).

[35] Southampton Electrochemistry Group. *Instrumental Methods in Electrochemistry*, Chichester, UK, Horwood Publishing (1985).

[36] R.M. Wightman, J.A. Jankowski, R.T. Kennedy, K.T. Kawagoe, T.J. Schroeder, D.J. Leszczyszyn, J.A. Near, E.J. Diliberto, O.H. Viveros. Temporally resolved catecholamine spikes correspond to single vesicle release from individual chromaffin cells. *Proceedings of the National Academy of Science, USA* **88**, 10754-10758 (1991).

[37] W.-L. Yeh, Y.-R. Kuoa, S.-H. Cheng. Voltammetry and flow-injection amperometry for indirect determination of dopamine. *Electrochemistry Communications* **10**, 66-70 (2008).

[38] N.J. Ke, S.-S. Lu, S.-H. Cheng. A strategy for the dermination of dopamine at a bare glassy carbon electrode: p-phenylenediamine as a nucleophile. *Electrochemistry Communications* **8**, 1514-1520 (2006).

[39] C.H. Görbitz. Theoretical basis of biological self-assembly. In: J. Castillo-León, L. Sasso, W.E. Svendsen (Eds.), *Title of book* (Chapter 1), Place of publication, publisher.

[40] M. Reches, E. Gazit. Casting Metal Nanowires Within Discrete Self-Assembled Peptide Nanotubes. *Science* **300**, 625-627 (2003).

[41] S. Scanlon, A. Aggeli. Self-assembling peptide nanotubes. *Nano Today* **3**, 22-30 (2008).

[42] X.H. Yan, P.L. Zhu, J.B. Li. Self-assembly and application of diphenylalanine-based nanostructures. *Chemical Society Review* **39**, 1877-1890 (2010).

[43] C.H. Gorbitz. The structure of nanotubes formed by diphenylalanine, the core recognition motif of Alzheimer's ?-amyloid polypeptide. *Chemical Communications* 2332-2334 (2006).

[44] J. Castillo-León, R. Rodriguez-Trujillo, S. Gauthier, A.C.O. Jensen, W.E. Svendsen. Micro-factory for self-assembled nanostructures. *Microelectronic Engineering* **88**, 1685-1688 (2011).

[45] K.B. Andersen, J. Castillo-León, M. Hedstrom, W.E. Svendsen. Stability of diphenylalanine peptide nanotubes under liquid conditions. *Nanoscale* **3**, 994-998 (2011).

[46] J. Castillo, S. Tanzi, M. Dimaki, W. Svendsen. Manipulation of self-assembly amyloid peptide nanotubes by dielectrophoresis (DEP). *Electrophoresis* **29**, 5026-5032 (2008).

[47] C.H. Clausen, M. Dimaki, S.P. Pantagos, E. Kasotakis, A. Mitraki, W.E. Svendsen, J. Castillo. Electrostatic Force Microscopy of Self Assembled Peptide Structures. *Scanning* **33**, 201-207 (2011).

[48] C.H. Clausen, J. Jensen, J. Castillo, M. Dimaki, W.E. Svendsen. Qualitative Mapping of Structural Different Polypeptide Nanotubes. *Nano Letters* **8**, 4066-4069 (2008).

[49] M. Reches, E. Gazit. Biological and chemical decoration of peptide nanostructures via biotin-avidin interactions. *Journal of Nanoscience and Nanotechnology* **7**, 2239-2245 (2007).

[50] M. Larsen, K. Andersen, W.E. Svendsen, J. Castillo-León. Self-assembled peptide nanotubes as an etching material for the rapid fabrication of silicon wires. *BioNanoScience* **1**, 31-37 (2011).

[51] A. Mahler, M. Reches, M. Rechter, S. Cohen, E. Gazit. Rigid, Self-Assembled Hydrogel Composed of a Modified Aromatic Dipeptide. *Advanced Materials* **18**, 1365-1370 (2006).

[52] J. Ryu, C.B. Park. High Stability of Self-Assembled Peptide Nanowires Against Thermal, Chemical, and Proteolytic Attacks. *Biotechnology and Bioengineering* **105**, 221-230 (2010).

[53] T.C. Cipriano, P.M. Takahashi, D. de Lima, V.X. Oliveira, J.A. Souza, H. Martinho, W.A. Alves. Spatial organization of peptide nanotubes for electrochemical devices. *Journal of Materials Science 45*, 5101-5108 (2010).

[54] M. Yemini, M. Reches, E. Gazit, J. Rishpon. Peptide Nanotubes Modified Electrodes for Enzyme-Biosensors Applications. *Analytical Chemistry* **77**, 5155-5159 (2005).

[55] M. Yemini, M. Reches, J. Rishpon, E. Gazit. Novel Electrochemical Biosensing Platform Using Self-Assembled Peptide Nanotubes. *Nano Letters* **5**, 183-186 (2005).

[56] J.H. Kim, S.Y. Lim, D.H. Nam, J. Ryu, S.H. Kum, C.B. Park. Self-assembled, photoluminescent peptide hydrogel as a versatile platform for enzyme-based optical biosensors. *Biosensors & Bioelectronics* **26**, 1860-1865 (2011).

[57] X.H. Yan, Y. Cui, Q. He, K.W. Want, J.B. Li. Organogels based on self-assembly of diphenylalanine peptide and their application to immobilize quantum dots. *Chemistry of Materials* **20**, 1522-1526 (2008).

[58] J.H. Kim, J. Ryu, C.B. Park. Selective Detection of Neurotoxin by Photoluminescent Peptide Nanotubes. *Small* **7**, 718-722 (2011).

[59] O. Carny, D.E. Shalev, E. Gazit. Fabrication of coaxial metal nanocables using a self-assembled peptide nanotube scaffold. *Nano Letters* **6**, 1594-1597 (2006).

[60] E. Gazit. Self-assembled peptide nanostructures: the design of molecular building blocks and their technological utilization. *Chemical Society Reviews* **36**, 1263-1269 (2007).

[61] H.I. Ryoo, J.S. Lee, C.B. Park, D.P. Kim. A microfluidic system incorporated with peptide/Pd nanowires for heterogeneous catalytic reactions. *Lab on a Chip* **11**, 378-380 (2011).

[62] E.C. Wu, S. Zhang, C.A.E. Hauser. Self-Assembling Peptides as Cell-Interactive Scaffolds. *Advanced Functional Materials* **22**, 456-468 (2011).

[63] A. Lakshmanan, S. Zhang, C.A.E. Hauser. Short Self-Assembling Peptides as Building Blocks for Modern Nanodevices. *Trends in Biotechnology* **30**, 155-165 (2011).

[64] Y. Loo, S. Zhang, C.A.E. Hauser. From Short Peptides to Nanofibers to Macromolecular Assemblies in Biomedicine. *Biotechnology Advances* **30**, 593-603 (2011).

[65] M. Schindler, A. Nur-E-Kamal, I. Ahmed, J. Kamal, H.Y. Liu, N. Amor, A.S. Ponery, D.P. Crockett, T.H. Grafe, H.Y. Chung, T. Weik, E. Jones, S. Meiners. Living in three dimensions - 3D nanostructured environments for cell culture and regenerative medicine *Cell Biochemistry and Biophysics* **45**, 215-227 (2006).

[66] C. Dionigi, M. Bianchi, P. D'Angelo, B. Chelli, P. Greco, A. Shehu, I. tonazzini, A.N. Lazar, F. Biscarini. Control of neuronal cell adhesion on single-walled carbon nanotube 3D patterns. *Journal of Materials Chemistry* **20**, 2213-2218 (2010).

[67] J. Ryu, C.B. Park. High-Temperature Self-Assembly of Peptides into Vertically Well-Aligned Nanowires by Aniline Vapor. *Advanced Materials* **20**, 3754-3758 (2008).

[68] N. Wiradharma, M. Khan, L.-K. Yong, C.A.E. Hauser, S.V. Seow, S. Zhang, Y.-Y. Yang. The effect of thiol funcitonal group incorporation into cationic helical peptides on antimicrobial activities and spectra. *Biomaterials* **32**, 9100-9108 (2011).

[69] R. R. Traut, A. Bollen, T.T. Sun, J.W. Hershey, J. Sundberg, L.R. Pierce. Methyl 4-mercaptobutyrimidate as a cleavable cross-linking reagent and its application to the Escherichia coli 30S ribosome, *Biochemistry* **12**, 3266-3273 (1973).

[70] W.F. Scherer, J.T. Syverton, G.O. Gey. Studies on the propagation in vitro of poliomyelitis viruses. IV. Viral multiplication in a stable strain of human malignant epithelial cells (strain HeLa) derived from an epidermoid carcinoma of the cervix. *Journal of Experimental Medicine* **97**, 695-710 (1953).

[71] A. Starr, K.D. Wise, J. Csongradi. An evaluation of photoengraved-microelectrodes for extracellular single-unit recording, *IEEE Transactions on Biomedical Engineering* **20**, 291-293 (1973).

[72] D.J. Anderson, K. Najafi, S.J. Tanghe, D.A. Evans, K.L. Levy, J.F. Hetke, X. Xue, J.J. Zappia, K.D. Wise. Batch-fabricated thin-film electrodes for stimulation of the central auditory system, *IEEE Transactions on Biomedical Engineering* **36**, 693-704 (1989).

[73] P.K. Campbell, K.E. Jones, R.J. Huber, K.W. Horch, R.A. Normann. A silicon-based, three-dimensional neural interface: manufacturing processes for an intracortical electrode array, *IEEE Transactions on Biomedical Engineering* **38**, 758-768 (1991).

[74] F. Ejserholm, P. Kohler, M. Bengtsson, J. Jorntell, J. Schouenborg, L. Wallman. A polymer based electrode array for recordings in the cerebellum, *Proceedings of the 5th International IEEE EMBS Conference on Neural Engineering*, 376-379 (2011).

[75] C.K. Chiang, C.R. Fincher Jr., Y.W. Park, A.J. Heeger, H. Shirakawa, E.J. Louis, S.C. Gau, A.G. MacDiarmid. Electrical conductivity in doped polyacetylene, *Physical Review Letters* **39**, 1098-1101 (1977).

[76] "The Nobel Prize in Chemistry 2000 - Press Release". Nobelprize.org (2000).

[77] A.G. MacDiarmid. "Synthetic Metals": A Novel Role for Organic Polymers (Nobel Lecture). *Angew. Chem. Int. Ed.* **40**, 2581-2590 (2001).

[78] "The Nobel Prize in Physics 2010 - Press Release". Nobelprize.org (2010).

[80] J. Janata, M. Josowicz. Conducting polymers in electronic chemical sensors. *Nature Materials* **2**, 19-24 (2003).

[81] C.M. Hangarter, M. Bangar, A. Mulchandani, N.V. Myung. Conducting polymer nanowires for chemiresistive and FET-based bio/chemical sensors. *Journal of Material Chemistry* **20**, 3131-3140 (2010).

[82] Z. Zhang, R. Roy, F.J. Dugré, D. Tessier, L.H. Dao. In vitro biocompatibility study of electrically conductive polypyrrole-coated polyester fabrics. *Journal of Biomedical Materials Research* **57**, 63-71 (2001).

[83] P.G. Bruce, E.S. McGregor, C.A. Vincent. The perfectly polarized polymer electrolyte/electrode interface. *Electrochimica Acta* **37**, 1525-1527 (1992).

[84] S. Chao, M.S. Wrighton. Solid-state microelectrochemistry - electrical characteristics of a solid-state microelectrochemical transistor based on poly(3-methylthiophene). *Journal of the American Chemical Society* **109**, 2197-2199 (1987).

[85] M.M. Ayad, N.A. Salahuddin, M.O. Alghaysh, R.M. Issa. Phosphoric acid and pH sensors based on polyaniline films. *Current Applied Physics* **10**, 235-240 (2010).

[86] P.N. Bartlett, J.M. Cooper. A review of the immobilization of enzymes in electropolymerized films. *Journal of Electroanalytical Chemistry* **362**, 1-12 (1993).

[87] T. Sata. Anti-organic fouling properties of composite membranes prepared from anion exchange membranes and polypyrrole. *Journal of the Chemical Society, Chemical Communications* **14**, 1122-1124 (1993).

[88] A. Galal, N.F. Atta, J.F. Rubinson, H. Zimmer, H.B. Mark. Electrochemistry and detection of some organic and biological molecules at conducting polymer electrodes. *Analytical Letters* **26**, 1361-1381 (1993).

[89] V.-T. Truong, P.K. Lai, B.t. Moore, R.F. Muscat, M.S. Russo. Corrosion protection of magnesium by electroactive polypyrrole/paint coatings. *Synthetic Metals* **110**, 7-15 (2000).

[90] S. Rapi, V. Bocchi, G.P. Gardini. Conducting polypyrrole by chemical synthesis in water. *Synthetic Metals* **24**, 217-221 (1988).

[91] Y. Wei, J. Tian, D.C. Yang. A new method for polymerization of pyrrole and derivatives. *Makromolekulare Chemie - Rapid Communications* **12**, 617-623 (1991).

[92] S.P. Armes. Optimum reaction condictions for the polymerization of pyrrole by iron (III) chloride in aqueous solution. *Synthetic Metals* **20**, 365-371 (1987).

[93] E.M. Genies, G. Bidan. Spectroelectrochemical Study of Polypyrrole Films. *Journal of Electroanalytical Chemistry* **149**, 101-113 (1983).

[94] C.A. Thomas, P.A. Springer, G.E. Loeb, Y. Berwald-Netter, L.M. Okun. A miniature microelectrode array to monitor the bioelectric activity of cultured cells. *Experimental Cell Research* **74**, 61-66 (1972).

[95] G.W. Gross, E. rieske, G.W. Kreutzberg, A. Mayer. A new fixed-array multi-microelectrode system designed for long-term monitoring of extracellular single unit neuronal activity in vitro. *Neuroscience Lett* **6**, 101-105 (1977).

[96] M.P. Maher, J. Pine, J. Wright, Y.-C. Tai. The neurochip: A new multielectrode device for stimulating and recording from cultured neurons. *Journal of Neuroscience Methods* **87**, 45-56 (1999).

[97] G. Xiang, L. Pan, L. Huang, Z. Yu, X. Song, J. Cheng, W. Xing, Y. Zhou. Microelectrode array-based system for neuropharmacological applications with cortical neurons cultured in vitro. *Biosensensors & Bioelectronics* **22**, 278-2484 (2007).

[98] F. Greve, J. Lichtenberg, K.-U. Kirstein, U. Frey, J.-C. Perriard, A. Hierlemann. A perforated CMOS microchip for immobilization and activity monitoring of electrogenic cells. *Journal of Micromechanics and Microengineering* **17**, 462-471 (2007).

[99] C. Ionescu-Zanetti, R.M. Shaw, J.g. Seo, Y.N. Jan, L.Y. Jan, L.P. Lee. Mammalian electrophysiology on a microfluidic platform. *Proceedings of the National Academy of Science, USA* **102**, 9112-9117 (2005).

[100] R. Huys, D. Braken, B. Van Meerbergen, K. Winters, W. Eberle, J. Loo, D. Tsvetanova, C. Chen, S. Severi, S. Yitzchaik, M. Spira, J. Shappir, G. Callewaert, G. Borghs, C. Bartic. Novel concepts for improved communication between nerve cells and silicon electronic devices. *Solid State Electronics* **52**, 533-539 (2008).

[101] M.O. Heuschkel, M. Fejtl, M. Raggenbass, D. Bertrand, P. Renaud. A three-dimensional multi-electrode array for multi-site stimulation and recording in acute brain slices. *Journal of Neuroscience Methods* **114**, 135-148 (2002).

[102] P. Thiebaud, C. Beuret, N.F. de Rooij, M. Koudelka-Hep. Microfabrication of Pt-tip microelectrodes. *Sensors and Actuators B: Chemical* **70**, 51-56 (2000).

[103] P. Vazquez, M. Dimaki, W.E. Svendsen. Metallization of High Aspect Ratio, out of Plane Structures. *Proceedings of 3rd International Workshop on Advances in Sensors and Interfaces*, New York, NY, USA, 184-187 (2009).

[104] J.-R. Rau, J.-C. Lee, S.-C. Chen. Study of Au(I)-polypyrrole interaction. *Synthetic Metals* **79**, 69-74 (1996).

[105] S. Asavapiriyanont, G.K. Chandler, G.A. Gunawardena, D. Pletcher. The electrodeposition of polypyrrole films from aqueous solutions. *Journal of Electroanalytical Chemistry and Interfacial Electrochemistry* **177**, 229-224 (1984).

[106] C.A. Ferreira, S. Aeiyach, M. Delamar, P.C. Lacaze. Electropolymerization of pyrrole on iron electrodes - influence of solvent and electrolyte on the nature of the deposits. *Journal of Electroanalytical Chemistry and Interfacial Electrochemistry* **284**, 351-369 (1990).

[107] R.J. Mammone, M. Binder. Influence of dopant ions on dielectric and physical properties of electrochemically formed poly-n-methylpyrrole. *Journal of the Electrochemical Society* **137**, 2135-2139 (1990).

[108] S. Kuwabata, J. Nakamura, H. Yoneyama. Dependence of conductivity of polypyrrole film doped with para-phenol sulfonate on solution pH. *Journal of the Electrochemical Society* **137**, 2147-2150 (1990).

[109] M. Ogasawara, K. Funahashi, T. Demura, T. Hagiwara, K. Iwata. Enhancement of electrical conductivity of polypyrrole by stretching. *Synthetic Metals* **14**, 61-69 (1986).

[110] A. Witkowski, M.S. Freund, A. Brajter-Toth. Effect of electrode substrate on the morphology and selectivity of overoxidized polypyrrole films. *Analytical Chemistry* **63**, 622-626 (1991).

[111] G. Zotti, S. Cattarin, N. Comisso. Cyclic potential sweep electropolymerization of aniline: The role of anions in the polymerization mechanism. *Journal of Electroanalytical Chemistry and Interfacial Electrochemistry* **239**, 387-396 (1988).

[112] A.F. Diaz, J.I. Castillo, J.A. Logan, W.-Y. Lee. Electrochemistry of conducting polypyrrole films. *Journal of Electroanalytical Chemistry* **129**, 115-132 (1981).

[113] S.M. Sayyah, S.S. Abd El-Rehim, M.M. El-Deep. Electropolymerization of Pyrrole and Characterization of the Obtained Polymer Films. *Journal of Applied Polymer Science* **90**, 1783-1792 (2003).

[114] S. Sadki, P. Schottland, N. Brodie, G. Sabouraud. The mechanisms of pyrrole electropolymerization. *Chemical Society Reviews* **29**, 283-293 (2000).

[115] H.N. Dinh, V.I. Birss. Effect of substrate on polyaniline film properties - a cyclic voltammetry and impedance study. *Journal of the Electrochemical Society* **147**, 3775-3784 (2000).

[116] K. Raimer, C. Kohler, T. Lisec, U. Schnakenberg, G. Fuhr, R. Hintsche. Fabrication of Electrode Arrays in the Quarter Micron Regime for Biotechnological Applications.*Sensors and Actuators A: Physical* **46-47**, 66-70 (1995).

[117] L.M. Fischer, M. Tenje, A.R. Heiskanen, N. Masuda, J. Castillo, A. Bentien, J. Emneus, M.H. Jakobsen, A. Boisen. Gold cleaning meth-

ods for electrochemical detection applications. *Microelectronics Engineering* **86**, 1282-1285 (2009).

[118] E.M. Genies, G. Bidan, A.F. Diaz. Spectroelectrochemical study of polypyrrole films. *Journal of Electroanalytical Chemistry and Interfacial Electrochemistry* **149**, 101-113 (1983).

[119] F. Beck, R. Michaelis, F. Schloten, B. Zinger. Filmforming Electropolymerization of Pyrrole on Iron in Aqueous Oxalid-Acid.*Electrochimica Acta* **39**, 229-234 (1994).

[120] H. Ge, G. Qi, E.-T. Kang, N.G. Neoh. Study of Overoxidized Polypyrrole Using X-Ray Photoelectron-Spectroscopy. *Polymer* **35**, 504-508 (1994).

[121] P.A. Christensen, A. Hamnett. In situ spectroscopic investigations of the growth, electrochemical cycling and overoxidation of polypyrrole in aqueous solution. *Electrochimica Acta* **36**, 1263-1286 (1991).

[122] K. Pihel, D. Walker, R.M. Wightman. Overoxidized polypyrrole-coated carbon fiber microelectrodes for dopamine measurements with fast-scan cyclic voltammetry. *Anal. Chem.* **68**, 2084-2089 (1996).

[123] T. Shimidzu, A. Ohtani, T. Iyoda, K. Honda. Charge-controllable polypyrrole polyelectrolyte composite membranes: Effect of incorporated anion size on the electrochemical oxidation reduction process. *Electroanalytical Chemistry* **224**, 123-135 (1987).

[124] K. Naoi, M. Lien, W.H. Smyrl. Quartz Crystal Microbalance Study - ionic motion across conducting polymers. *Journal of the Electrochemical Society* **138**, 440-445 (1991).

[125] R. Yang, K. Naoi, D.F. Evans, W.H. Smyrl, W.A. Hendrickson. Scanning Tunneling Microscope Study of Electropolymerized Polypyrrole with Polymeric Anion. *Langmuir* **7**, 556-558 (1991).

[126] L. Atanasoska, K. Naoi, W.H. Smyrl. XPS studies on conducting polymers - polypyrrole films doped with perchlorate and polymeric anions. *Chemistry of Materials* **4**, 988-994 (1992).

[127] U. Wollenberger, B. Neumann. Quinoprotein Glucose Dehydrogenase Modified Carbon Paste Electrode for the Detection of Phenolic Compounds. *Electroanalysis* **9**, 366-371 (1997).

[128] F. Lisdat, U. Wollenberger, A. Makower, H. Hortnagl, D. Pfeiffer, F.W. Scheller. Catecholamine detection using enzymatic amplification. *Biosensors & Bioelectronics* **12**, 1199-1211 (1997).

[129] F. Lisdat, U. Wollenberger, M. Paeschke, F.W. Scheller. Sensitive catecholamine measurement using a monoenzymatic recyclic system. *Analytica Chimica Acta* **368**, 233-241 (1998).

[130] A. Rose, F.W. Scheller, U. Wollenberger, D. Pfeiffer. Quinoprotein glucose dehydrogenase modified thick-film electrodes for the amperometric detection of phenolic compounds in flow injection analysis. *Journal of Analytical Chemistry* **369**, 145-152 (2001).

[131] K. Streffer, E. Vijgenboom, A.W.J.W. Tepper, A. Makower, F.W. Scheller, G.W. Canters, U. Wollenberger. Determination of phenolic compounds using recombinant tyrosinase from Streptomyces antibioticus. *Analytical Chimica Acta* **427**, 201-210 (2001).

[132] A. Dalmia, C.C. Liu, R.F. Savinell. Electrochemical behavior of gold electrodes modified with self-assembled monolayers with an acidic end group for selective detection of dopamine. *Journal of Electroanalytical Chemistry* **430**, 205-214 (1997).

[133] C. Spegel, A. Heiskanen, J. Acklid, A. Wolff, R. Taboryski, J. Emneus, T. Ruzgas. On-chip determination of dopamine exocytosis using mercaptopropionic acid modified microelectrodes. *Electroanalysis* **19**, 263-271 (2007).

[134] R.F. Lane, A.T. Hubbard. Differential double pulse voltammetry at chemically modified platinum electrodes or in vivo determination of catecholamines. *Analytical Chemistry* **48**, 1287-1293 (1976).

[135] L.A. Sombers, M.M. Maxson, A.G. Ewing. Loaded dopamine is preferentially stored in the halo portion of PC12 cell dense core vesicles. *Journal of Neurochemistry* **93**, 1122-1131 (2005).

[136] M. Vergani, M. Carminati, G. Ferrari, E. Landini, C. Caviglia, A. Heiskanen, C. Comminges, K. Zor, D. Sabourin, M. Dufva, M. Dimaki, R. Raiteri, U. Wollenberger, J. Emneus, M. Sampietro. Multichannel Bipotentiostat Integrated With a Microfluidic Platform for Electrochemical Real-Time Monitoring of Cell Cultures. *IEEE Transactions on Biomedical Circuits and Systems* - accepted (2012).

[137] C. Spegel, A. Heiskanen, S. Pedersen, J. Emneus, T. Ruzgas, R. Taboryski. Fully automated microchip system for the detection of

quantal exocytosis from single and small ensembles of cells. *Lab Chip* **8**, 323-329 (2008).

[138] P. Roach, T. Parker, N. Gadegaard, M.R. Alexander. Surface strategies for control of neuronal cell adhesion: A review. *Surface Science Reports* **65**, 145-173 (2010).

[139] C. Amatore, S. Arbault, M. Guille, F. Lemaitre. Electrochemical monitoring of single cell secretion: Vesicular exocytosis and oxidative stress. *Chemical Reviews* **108**, 2585-2621 (2008).

[140] C. Krabbe, E. Courtois, P. Jensen, J.R. Jorgensen, J. Zimmer, A. Martinez-Serrano, M. Meyer. Enhanced dopaminergic differentiation of human neural stem cells by synergistic effect of Bcl-x(L) and reduced oxygen tension. *Journal of Neurochemistry* **110**, 1908-1920 (2009).

[141] A. Villa, I. Liste, E.t. Courtois, E.g. Seiz, M. Ramos, M. Meyer, B. Juliusson, P. Kusk, A. Martinez-Serrano. Generation and properties of a new human ventral mesencephalic neural stem cell line. *Experimental Cell Research* **315**, 1860-1874 (2009).

[142] Z. Gao, A. Ivaska. Electrochemical Behavior of Dopamine and Ascorbic Acid at Overoxidized Polypyrrole (Dodecyl Sulfate) Film-Coated Electrodes. *Analytica Chimica Acta* **284**, 393-404 (1993).

[143] J. Ryu, C.B. Park. Synthesis of Diphenylalanine/Polyaniline Core/Shell Conducting Nanowires by Peptide Self-Assembly. *Angewandte Chemie - International Edition* **48**, 4820-4823 (2009).

[144] J.C. Miller, J.N. Miller. Statistics for Analytical Chemistry, Ellis Horwood Limited, West Sussex (1984).

[145] J. Njagi, M.M. Chernov, J.C. Leiter, S. Andreescu. Amperometric Detection of Dopamine in Vivo with an Enzyme Based Carbon Fiber Microbiosensor. *Analytical Chemistry* **82**, 989 (2010).

[146] F.-L. Zhan, L.-M. Kuo, S.-W. Wang, M. S.-C. Lu, W.-Y. Chang, C.-H. Lin, Y.-S. Yang. An electrochemical dopamine sensor with CMOS detection circuit. *6th IEEE Sensors* **1-3**, 1448 (2007).

[147] F. Agnesi, S.J. Tye, J.M. Bledsoe, C.J. Griessenauer, C.J. Kimble, G.C. Sieck, K.E. Bennet, P.A. Garris, C.D. Blaha, K.H. Lee. Wireless Instantaneous Neurotransmitter Concentration System-based amperometric detection of dopamine, adenosine, and glutamate for intraop-

erative neurochemical monitoring Laboratory investigation. *Journal of Neurosurgery* **111**, 701 (2009).

[148] The International Organization for Standardization (ISO), *http://www.iso.org/*.

Appendices

Appendix A

List of Publications and Submitted Papers

A.1 Articles in Peer-reviewed Journals

Publication I.

Conducting Polymer 3D Microelectrodes.
L. Sasso, P. Vazquez, I. Vedarethinam, J. Castillo-León, J. Emnéus, W.E. Svendsen, *SENSORS* **10**, 10986-11000 (2010).

Publication II.

Self-Assembled Diphenylalanine Nanowires for Cellular Studies and Sensor Applications.
L. Sasso, I. Vedarethinam, J. Emnéus, W.E. Svendsen, J. Castillo-León, *Journal of Nanoscience and Nanotechnology* **12**, 3077-3083 (2012).

Publication III.

Doped Overoxidized Polypyrrole Microelectrodes as Sensors for Detection of Cellular Dopamine Release.
L. Sasso, A. Heiskanen, F. Diazzi, M. Dimaki, J. Castillo-León, M. Vergani, E. Landini, R. Raiteri, G. Ferrari, M. Carminati, M. Sampietro, W.E. Svendsen, J. Emnéus, *Biosensors and Bioelectronics*, submitted.

Publication IV.

Fabrication and Characterization of 3D Micro- and Nanoelectrodes for Neuron Recordings.
M. Dimaki, P. Vazquez, M.H. Olsen, L. Sasso, R. Rodriguez-Trujillo, I. Vedarethinam, W.E. Svendsen, *SENSORS* **10**, 10339-10355 (2010).

Publication V.

Microfabricated 3D micro/- and nanoelectrodes for neuron studies.
M. Dimaki, P. Vazquez, A. Aimone, M.H. Olsen, L. Sasso, R. Rodriguez-Trujillo, W.E. Svendsen, *Microelectronic Engineering*, submitted.

Publication VI.

Micro and nano-platforms for biological cell analysis.
W.E. Svendsen, J. Castillo-León, J.M. Lange, L. Sasso, M.H. Olsen, M. Abaddi, L. Andresen, S. Levinsen, P. Shah, I. Vedarethinam, M. Dimaki, *Sensors and Actuators A: Physical* **172**, 54-60 (2011).

A.2 Conference Proceedings

Publication VII.

Micro and nano-platforms for biological cell analysis.
W.E. Svendsen, J. Castillo-León, J.M. Lange, L. Sasso, M.H. Olsen, L. Andresen, S. Levinsen, M. Dimaki, *Procedia Engineering: Eurosensors XXIV Conference* **5**, 33-36 (2010).

Publication VIII.

Vertically Aligned Patterned Peptide Nanowires for Cellular Studies.
M.B. Taskin, L. Sasso, I. Vedarethinam, W.E. Svendsen, J. Castillo-León, *Proceedings of Nanotech Conference and Expo 2012*, submitted.

A.3 Edited Books and Book Chapters

Publication IX.

Chapter 5: Manipulation of Self-assembled Peptide Nanostructures.
J. Castillo-León, L. Sasso, W.E. Svendsen

in:

Publication X.

Self-Assembled Peptide Nanostructures: Advances and Applications in Nanobiotechnology.
J. Castillo-León, L. Sasso, W.E. Svendsen (Eds.), Pan Stanford Publishing, in press.

A.4 Articles in Popular Science Journals

Publication XI.

Diphenylalanine: a short molecule with a big impact.
J. Castillo-León, L. Sasso, W.E. Svendsen, *Kemivärlden Biotech med Kemisk Tidskrift* **3**, 35-36 (2012).

Appendix B

Conference Contributions

Peptide Nanowires for Cellular Sensing.
L. Sasso, J. Castillo-León, J. Emnéus, W.E. Svendsen.
4th International Conference on Surface, Coatings and Nanostructured Materials (NanoSMat), Rome, Italy, October 19-22, 2009 - **Poster Presentation**

Peptide Nanowires/Conductive Polymer Systems for Biosensing.
L. Sasso, J. Castillo-León, J. Emnéus, W.E. Svendsen.
3rd International Conference on Advanced Nano Materials (ANM), Agadir, Morocco, 2010 - **Oral Presentation**

Peptide-based Nanosensors.
L. Sasso, J. Castillo-León, J. Emnéus, W.E. Svendsen.
20th Anniversary World Congress on Biosensors (Biosensors), Glasgow, UK, May 26-28, 2010 - **Oral Presentation**

Diphenylalanine Peptide Nanowires for Sensing Applications.
L. Sasso, I. Vedarethinam, J. Castillo-León, J. Emnéus, W.E. Svendsen.
Brain-Machine Interface Symposium, Ystad, Sweden, August 26-29, 2010 - **Poster Presentation**

Diphenylalanine Peptide Nanowires for Sensing Applications.
L. Sasso, I. Vedarethinam, J. Castillo-León, J. Emnéus, W.E. Svendsen.

Annual Meeting of the Danish Electrochemical Society, Kgs. Lyngby, Denmark, September 30-October 1, 2010 - **Oral Presentation**

Peptide Nanowires for Cellular Studies.
L. Sasso, J. Castillo-León, J. Emnéus, W.E. Svendsen.
Nano Connect Scandinavia Workshop, Gothenburg, Sweden, October 28-29, 2010 - **Poster Presentation**

Diphenylalanine Peptide Nanowires for Sensing Applications.
L. Sasso, J. Castillo-León, J. Emnéus, W.E. Svendsen.
Pittsburgh Conference on Analytical Chemistry and Applied Spectroscopy (PITTCON), Atlanta, GA, USA, March 13-18, 2011 - **Oral Presentation**

Self-Assembled Peptide Nanowires as a Multifunctional Platform for Cellular Studies.
L. Sasso, I. Vedarethinam, J. Castillo-León, J. Emnéus, W.E. Svendsen.
2nd Nano Today Conference, Waikoloa Beach, HI, USA, Dec 11-15, 2011 - **Oral Presentation**

Appendix C

Publications' Abstracts and Experimental Details

This appendix outlines the "Materials and Methods" sections of each publication on which this thesis is based. For each article, only the title page, the abstract and the relevant sections holding details about the experimental protocols are shown.

C.1 Publication I

Sensors **2010**, *10*, 10986-11000; doi:10.3390/s101210986

OPEN ACCESS

sensors

ISSN 1424-8220

www.mdpi.com/journal/sensors

Article

Conducting Polymer 3D Microelectrodes

Luigi Sasso *,†, Patricia Vazquez †, Indumathi Vedarethinam, Jaime Castillo-León, Jenny Emnéus and Winnie E. Svendsen

Department of Micro- and Nanotechnology, Technical University of Denmark, Ørsteds Plads 345ø, 2800 Kgs. Lyngby, Denmark; E-Mails: patricia.vazquez@nanotech.dtu.dk (P.V.); indumathi.vedarethinam@nanotech.dtu.dk (I.V.); jaime.castillo@nanotech.dtu.dk (J.C.-L.); jenny.emneus@nanotech.dtu.dk (J.E.); winnie.svendsen@nanotech.dtu.dk (W.E.S.)

* Author to whom correspondence should be addressed; E-Mail: luigi.sasso@nanotech.dtu.dk; Tel.: +45-4525-5829; Fax: +45-4588-7762.

† Both authors contributed equally to this article and therefore order of authorship is arbitrary.

Received: 20 October 2010; in revised form: 22 November 2010 / Accepted: 25 November 2010 / Published: 3 December 2010

Abstract: Conducting polymer 3D microelectrodes have been fabricated for possible future neurological applications. A combination of micro-fabrication techniques and chemical polymerization methods has been used to create pillar electrodes in polyaniline and polypyrrole. The thin polymer films obtained showed uniformity and good adhesion to both horizontal and vertical surfaces. Electrodes in combination with metal/conducting polymer materials have been characterized by cyclic voltammetry and the presence of the conducting polymer film has shown to increase the electrochemical activity when compared with electrodes coated with only metal. An electrochemical characterization of gold/polypyrrole electrodes showed exceptional electrochemical behavior and activity. PC12 cells were finally cultured on the investigated materials as a preliminary biocompatibility assessment. These results show that the described electrodes are possibly suitable for future *in-vitro* neurological measurements.

Keywords: conducting polymers; micro-fabrication; micro-electrodes

deposition [32]. The patterning of the polymer film is then done by a traditional sacrificial lithography technique, which does not require any etching steps, and is therefore also more cost effective. The experimental details for the formation of a PAni or PPy layer are slightly different since different conditions yield lead to better results for each of these materials (in terms of polymerization time and film thickness) [31], according to the following procedure: For the formation of a PAni layer, the polymerizing solution consisted of a combination of the monomer, aniline (Sigma-Aldrich, St. Louis, MO, USA), and ammonium persulfate (APS) (ICN Biomedicals, Inc., Aurora, OH, USA), an oxidizing agent needed for the chemical oxidative synthesis. A 10 mL solution containing APS (40 mM) in 1 M HCl (Sigma-Aldrich) was prepared. Aniline was added to a final concentration of 160 mM, and the solution was stirred. The samples, consisting of a silicon wafer covered with silicon nitride and a patterned layer of photoresist, were quickly immersed in the polymerizing solution and then left for 70 min unstirred. The samples were finally washed with 1M HCl and dried with nitrogen gas. The PPy synthesis was carried out in a similar way: A polymerizing solution was prepared by first dissolving 0.08 g of $FeCl_3$ in 19 mL of double distilled (dd) water, and sequentially adding 300 μL of pyrrole monomer (Sigma-Aldrich). The silicon wafer was in this case immersed and left in the polymerizing solution for 10 min in order to achieve a polymer film of thickness in the order of 50 nm [31]. In this case the samples were washed with dd water and dried with nitrogen gas.

3. Cell Culturing

Untreated T25 flasks (NUNC, Thermo Scientific, Denmark) were coated with laminin (20 μg/mL, Sigma Aldrich, Denmark) in 1X Phosphate Buffered Saline (PBS) (Sigma Aldrich, Denmark) and left overnight. Later, excess laminin was removed and the flasks were washed twice with sterile water (Sigma Aldrich, Denmark). The Dulbecco's Modified Eagle medium/Ham's Nutrient Mixture F12 supplemented with 10% fetal bovine serum, 10% horse serum, 100 Units/mL penicillin and 100 μg/mL streptomycin and 25 mM HEPES (referred to as DMEM/F12 from now on) was added in the flasks and placed at 37 ℃ in humid atmosphere containing 95% air and 5% CO_2.

Undifferentiated PC12 cells (PC12—pheochromocytoma of rat adrenal medulla, DSMZ GmbH, Germany) approximately 4×10^6 cells were thawed and transferred to the above-mentioned flasks and placed in the incubator. After 5 days, neuronal differentiation was initiated by replacing the media with DMEM/F-12 supplemented with 100 ng/mL NGF. The cell media was changed every 2 days. After 5 days of culturing, the cells were detached by adding 0.05% trypsin-EDTA (Sigma Aldrich, Denmark) at 37 ℃ for 3 min. The cell suspension was transferred to a 10 mL Falcon tube with fresh media and centrifuged at 1,100 rpm for 3 min. The supernatant was removed and the pellet was resuspended with media at 1×10^6 cells/mL. The centrifugation process and the resuspension of the cells in fresh media are done in order to remove the trypsin.

The differentiated cells were then seeded in a Petri dish containing the electrode chip and it was supplemented with DMEM/F-12 and 100 ng/ml NGF. Before seeding the cells, the electrode chips were sterilised with acetone at 70 ℃ for 5 min followed by three times wash in 70% ethanol for 5 min. The chips were washed with 1X PBS three times and then coated with laminin, as previously described.

C.2 Publication II

Journal of
Nanoscience and Nanotechnology
Vol. 12, 1–7, 2012

Self-Assembled Diphenylalanine Nanowires for Cellular Studies and Sensor Applications

Luigi Sasso*, Indumathi Vedarethinam, Jenny Emnéus, Winnie E. Svendsen, and Jaime Castillo-León

Technical University of Denmark, Department of Micro- and Nanotechnology, Ørsteds Plads 345ø, 2800 Kongens Lyngby, Denmark

In this paper we present a series of experiments showing that vertical self-assembled diphenylalanine peptide nanowires (PNWs) are a suitable candidate material for cellular biosensing. We grew HeLa and PC12 cells onto PNW modified gold surfaces and observed no hindrance of cell growth caused by the peptide nanostructures; furthermore we studied the properties of PNWs by investigating their influence on the electrochemical behavior of gold electrodes. The PNWs were functionalized with polypyrrole (PPy) by chemical polymerization, therefore creating conducting peptide/polymer nanowire structures vertically attached to a metal electrode. The electroactivity of such structures was characterized by cyclic voltammetry. The PNW/PPy modified electrodes were finally used as amperometric dopamine sensors, yielding a detection limit of 3,1 μM.

Keywords:

1. INTRODUCTION

Molecular self-assembly is a powerful method for fabricating novel biomaterials that are indispensable to the integration between nanotechnology and biology due to their structural variety, their application in cell culture and tissue engineering and their molecular recognition capability.[1] Peptide-based materials, in particular, have attracted interest because of their diverse chemical and physical properties, their simple synthesis and their possibility to be functionalized.[2] Ways have also been found for manipulating peptide nanostructures, for example by dielectrophoresis[3] or using microfluidics.[4]

Several sub-micron sized structures can be obtained from peptide building-blocks. Structures such as tubes, wires, spheres, fibrils and tapes can be attained by tweaking the self-assembly process during the synthesis.[2] Particularly, diphenylalanine has been proved to be useful in the creation of both tubes and wires.[5] Although these two nanostructures are synthesized from the same peptide monomer, they have shown to hold very different properties, especially when it comes to stability.[6, 7]

Vertically organized self-assembled peptide nanowires (PNWs) can be synthesized from an amorphous diphenylalanine film by a high-temperature aniline vapor treatment.[8] The obtained structures are about 150–300 nm in diameter and 6–10 μm in length. These structures have been found to have excellent chemical and thermal stability and to be resistant to proteolytic attacks, in comparison to the less stable and resistant peptide nanotubes which can be synthesized from the same diphenylalanine monomer.[6] Moreover, the peptide nanowires been shown to have unique properties, such as superhydrophobicity[9] and suitability to be applied to energy storage.[10]

Much scientific interest has risen in the past decades concerning the use of micro- and nanotechnology for cellular biosensors, aiming towards *in-vitro* intra-cellular analyses with micro-fabricated electrodes created in a variety of materials with a vast number of techniques.[11, 12] Cellular functions can be better understood with the use of intra-cellular probing and sensing. New technologies are quickly developing in order to better mimic *in-vivo* conditions during *in-vitro* cellular analyses, since the current cell culturing techniques (i.e., culturing on smooth glass and plastic surfaces) are quite far from *in-vivo* conditions. Although cells have been shown to survive when penetrated by nanostructures,[13] the investigation of new nanobiomaterials for cellular studies and sensing can lead to better biocompatibility of the sensing electrodes and therefore cellular analysis with more *in-vivo*-like conditions.

We show here that self-assembled diphenylalanine PNWs can be suited for cellular studies and sensing applications. It is because of their distinctive properties, especially regarding stability and resistance, that the peptide nanowires have been investigated instead of other nano- and microstructures available from the

*Author to whom correspondence should be addressed.

RESEARCH ARTICLE

same diphenylalanine peptide, although the diphenylalanine nanotubes have for example been shown to exhibit an excellent electrochemical behavior, increasing electrode current responses.[14]

The PNWs were tested as a scaffold for cell growth, by culturing HeLa and PC12 cells onto a sample of peptide nanograss grown on gold. The PNWs' aptness for electrode modification was also investigated. Gold disk electrodes covered by peptide nanograss were tested electrochemically by amperometric detection of hydrogen peroxide. Lastly, the PNWs were functionalized with polypyrrole by chemical polymerization. Polypyrrole (PPy) is a conducting polymer interesting to research for its facile chemical and electrochemical synthesis, doping properties, and thermal stability in air.[15] PPy is a favorable candidate for biosensing applications because it is one of the most versatile conducting polymer when it comes to selectivity properties.[16] PNW/PPy modified electrodes were electrochemically characterized by cyclic voltammetry and chronoamperometric dopamine detection.

2. EXPERIMENTAL DETAILS

2.1. Materials

Diphenylalanine was purchased from BACHEM (Bubendorf, Switzerland). 1,1,1,3,3,3-hexafluoro-2-propanol (HFP), hydrogen peroxide (30% by weight) and glutaraldehyde were obtained from Fluka Analytical (Buchs, Switzerland). Aniline, pyrrole, phosphate buffer solution (PBS, pH 7.2), dopamine hydrochloride (3-Hydroxytyramine hydrochloride), Laminin, Fetal Calf Serum (10%), penicillin, paraformaldehyde, streptomycin and trypsin-EDTA were acquired from Sigma-Aldrich (St. Louis, MO, USA). Iron (III) chloride was purchased from Merck (Darmstadt, Germany). Dulbecco's Modified Eagle Medium (DMEM) and DAPI (4′-6-Diamidino-2-phenylindole) was purchased from Invitrogen (Paisley, UK). Commercial gold disk electrodes of diameter 0.1 cm^2 (AC1.W1.R2) were obtained from BTV Technologies (Brno, Czech Republic). T25 cell culturing flasks were purchased from NUNC, Thermo Scientific (Denmark).

2.2. PNW Synthesis

Peptide nanowires were synthesized onto commercial gold electrodes by dissolving different amounts of diphenylalanine powder into 1 mL of HFP. 10 μL drops of peptide solutions in HFP of concentrations ranging from 0.05 to 25 mg/mL were pipetted onto the working surface of commercial gold electrodes. The samples were allowed to dry under anhydrous conditions in a vacuum desiccator in order to obtain the formation of an amorphous film. The aniline vapor treatment was carried out in a Petri-dish containing two separate compartments, one for the sample and one for the aniline solvent, in order to only allow the solvent vapor to reach the film. The chamber system was sealed with aluminum sealing film and placed in the oven for 16 hours at 100 °C.

2.3. Functionalization with PPy

Dipheylalanine/polypyrrole hybrid nanowires were synthesized by immersing the previously grown peptide nanowire samples (1.0 mg/mL) into a polymerizing solution, prepared by rapidly mixing a pyrrole solution (300 μL pyrrole in 12 mL milliQ H_2O) with an iron chloride solution (0.08 g of $FeCl_3$ in 7 mL of milliQ H_2O).[17] The reaction was allowed to run for 15 minutes at room temperature. After the completion of the polymerization reaction, the samples were washed with water and dried with nitrogen gas.

2.4. Characterization

The electrochemical activity of the PNW-modified electrodes was studied by chronoamperometric experiments at 600 mV[18] versus Ag/AgCl in 0.1 M KCL under stirred conditions with subsequent additions of H_2O_2 (12 M) every 20 seconds. Several electrodes were used containing peptide nanograss obtained from different concentrations of the original peptide solution.

Low-vacuum Scanning Electron Microscopy (SEM) images were obtained using a FEI Nova 600 NanoSEM system (FEI Company, Oregon, USA) at 5 kV (spot size 4.0). The samples were tilted up to 45 degrees for imaging.

The synthesized PNW/PPy hybrid nanowires were characterized by cyclic voltammetry at potential scan rates ranging from 50–300 mV/s in a 0.1 M KCl solution under stirred conditions, using a Reference 600 potentiostat/galvanostat/ZRA (Gamry Instruments, Warminster, PA, USA) with a gold counter electrode and an Ag/AgCl (3M KCl) reference electrode (Metrohm, Glostrup, DK). Amperometric dopamine detection was carried out in the same 3-electrode system in PBS (pH 7.2) at 0.5 mV. Aliquots of a 10 μM dopamine stock solution in PBS were added stepwise and the current was measured after each addition. Ten measurements were carried out for each dopamine concentration, in order to investigate the reproducibility of the modified electrodes. Averages and standard deviations were calculated from current response values after stabilization of the system.

2.5. Cell Growth

Sterility is an important factor because of its influence on the stability of the PNWs for use in cell culture work. In our study, we took advantage of the PNWs stability[6] when subjected to the following sterilization condition. The gold surfaces (with and without PNW modification) were washed three times in 70% ethanol for 5 min, followed by three washes in 1X PBS for 5 min. HeLa cells

were cultured in DMEM supplemented with 10% Fetal Calf Serum, 100 U/ml penicillin, 10 mg/ml streptomycin at 37 °C in humid atmosphere containing 95% air and 5% CO_2. Cells were plated on the modified and unmodified gold surfaces at a seeding concentration of 10000/ml and cultured for 3 days.

On the 3rd day, 2/3rd of culture medium was removed, the culture was fixed on the surfaces with 4% paraformaldehyde fixative solution (4% of paraformaldehyde in 0.1 M PBS) for 15 min and the fixative solution was removed and stained with DAPI for 20 min. The sample was analyzed using Olympus BX51 microscope/20X objective.

For the PC12 cell culturing, untreated T25 flasks were coated with laminin (20 μg/mL) in 1X PBS and left overnight. Later, excess laminin was removed and the flasks were washed twice with sterile water. The Dulbecco's Modified Eagle medium/Ham's Nutrient Mixture F12 supplemented with 10% fetal bovine serum, 10% horse serum, 100 Units/mL penicillin, 100 μg/mL streptomycin and 25 mM HEPES (referred to as DMEM/F12 from now on) was added in the flasks and placed at 37 °C in humid atmosphere containing 95% air and 5% CO_2. Undifferentiated PC12 cells (PC12—pheochromocytoma of rat adrenal medulla), approximately 4×10^6 cells, were thawed and transferred to the above-mentioned flasks and placed in the incubator. After 5 days, neuronal differentiation was initiated by replacing the media with DMEM/F-12 supplemented with 100 ng/mL neuronal growth factor (NGF). The cell media was changed every 2 days. After 5 days of culturing, the cells were detached by adding 0.05% trypsin-EDTA at 37 °C for 3 min. The cell suspension was transferred to a 10 mL Falcon tube with fresh media and centrifuged at 1,100 rpm for 3 min. The supernatant was removed and the pellet was resuspended with media at 1×10^6 cells/mL. The centrifugation process and the resuspension of the cells in fresh media are done in order to remove the trypsin. The differentiated cells were then seeded in a Petri dish containing the PNW sample (washed with 1X PBS three times and coated with laminin as previously described) and it was supplemented with DMEM/F-12 and 100 ng/ml NGF. Before seeding the cells, the PNW samples were sterilised with acetone at 70 °C for 5 min followed by three times wash in 70% ethanol for 5 min.

For SEM imaging, the culture was fixed in 2% glutaraldehyde in 0.1 M phosphate buffer for 1 hour. The culture was rinsed in 0.1 M PBS for 15 minutes at 4 °C and washed with deionized water for 5 minutes. The sample was dehydrated with increased percentage of ethanol (50, 60, 70, 80, 90, and finally 100%) and air-dried.

3. RESULTS AND DISCUSSION

3.1. Electrochemical Behavior of PNW Modified Electrodes

An electrochemical investigation of PNW modified gold electrodes was carried out in order to study their behavior as possible sensor material. Figure 1 shows the amperometric response of the modified gold electrodes to subsequent additions of a 30% hydrogen peroxide stock solution. The PNW modified electrodes demonstrated a direct response to hydrogen peroxide, meaning that the current response increased with each addition.

Several concentrations of diphenylalanine solutions, ranging from 0.05 to 25 mg/mL, were used in order to investigate the effect of peptide concentration on current response. High concentrations yield densely packed peptide nanograss, whereas lower concentrations lead to the formation of less organized and not as vertical patches of peptide nanostructures (see Fig. 2). The PNW modified

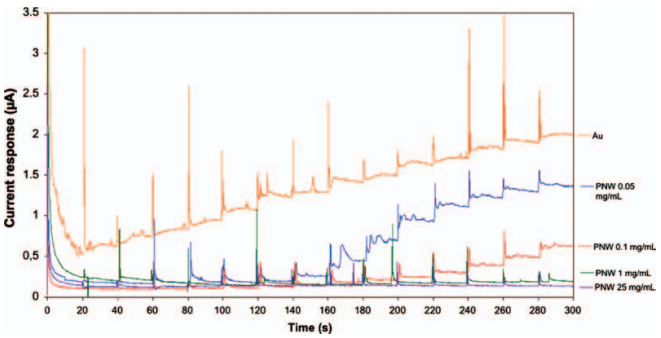

Fig. 1. Chronoamperometric measurements of the PNW modified gold electrodes with different concentrations of diphenylalanine solution in HFP at 600 mV versus Ag/AgCl in 0.1 M KCl under stirred conditions with subsequent additions of hydrogen peroxide (30 wt.%) every 20 seconds.

RESEARCH ARTICLE

C.3 Publication III

Doped Overoxidized Polypyrrole Microelectrodes as Sensors for Detection of Cellular Dopamine Release

Luigi Sasso[a], Arto Heiskanen[a], Francesco Diazzi[a,1], Maria Dimaki[a], Jaime Castillo-León[a], Marco Vergani[b], Ettore Landini[c], Roberto Raiteri[c], Giorgio Ferrari[b], Marco Carminati[b], Marco Sampietro[b], Winnie E. Svendsen[a]*, and Jenny Emnéus[a].

[a]*Dept. of Micro- and Nanotechnology, Technical University of Denmark, Ørsted Plads 345B, 2800 Kgs. Lyngby, Denmark.*

[b]*Dept. of Electronics and Information Technologies, Politecnico di Milano, Via Golgi 42, 20133 Milano, Italy.*

[c]*Dept. of Biophysical and Electronic Engineering, University of Genova, Via Opera Pia 11A, 16145 Genova, Italy.*

*Corresponding author: Winnie E. Svendsen (e-mail: winnie.svendsen@nanotech.dtu.dk, telephone: +45 4525 5741, fax: +45 4588 7762

[1]Present address: STMicroelectronics, Via Tolomeo 1, 20010 Cornaredo (MI), Italy

E-mail addresses of authors

Luigi Sasso:	luigi.sasso@nanotech.dtu.dk
Arto Heiskanen:	arto.heiskanen@nanotech.dtu.dk
Francesco Diazzi:	francesco.diazzi@gmail.com
Maria Dimaki:	maria.dimaki@nanotech.dtu.dk
Jaime Castillo-León:	jaime.castillo@nanotech.dtu.dk
Marco Vergani:	vergani@elet.polimi.it
Ettore Landini:	ettore.landini@unige.it
Roberto Raiteri:	rr@unige.it
Giorgio Ferrari:	ferrari@elet.polimi.it
Marco Carminati:	carminati@elet.polimi.it
Marco Sampietro:	sampietr@elet.polimi.it
Winnie E. Svendsen:	winnie.svendsen@nanotech.dtu.dk
Jenny Emnéus:	jenny.emneus@nanotech.dtu.dk

Abstract

A surface modification of interdigitated gold microelectrodes (IDEs) with a doped polypyrrole (PPy) film for detection of dopamine released from populations of differentiated PC12 cells is presented. A thin PPy layer was potentiostatically electropolymerized from an aqueous pyrrole solution onto electrode surfaces. The conducting polymer film was doped during electropolymerization by introducing counter ions in the monomer solution. Several counter ions were tested and the resulting electrode modifications were characterized electrochemically to find the optimal dopant that increases sensitivity in dopamine detection. Overoxidation of the PPy films was shown to contribute to a significant enhancement in sensitivity to dopamine. The changes caused by overoxidation in the film morphology and electrochemical behaviour were investigated by SEM and AFM as well as cyclic voltammetry, respectively. The optimal dopant for dopamine detection was found to be polystyrenesulfonate anion (PSS^-). Rat pheochromocytoma (PC12) cells, a suitable model to study exocytotic dopamine release, were differentiated on IDEs functionalized with an overoxidized PSS^- doped PPy film. The modified electrodes were used to amperometrically detect dopamine released by populations of cells upon triggering cellular exocytosis with an elevated K^+ concentration. A comparison between the generated current on bare gold electrodes and gold electrodes modified with overoxidized doped PPy illustrates the clear advantage of the modification, yielding 2.6-fold signal amplification. The results also illustrate how to use cell population based dopamine exocytosis measurements to obtain biologically significant information that can be relevant in, for instance, the study of neural stem cell differentiation into dopaminergic neurons.

Keywords (max 6)

Conducting polymer, Doped polypyrrole, Overoxidation, Microelectrode arrays, Dopamine detection, PC12 cell exocytosis

oxidation on an electrode surface (Adams, 1976) has resulted in numerous studies that have revealed, for instance, the fundamental mechanism of neurotransmitter release in the process known as exocytosis. Inside neurons, the neurotransmitters are sequestered in vesicles that upon stimulation are fused with the plasma membrane in a Ca^{2+}-influx mediated process, resulting in the release of the vesicular contents into the extracellular environment. Electrochemical investigation has demonstrated that neurotransmitters are released as small packages upon fusion of one vesicle at a time (Wightman, 1991), known as quantal release. Typically, carbon fibre microelectrodes (CFMEs) have been applied in electrochemical detection of released dopamine (Wightman, 1991), however, during recent years metal electrode systems based on lithographic microsensor technology have gained increasing attention (Spégel et al., 2008a). Since electrooxidation of dopamine results in electrode fouling due to polymerization on the electrode surface (Lane and Hubbard, 1976) and negatively charged interferences, such as ascorbate, can hamper the detection of dopamine (Gao and Ivaska, 1993), different electrode modifications, e.g., thiol self-assembled monolayers (SAMs) (Spégel, 2007) and overoxidized PPy (Gao and Ivaska, 1993), have been utilized to overcome the problems.

In this paper, we describe PPy modification of interdigitated gold microelectrodes based on an optimized counter-ion doping during electropolymerization and overoxidation of the polymer layer to increase sensitivity for detection of dopamine released from populations of differentiated PC12 cells.

2. Materials and Methods

2.1. Chemicals

Potassium chloride (BioXtra), sodium sulfate (ReagentPlus), monobasic potassium phosphate (cell culture tested), sodium dodecyl sulfate (DS^-, M_w 288.4 g/mol (molecular biology grade), poly(sodium 4-styrenesulfonate) (PSS^-) (average M_w ~70,000 Da, 30% wt. in water), hydrochloric acid (BioReagent), magnesium chloride hexahydrate (BioReagent), calcium chloride dihydrate (BioReagent), sodium chloride (BioReagent), glucose (BioXtra), 4-(2-hydroxyethyl)piperazine-1-ethanesulfonic acid (HEPES) 1M solution (BioReagent), 2-(3,4-dihydroxyphenyl)ethylamine hydrochloride (Dopamine), 3-(3,4-dihydroxyphenyl)-L-alanine (L-DOPA), sodium hydroxide (BioXtra), pyrrole (Reagent), hydrogen peroxide (30% in water), potassium hydroxide (semiconductor grade), polyethylenimine (PEI) (branched, average M_w ~25,000), nerve growth factor-β from rat (NGF), laminin from Engelbreth-Holm Swarm murine sarcoma basement membrane, horse serum (HS), glutaraldehyde (25% in H_2O, specially purified for use as an electron microscopy fixative), and water (cell culture tested) were purchased from Sigma-Aldrich Corporation (St. Louis, MO, USA). Dulbecco's Modified Eagle Medium/Ham's Nutrient Mixture F12 with GlutaMAX (DMEM/F12), Trypsin-EDTA (0.05%) and penicillin/streptomycin (P/S) were purchased from Life Technologies Ltd (Paisley, UK). Foetal bovine serum (FBS) and cell culture

tested phosphate buffered saline (PBS) were from Biowest S.A.S. (Nuaillé, France) and Lonza Group Ltd (Basel, Switzerland), respectively. All solutions used for electropolymerization and electrochemical characterization were prepared in ultra pure water (resistivity 18.2 MW·cm) from a Milli-Q® water purification system (Millipore Corporation, Billerica, MA, USA).

2.2. Solutions and Buffers

The following solutions and buffers were used throughout the experimental work:

Electropolymerization solutions (with dopant counter ions): Pyrrole was used as received to prepare a 0.05 M solution in water. When using dopant counter-ions (Cl^-, SO_4^{2-}, PO_4^{3-}, DS^- or PSS^-) each of them was added in a 10-mL aliquot of the pyrrole solution to obtain the concentration of 0.1 M.

Dopamine solution: A 1 mM stock solution was prepared in PBS that had been purged with nitrogen for at least 20 minutes before use. Purging of the stock solution was continued throughout the sensor characterization. Each dilution (e.g. 100 µM, 10 nM) was prepared immediately before use.

Cell Media: All cell media were prepared using DMEM/F12. The growth medium was supplemented with 15% HS, 2.5% FBS, 1% P/S, and 0.5% HEPES. The differentiation medium had a lowered serum contents (0.5% HS and 0.5% FBS). The L-DOPA (100 µM) medium was prepared by adding L-DOPA from a 10-mM stock solution in PBS into the differentiation medium. The stock solution was prepared by first dissolving L-DOPA (40 mg/ml) in 0.5 M HCl followed by dilution with PBS and sterile filtration.

Buffers for exocytosis measurements: All the buffers were prepared using cell culture tested water. The low K^+ buffer contained 10 mM HEPES, 5 mM glucose, 1.2 mM Mg^{2+}, 2 mM Ca^{2+}, 150 mM Na^+, and 5 mM K^+. In the high K^+ buffer, the concentration of Na^+ and K^+ were 5 mM and 450 mM, respectively. Both buffers were sterile filtered before use.

2.3. Electrode microchip fabrication

The microchips having 12 electrode sets, each comprising an interdigitated electrode (IDE), a counter electrode (CE) and a reference electrode (RE) (see Fig. 1), were fabricated using standard cleanroom-based micromachining techniques. A 670 nm layer of thermal oxide (SiO_2) was grown on a silicon wafer (one side polished) in a drive-in furnace at 1050 ^oC in the presence of water vapour (wet growth). The gold structures, i.e. electrodes, leads and contact pads, were photolithographically defined in positive photoresist (AZ® 5214E from MicroChemicals GmbH, Ulm, Germany) using an image reversal process, followed by metal deposition (10 nm thick Ti adhesion layer and 150 nm thick gold layer) through electron beam evaporation and lift-off in acetone. Prior to metal deposition, the SiO_2 was etched for 100 s in the areas having opened resist using buffered HF solution to form ca. 150 nm deep isotropic undercuts (Reimer et al., 1995) that eliminate the formation of lift-off ears at the edges of the metal structures. The non-active gold areas (the leads connecting the electrodes to the contact pads) were passivated with 500 nm thick silicon nitride deposited using plasma-enhanced chemical vapour deposition. A second photolithography

step coupled with reactive ion etching of the silicon nitride was used to expose the active electrode areas and contact pads. Removal of the final photoresist was achieved by ultrasonication in acetone followed by intermediate rinsing with ethanol and final rinsing with deionized water.

2.4. Polypyrrole electropolymerization, overoxidation and characterization

For the electropolymerization and electrode characterization, the electrode chips were placed in a micromilled poly(methyl methacrylate) (PMMA) holder (for details see the Supplementary Data). The holder formed a 500-µL vial on top of the electrode chip to facilitate liquid handling during experiments. Interconnections between the electrode chip and the potentiostat (1010 eight-channel potentiostat from CH Instruments, Austin, USA) were obtained using a tailor-made PCB having gold plated spring loaded pins (Mill-Max Mfg. Corp., Oyster Bay, NY, USA). Before use, the electrode chips were cleaned for 10 minutes in a solution containing 50 mM KOH and 25% H_2O_2, followed by a potential sweep on the IDE working electrodes (WE) from -200 mV to -1200 mV in 50 mM KOH at 50 mV/s to remove the gold oxides formed during the chemical cleaning (Fischer et al., 2009). The polypyrrole (PPy) electrode modification was achieved by electropolymerizing pyrrole monomers under potentiostatic conditions for 10 seconds at 700 mV with or without dopant counterions. The IDEs of the microchip were used as WEs together with the RE and CE from each respective electrode set. Overoxidation of the PPy layer was carried out by cyclic voltammetry in a 0.1 M NaOH solution by applying 50 cycles in a potential window from 0 to 1000 mV at the sweep rate of 100 mV/s. The electrochemical behaviour of the doped PPy-modified electrodes was characterized by cyclic voltammetry in a potential window from 0 to 700 mV at a potential sweep rate of 50 mV/s in solutions having various dopamine concentrations. A morphological comparison of the polymer layer was done by low-vacuum scanning electron microscopy (SEM) using a FEI Nova 600 NanoSEM system (FEI Company, Oregon, USA) at 5 kV (spot size 4.0). Atomic Force Microscopy (AFM) characterization was carried out with a Veeco di CP-II microscope (Veeco Instruments Inc., Plainview, NY, USA). The results showing the average thickness of the obtained PPy films are presented +/- standard error of mean (s.e.m.).

2.5. Cell culturing and differentiation

The cell-based experiments were conducted using rat pheochromocytoma (PC12) cells from Deutsche Sammlung von Microorganismen und Zellkulturen GmbH (Braunschweig, Germany). Initially, PC12 cells were grown for 48 hours in PEI-coated (2-hour coating at room temperature using sterile filtered 50 µg/mL PEI diluted in PBS followed by rinsing twice with PBS) T25 culture flasks from Nunc A/S (Roskilde, Denmark) using growth medium. 24 hours prior to seeding the cells onto an electrode chip, the growth medium was changed for the differentiation medium to initiate the cellular response to NGF. Sterilization of all microfabricated cell culture substrates and materials was done by immersing them in 0.5 M NaOH for 30 minutes followed by rinsing with PBS trice. Electrode chips were coated with

laminin (20 µg/mL laminin diluted in PBS) in a Petri dish for 2 hours to ensure cellular adhesion. Adsorption of laminin, and hence adhesion of cells, only in the central part of an electrode chip where the electrode sets are located was achieved using a hydrophobic pen from Dako Denmark A/S (Glostrup, Denmark). The pre-differentiated PC12 cells were rinsed with PBS and trypsinized for 5 minutes followed by 5-minute centrifugation at 850 rpm at 20 ºC. The cell pellet was resuspended in the differentiation medium and the cells were seeded onto the coated electrode chips with a surface density of 10^5 cells/cm^2. All cell culturing and differentiation was done in an incubator at 37 ºC in a humidified atmosphere of 5% CO2/95% air. SEM imaging of the differentiated cells was done using a FEI Nova 600 NanoSEM system after fixation with 2% glutaraldehyde solution diluted in PBS for 1 hour followed by rinsing with PBS (twice for 15 min) and cell culture tested water (twice for 5 min). Cell counting on microchips was done using a Zeiss Axio Imager M1m microscope equipped with an AxioCam MRc5 computer controlled CCD camera (Carl Zeiss AG, Göttingen, Germany).

2.6. Exocytosis measurements

After 4 days of differentiation, the differentiation medium was replaced by the L-DOPA medium and the cells were kept in the incubator for one hour to increase the dopamine load in the vesicles (Sombers et al., 2005). Before conducting the exocytosis measurements, each electrode chip with the differentiated PC12 cells was placed in a micromilled PMMA holder (described in section 2.4) to facilitate contact between the individual electrode sets and the 24-channel potentiostat with a tailor-made acquisition software (Vergani et al., 2011). The open vial in the holder facilitated the addition of the necessary buffer solutions during exocytosis measurements. The medium was immediately replaced by 160 µL of the low K^+ buffer to record a baseline for the measurements. Each array of interdigitated WEs was poised at 400 mV vs. the gold RE adjacent to the array. After a stable baseline had been recorded, exocytosis was triggered by pipetting 80 µL of the high K^+ buffer directly into the vial of the PMMA holder to elevate the K^+ concentration to 150 mM (Spegel et al., 2008b). The current peaks corresponding to the oxidation of the dopamine released by the cells were obtained shortly after triggering the exocytosis. Recording of the exocytotic events was done simultaneously on each IDE array. Exocytosis experiments were carried out on 3 different electrode chips, each having non-modified IDE arrays and IDE arrays modified with overoxidized PSS^--doped PPy. All the amperometric recordings were done at room temperatrure (~ 22 ºC). All calculated results from cell-based measurements are presented +/- (s.e.m.).

3. Results and discussion

All electrodes used in this work were fabricated onto a silicon-based microchip using standard cleanroom technology. Each set of interdigitated electrodes used as working electrode was coupled with its own counter and reference electrode present in the microchip, as shown in Fig. 1A.

C.4 Publication IV

Sensors **2010**, *10*, 10339-10355; doi:10.3390/s101110339

OPEN ACCESS

sensors

ISSN 1424-8220

www.mdpi.com/journal/sensors

Article

Fabrication and Characterization of 3D Micro- and Nanoelectrodes for Neuron Recordings

Maria Dimaki *, Patricia Vazquez, Mark Holm Olsen, Luigi Sasso, Romen Rodriguez-Trujillo, Indumathi Vedarethinam and Winnie E. Svendsen

Department of Micro- and Nanotechnology, Technical University of Denmark, DTU Nanotech, Building 345E, Kgs. Lyngby, Denmark; E-Mails: Patricia.Vazquez@nanotech.dtu.dk (P.V.); Mark.Olsen@nanotech.dtu.dk (M.H.O.); Luigi.Sasso@nanotech.dtu.dk (L.S.); Romen.Trujillo@nanotech.dtu.dk (R.R.-T.); Indumathi.Vedarethinam@nanotech.dtu.dk (I.V.); Winnie.Svendsen@nanotech.dtu.dk (W.E.S.)

* Author to whom correspondence should be addressed; E-Mail: Maria.Dimaki@nanotech.dtu.dk; Tel.: +45-45256837; Fax: +45-45887762.

Received: 18 October 2010; in revised form: 28 October 2010 / Accepted: 15 November 2010 / Published: 17 November 2010

Abstract: In this paper we discuss the fabrication and characterization of three dimensional (3D) micro- and nanoelectrodes with the goal of using them for extra- and intracellular studies. Two different types of electrodes will be described: high aspect ratio microelectrodes for studying the communication between cells and ultimately for brain slice recordings and small nanoelectrodes for highly localized measurements and ultimately for intracellular studies. Electrical and electrochemical characterization of these electrodes as well as the results of PC12 cell differentiation on chip will be presented and discussed.

Keywords: 3D electrodes; fabrication; neuron differentiation on chip

1. Introduction

Recording electrical or chemical signals from cells can provide a lot of information about how they respond to different stimuli, how they communicate with each other and how they function in general.

The characterization was done in a 1% NaCl solution following the example of [15]. For the small 3D electrodes measurements were additionally taken in de-ionized (DI) water as well as a 0.1% NaCl solution. The impedance of the tall electrodes was measured in the biologically relevant range of 40 Hz to 100 kHz. As the impedance of the small electrodes is expected to be large, the frequency range for the measurements was from 100 Hz to 80 MHz. The input voltage amplitude was 100 mV in both cases. Impedance measurements were also done at 10 mV but apart from a higher noise at the lowest frequencies in this case, the impedance values were identical for 10 mV and 100 mV. Therefore 100 mV were chosen as the voltage amplitude to avoid high noise levels. Frequencies down to 1 Hz would also be relevant for this characterization considering the application, but due to the experimental equipment these were not possible to test.

2.4. Electrochemical Characterization

Using a Reference 600 potentiostat/galvanostat/ZRA (Gamry Instruments, Warminster, PA, USA) Polyaniline (PAni) was electrodeposited on selected small electrodes by varying the potential from 0 to 1 V at a potential sweep rate (PSR) of 100 mV/s for 25 cycles in a 1.0 M HCl solution containing 1.0 M of the aniline monomer using an Ag/AgCl (1.0 M KCl) reference electrode. The same instrument was used afterwards for getting cyclic voltammograms from the PAni covered electrodes at PSR from 50 to 300 mV/s.

2.5. Energy Dispersive X-Ray (EDX) Analysis

EDX analysis (Oxford Inca EDX system, Oxford Instruments, UK) on the small electrodes was done inside a Scanning Electron Microscope (SEM) from FEI Corporation in order to check the electrodeposition of PAni on the selected electrodes and whether the silicon nitride layer was properly removed during the nitride etch (step 18, Figure 2). Spectra were taken at 15 kV on three locations: 1) An electrode location that had not been contacted during electrodeposition of PAni 2) An electrode location that was contacted during electrodeposition of PAni and 3) A test electrode for which the nitride layer had not been removed during the nitride etch step.

2.6. PC12 Cell Culture and Differentiation

Untreated T25 flasks (Nunc, Thermo Scientific, Denmark) were coated with laminin (20 μg/mL, Sigma Aldrich, Denmark) in 1X Phosphate Buffered Saline (PBS) (Sigma Aldrich, Denmark) and left overnight. Later, excess laminin was removed and the flasks were washed twice with sterile water (Sigma Aldrich, Denmark). The Dulbecco's Modified Eagle medium/Ham's Nutrient Mixture F12 supplemented with 10% fetal bovine serum, 10% horse serum, 100 Units/mL penicillin and 100 μg/mL streptomycin and 25 mM HEPES (referred to as DMEM/F12 from now on) was added in the flasks and placed at 37 ℃ in humid atmosphere containing 95% air and 5% CO_2.

A vial containing approximately 4×10^6 cells (PC12-pheochromocytoma of rat adrenal medulla, DSMZ GmbH) was thawed and transferred to the above flasks and placed in the incubator. After 2 days the media was removed and replaced with DMEM/F-12 supplemented with 100 ng/mL Neurite Growth Factor (NGF). The cell media was changed every 2 days. After 5 days, the cells were

detached by adding 0.05% trypsin-EDTA (Sigma Aldrich, Denmark) at 37 ℃ for 3 min. The cell suspension was transferred to a 10 mL Falcon tube with fresh media and centrifuged at 1,100 rpm for 3 minutes. The supernatant was removed and the pellet was resuspended with media at 1×10^6 cells/mL. The centrifugation process and the resuspension of the cells in fresh media are done in order to remove the trypsin.

The cells were then seeded in a Petri dish containing the electrode chip and supplemented with DMEM/F-12 with NGF. Before seeding the cells, the electrode chips were sterilised with acetone at 70 ℃ for 5 min followed by three times wash in 70% ethanol for 5 min. The chips were washed with 1× PBS three times and then coated with laminin, as previously described. After 32 hrs, two thirds of the culture medium was removed, the culture was fixed on the surfaces with 4% paraformaldehyde fixative solution (4% of paraformaldehyde in 0.1 M PBS) for 15 min and the fixative solution was removed. The sample was analyzed using a ZEISS Axio microscope with 20× and 50× magnification.

For Scanning Electron Microscope (SEM) imaging, the cells were fixed in 2% glutaraldehyde in 0.1 M PBS for an hour. The sample was rinsed in 0.1 M PBS for 15 minutes at 4 ℃ and washed with deionized water for 5 minutes. The sample was dehydrated with increased percentages of ethanol (50, 60, 70, 80, 90, and finally 100%) and freeze dried overnight.

3. Results and Discussion

3.1. Fabrication of Tall Electrodes

The fabrication of the tall electrodes gives them a characteristic scalloped shape that increases their surface area as compared to a 2D electrode or a conical 3D electrode (Figure 4).

Figure 4. The measurement of the height of the pillar should be corrected with the tilted angle with which the picture was taken in the SEM (30°), giving a value of 63.8 μm.

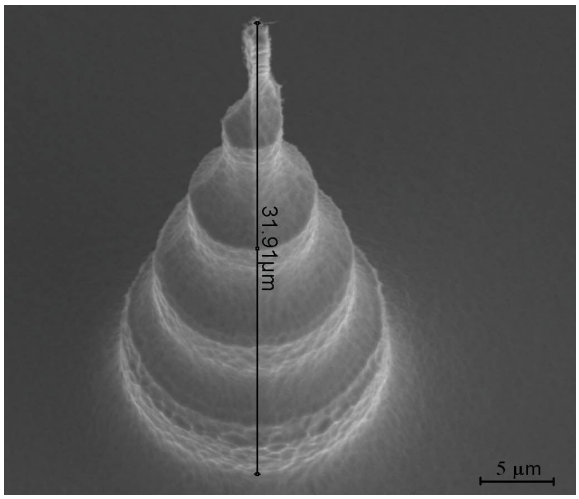

C.5 Publication V

Microfabricated 3D micro- and nanoelectrodes for neuron studies

Maria Dimaki[a*], Patricia Vazquez[b], Alessandro Aimone[a], Mark H. Olsen[a], Luigi Sasso[a], Romen Rodriguez-Trujillo[a] and Winnie E. Svendsen[a]

[a]Department of Micro- and Nanotechnology, Technical University of Denmark, Bldg. 345B, 2800 Kgs. Lyngby, Denmark
[b]Tyndall National Institute, University College, Cork, Lee Maltings, Mardyke Parade, Cork, Ireland

[*]Corresponding author: maria.dimaki@nanotech.dtu.dk

The purpose of this work is to develop novel 3D micro- and nanoelectrodes and pipettes by use of carefully optimised standard microfabrication techniques such as wet (by KOH) and dry silicon etching. Two types of electrodes have been fabricated and characterized: small nanoelectrodes to be used for localised measurements on cell cultures and high aspect ratio scalloped microelectrodes for measurements in brain slices. All types of electrodes have been electrically and/or electrochemically characterized in order to confirm their functionality. Moreover, the high aspect ratio electrodes have been tested in terms of robustness by using them to penetrate a thick slice of PDMS. The pipettes fabricated have openings of the order of 500 nm, which makes them ideal candidates for localised stimulation of cell or brain slice cultures.

1. Introduction

Localised stimulation and measurement of signals from single neuron cells (both extra- and intracellular) in culture or inside brain slices is necessary in order to better understand the processes behind neuron communication and function. This kind of understanding can ultimately lead to the treatment of diseases for which little can be done today, e.g. Parkinson's disease, spinal cord injuries and even cancer [1,2].

Traditionally, planar electrodes in the form of the so called Micro Electrode Arrays (MEAs) have been used for recording signals from neurons and tissue slices, e.g. [3-8]. These, however, do not offer the possibility of intracellular measurements and in the case of brain slices, are placed far away from the signal source (the neurons deep inside the tissue), with a decreased signal-to-noise ratio as the consequence. 3D microelectrodes have been successfully developed [9] to counter these problems and several examples of their use can be found in the literature, e.g. [10-13].

The realization that 3D electrodes present higher signal-to-noise ratios due to their increased surface area [9, 14] and ability to reach neurons inside the dead cell layer surrounding tissue slices, led to an increased interest for fabricating novel 3D structures on several materials and with a variety of fabrication techniques, though most work has been done on high aspect ratio electrodes and reports of fabrication of smaller 3D electrodes are limited.

In this paper we will present the fabrication and characterization of both large and small electrodes and small pipettes, utilising and optimising wet and dry etching techniques. The small electrodes are optimised to have steep sidewalls and tips around 100 nm in order to be able to penetrate cells without killing them, while the large electrodes are optimised to achieve a high surface area and a conical shape for ease of penetration in tissue slices. Finally, some preliminary work on fabricating nanopipettes for localised stimulation of neuron cells will be presented.

2. Materials and methods

We have previously presented a fabrication process for 3D micro- and nanoelectrodes [14]. In the case of the small electrodes, the KOH wet etch based process resulted in very sharp structures, however, after isolation (by silicon oxide deposition) and metal deposition, the tip size was extended to dimensions around 500 nm – 1 µm, which is too big for cell penetration. In the case of the large electrodes, fabricated by a modified Bosch process, an SOI wafer was used with a highly doped top silicon layer in order to create a conductive path through the silicon and compensate for possible gaps in the metallization layer. To improve on these two issues, we have made some small but important changes in the fabrication process of both types of electrodes.

The fabrication process for the small electrodes is similar to that presented in [14] but with two essential changes. First, by utilising a high resistivity wafer (10000 Ω·cm instead of the previously used 1-20 Ω·cm) we avoid having to isolate the resulting pillars by a thick oxide layer. Thus we only grow a thermal oxide of 50 nm for isolation instead of the previously deposited 500 nm. Moreover, instead of using the standard KOH bath for the silicon etch of the electrodes, where circulation is achieved by flow from the bottom of the container to the top and with several unknown parameters in terms of age of the bath and silicon etched, we utilise a manual KOH bath, where the solution is fresh every time and where KOH circulation is achieved by magnetic stirring.

In the case of the large electrodes, the fabrication process has been further optimised in order to achieve a smoother scalloped profile by adding a final maskless isotropic etch at the end of the modified Bosch process, as reported in [14]. We have moreover calculated the increase in surface area of the electrodes as compared to a simple conical electrode, such as the one in [9] to be

equal to 1.52 [15] for electrodes 60 µm in height and 20 µm in radius, a small but significant increase which will further improve the signal-to-noise ratio.

For fabricating the nanopipettes a multistep process on two wafers was followed based on previous work [16], as sketched in figure 1. Briefly, starting with a double polished silicon wafer (1), dry silicon etching is used with optimised parameters in order to create tapered holes with surface diameter of 2 µm and bottom diameter of 1 µm (2). The wafer is then thermally oxidized (3) with 200 nm of oxide and bonded to a wafer where microfluidic channels have previously been patterned (4). Then the wafer is etched by dry etching until the tips of the oxidised holes are visible (5) and these are etched away by wet (HF) or dry silicon oxide etch (6) until an opening is formed. The wafer is then further etched until the needles have the required height (7).

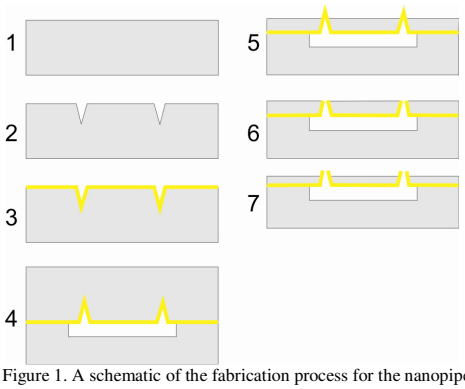

Figure 1. A schematic of the fabrication process for the nanopipettes.

Electrical characterization of the electrodes was performed with the setup previously described in [14] but for the small electrodes the solution for the characterization was a standard 1X phosphate buffered saline (PBS) solution. The electrochemical characterization of the small electrodes has been performed using a CH1000A multichannel potentiostat. The ferri/ferrocyanide redox reaction between $K_3[Fe(CN_6)]$ and $K_4[Fe(CN_6)]$ was monitored with the small 3D electrodes acting as the working electrodes, a Pt wire acting as the counter electrode and an Ag/AgCl electrode as reference. A potential scan rate of 200 mV/s was used and the voltage was varied between -0.2 V to 0.6 V since the peak of the test system is expected to be at 230 mV.

3. Results and discussion

We have previously reported [14] that due to the problems with the age and usage of the KOH bath the uniformity of the finished small electrodes was varying between 50 and 80%. By changing to the manual KOH bath with magnetic stirring the uniformity was almost perfect throughout the wafer. An image of an electrode before and after oxidation can be seen in figure 2, where it is evident that the electrode retains its structure and tip size even after the oxidation step. It can also be seen that the tips are formed by higher order planes in silicon, appearing due to the short etching times (4.5 – 5 min).

C.6 Publication VI

Sensors and Actuators A 172 (2011) 54–60

Contents lists available at ScienceDirect

Sensors and Actuators A: Physical

journal homepage: www.elsevier.com/locate/sna

Micro and nano-platforms for biological cell analysis

W.E. Svendsen*, J. Castillo-León, J.M. Lange, L. Sasso, M.H. Olsen, M. Abaddi, L. Andresen, S. Levinsen, P. Shah, I. Vedarethinam, M. Dimaki

DTU Nanotech, Technical University of Denmark, Building 345 East, 2800 Kgs, Lyngby, Denmark

ARTICLE INFO

Article history:
Available online 30 March 2011

Keywords:
Cell culturing
Cell sorting
Nanoelectrodes
Peptide nanotubes

ABSTRACT

In this paper some technological platforms developed for biological cell analysis will be presented and compared to existing systems. In brief, we present a novel micro cell culture chamber based on diffusion feeding of cells, into which cells can be introduced and extracted after culturing using normal pipettes, thus making it readily usable for clinical laboratories. To enhance the functionality of such a chamber we have been investigating the use of active or passive 3D surface modifications. Active modifications involve miniature electrodes able to record electrical or electrochemical signals from the cells, while passive modifications involve the presence of a peptide nanotube based scaffold for the cell culturing that mimics the *in vivo* environment. Two applications involving fluorescent in situ hybridization (FISH) analysis and cancer cell sorting are presented, as examples of further analysis that can be done after cell culturing. A platform able to automate the entire process from cell culturing to cell analysis by means of simple plug and play of various self-contained, individually fabricated modules is finally described.

1. Introduction

In vitro cellular analysis has paved the way to major breakthroughs in the history of biology and drug discovery. However, no matter how good *in vitro* experiments are, they will never be able to represent the *in vivo* situation fully. But since *in vivo* experiments are expensive and sometimes unethical, researchers strive towards developing modifications of lab-on-a-chip systems so that they better mimic the environment experienced by cells inside the body. Micro- and nanotechnology are two very promising technologies for achieving *in vivo* like conditions. A recent example is the mimicking of the human kidney using microfluidic chambers [1]. In this paper we will illustrate the advantage of microfluidic handling of cells in combination with nano- and microsensing platforms.

For cellular analysis it is often necessary to culture the cells. The standard methods used for this, e.g. culture flasks, do not in any way represent the *in vivo* situation. Here we will demonstrate a microfluidic culturing system for adherent and non adherent cells, with controlled environment and diffusion based feeding, but without flushing away important signalling chemicals. Then a discussion of the surface of the culturing system is given, where a novel 3D nanopattern method is investigated to mimic *in vivo* conditions, where no smooth glass or plastic surfaces exist.

Probing intercellular dynamics and intercellular signalling is at the research frontiers for understanding cellular function. Therefore, new technologies to address these issues are developing fast. It has been demonstrated that cells can survive penetration by nanoscale structures [2]. The obvious next step is to utilize this fact for probing the dynamics of the interior of living cells. Novel methods for fabricating 3D micro- and nanoelectrodes for this purpose will be presented.

Sorting of different types of cells is also an interesting research area and one that has received a fair amount of attention. Several methods have been used, both physical, based on cell dimensions alone, e.g. bumper arrays [3], biological, based on functionalizing substrates with proper markers binding on specific cell types [4], and electrical, based on differences in the dielectric properties of cells, e.g. dielectrophoresis [5] or electrorotation [6]. We here present the use of dielectrophoresis in order to sort cells expressing stress markers on their surfaces from cells without stress markers.

As a final point, the concept of a microfluidic motherboard, equipped with valves, simple microfluidic devices, e.g. mixers, and sockets for accepting microfluidic chips for specific applications will be presented. This motherboard can by plug-and-play integrate any chip that fits a standard general specification, irrespective of material and fabrication process.

2. Cell culture microfluidic bioreactor for adherent and non-adherent cells

Microfluidics enables cell culturing mimicking *in vivo* conditions [7,8], i.e. physical, biochemical and physicochemical properties such as pH, gas concentration and temperature, unlike the conventional culturing methods. Chemical gradients represent a very

* Corresponding author.
E-mail address: winnie.svendsen@nanotech.dtu.dk (W.E. Svendsen).

0924-4247/$ – see front matter © 2011 Elsevier B.V. All rights reserved.
doi:10.1016/j.sna.2011.02.027

C.7 Publication VII

Available online at www.sciencedirect.com

ScienceDirect

Procedia Engineering 00 (2009) 000–000

Procedia Engineering

www.elsevier.com/locate/procedia

Proc. Eurosensors XXIV, September 5-8, 2010, Linz, Austria

Micro And Nano-Platforms For Biological Cell Analysis

W. E. Svendsen, J. Castillo-Leon, J. M. Lange, L. Sasso, M. H. Olsen, L. Andresen, S. Levinsen and M. Dimaki

DTU Nanotech, Technical University of Denmark, Building 345 east, 2800 Kgs. Lyngby, Denmark

Abstract

In this paper some of the technological platforms developed in our group for biological cell analysis will be highlighted. The paper first presents a short introduction pinpointing the advantages of using micro and nano technology in cellular studies. The issues of requiring transient analysis while working in a biological environment maintaining the cells viability and adding analyte are addressed and discussed. An example of a cell culturing chamber useful for both adherent and non-adherent cells, with the capability of adding analyte is given, a small discussion of in vitro cellular studies mimicking the in vivo situation is presented and an example of surface modification for cellular growth is described. Then novel electronic sensor platforms are discussed and an example of a nanosensor with electronic readout is given utilizing both micro- and nanotechnology. Finally an example of sorting cells using dielectrophoresis will be given, aiming at early cancer detection.

cell culturing; cell sorting; nanoelectrodes; peptide nanotubes

1. Introduction

In vitro cellular analysis has paved the way to major breakthroughs in the history of biology and drug discovery. However, no matter how good in vitro experiments are, they will never be able to represent the in vivo situation. But since in vivo experiments are expensive and sometimes unethical, researchers strive towards making in vitro experiments as in vivo like as possible. Micro- and nanotechnology are two very promising technologies for this purpose. A recent example is the mimicking of the human kidney using microfluidic chambers [1]. In this paper we will illustrate the advantage of microfluidic handling of cells in combination with nano and micro sensing platforms.

Standard methods for culturing cells do not in any way represent the in vivo situation. An example is the surface of such systems; no smooth glass or plastic surfaces exist in vivo. For cellular analysis, probing intercellular dynamics and intercellular signaling is at the research frontiers for understanding cell function, therefore new technologies to address these issues are developing fast. It has been demonstrated that cells can survive penetration by nanoscale structures [2]. The obvious next step is to utilise this fact for probing the dynamics of the interior of living cells. Novel methods for fabricating 3D micro- and nanoelectrodes for this purpose are therefore needed. Sorting of different types of cells or of cells at different states is also a well developed field of research. Several methods have been used, e.g based on cell dimensions alone [3], on functionalising substrates with proper markers binding on specific cell types [4] or on differences in the dielectric properties of cells [5]. In this paper dielectrophoretic sorting of cells with and without cancer markers is demonstrated.

C.8 Publication VIII

Vertically Aligned Patterned Peptide Nanowires for Cellular Studies

M. B. Taskin[*], L. Sasso[*a], I. Vedarethinam[*b], W. E. Svendsen[*c] and J. Castillo-León[*d]

[*]Department of Micro-and Nanotechnology, DTU
Room 224, Kgs. Lyngby 2800, Denmark, mehta@nanotech.dtu.dk
[a] luigi.sasso@nanotech.dtu.dk
[b] indumathi.vedarethinam@nanotech.dtu.dk
[c] winnie.svendsen@nanotech.dtu.dk
[d] jaime.castillo@nanotech.dtu.dk

ABSTRACT

In this study, we present the influence of vertically aligned diphenylalanine peptide nanowires (PNWs) on cell growth and adherence using PC12 cells. Following the cell growth study, we simply concluded that the PNWs promoted PC12 cells' growth compared to bare gold surfaces. Moreover, we show a technique for the patterning of PNWs down to 10 micron wide strips to further investigate cell behavior and functionalization possibilities. We also investigated how the structural properties of patterned nanowire strips could be used as a cell scaffold in combination with adherence enhancers such as laminin (LAM) .

Keywords: self assembly peptide nanostructures, cell culture, patterning, PC12, diphenylalanine

1 INTRODUCTION

Over the years, scientific studies have shown that one crucial point when designing biological platforms is the strict environmental conditions required for cell and tissue culturing, such as pH, temperature, medium content and other parameters which affect the system's biocompatibility.

Diphenylalanine is reported to be the core recognition peptide in amyloid fibrils that are responsible for Alzheimer's disease [1]. Studies have revealed that diphenylalanine peptides with different functional groups and fabrication conditions can self-assemble into nanostructures such as nanowires, nanotubes, nanoparticles, and hydrogels. Self-assembled peptide nanostructures make an excellent candidate as a material for biological applications due to the inherent properties they hold, such as mechanical and chemical stability, various functionalization options, and mild, fast and inexpensive synthesis conditions [2].

Vertically aligned PNWs are grown by high temperature aniline vapor aging from thin amorphous diphenylalanine films [3]. Since their first report, PNWs aroused great attention among scientist. While some of the researches were focusing on discrete functionalization of PNWs to alter properties like hydrophobicity [4] and conductivity [5], others tooled with the patterning of PNWs and building up functional micro devices [6, 7]. Moreover it is strongly highlighted that we should expect a vast number of studies regarding 3D cell culture, drug delivery, bioimaging and biosensor development involving these biological nanostructures in the very near future [8].

Recently, our group has demonstrated that PNWs are a useful tool for cellular studies and sensor applications [9]. In this paper, we expand this study with different approaches. Firstly we cultured PC12 cells, which are neuronal stem cell models [10], onto different substrates (bare gold, laminin coated gold, PNWs on gold and laminin coated PNW on gold) to obtain an investigation of cell growth onto the mentioned surfaces. Secondly we patterned PNWs into strips of various widths onto a gold electrode surface by soft lithographic methods to evaluate the patterned structures' effects on cell growth and adherence using PC12 cells.

Combining this work with other approaches like discrete functionalization of PNW will reveal possible future platforms for cellular studies and biosensing.

2 EXPERIMENTAL

2.1 PNW Growth

PNWs were fabricated prior to experiments from freshly prepared 50 mg/ml diphenlyalanine solution in 1,1,1,3,3,3-hexafluoro-2-propanol (HFP) as described [3]. Gold surfaces were fabricated in cleanroom by e-beam evaporation on 10 nm titanium coated silicon wafers and were diced into 0.5 x 0.5 cm^2 squares. After placing a drop of peptide solution on the desired surfaces, samples were dried in a vacuum desiccator to obtain an amorphous film. Then the samples were located in a sealed chamber in the presence of aniline vapor, by including a separate container of aniline reagent in the chamber. The chamber was left for aniline aging in an oven for 14 hours at 120 °C.

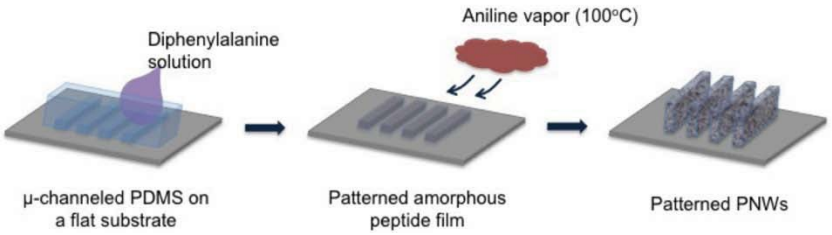

Figure 1 An illustration of PNW patterning using soft-lithorgapic methods.

2.2 PNW Patterning

PNWs were patterned onto substrates using a soft-lithographic method (see Fig. 1). PDMS stamps were fabricated in cleanroom using a patterned mask to etch channels with different dimensions on a silicon wafer. Etched silicon PDMS stamps with 10-20 μm wide micro channels used to fabricate PDMS molds. After locating the PDMS mold on a gold surface, a drop of peptide solution was introduced to the micro channels' openings and the channels were filled by capillary force. This process was followed by conventional PNW fabrication.

2.3 Cell Culturing

A thin laminin layer was introduced to the gold surfaces by 2 hours of direct contact with a 20 ug/mL laminin solution in cell culture tested water. The coated surfaces were washed two times with phosphate buffered saline solution (PBS).

PC12 cells in concentration of 10000 cells/ml were seeded onto the following surfaces: bare gold, LAM coated gold, PNWs on gold and LAM coated PNWs on gold. Cells were cultured in Dulbecco's Modified Eagle medium/Ham's Nutrient Mixture F12 supplemented with 10% fetal bovine serum, 10% horse serum, 100 Units/mL penicillin, 100 μg/mL streptomycin and 25 mM HEPES medium for one day before replacing the cell culture rmedium with a differentiating medium containing DMEM/F12 supplemented with 0.5% HS, 0.5% FBS, 100 μg/mL penicillin/streptomycin, 25 mM HEPES and 0.1 μg/mL Nerve Growth Factor (NGF). The samples were investigated after 48-96 by Optical and Scanning Electron Microscopy (SEM).

PC12 cells, in concentration of 330000 cell/ml were seeded on patterned PNWs on gold surfaces with and without LAM. The same cell culturing protocols and materials mentioned above were used for these experiments. Samples were investigated after 4 days of culturing.

2.4 Microscopy Imaging

Cell cultures were fixed prior to inspection with SEM. Direct contact of 2 wt/vol % gulataraldehyde solution in 0.1 M PBS was employed for fixation. After that, samples were rinsed twice with PBS for 5 minutes and washed with sterile water for 10 minutes. This step was followed by dehydration step using ethanol in concentration of 60-70-80-90-100 vol/vol % respectively and the samples were air dried.

A FEI Nova 600 NanoSEM system (FEI Company, Oregon, USA) was used to obtain Low Vacuum SEM images of Patterned PNW cell cultures.

For the cell growth study, an optical microscope was used to count cells on 48^{th}-96^{th} hours of culture. Several areas of samples were scanned and an average number of cells that were observed was used to plot cell growth bars including standard deviations.

3 RESULTS AND DISCUSSION

The cell growth study has shown that PNWs were suitable scaffolds for PC12 cells. PNWs clearly promoted cell adherence compared to bare gold surfaces (see Fig. 2). More over results indicated that introducing a standard protein adherence enhancer, laminin, increased cell growth as expected. It is also important to note that PNWs coated by LAM yielded a more favorable environment than LAM coated gold surfaces.

The patterning of PNW strips with widths of 10-20 μm were successfully done using the techniques mentioned above. The structures and morphology of the patterned nanostructures were found to be exactly the same as in the case of unpatterned PNWs.

C.9 Publications IX and X

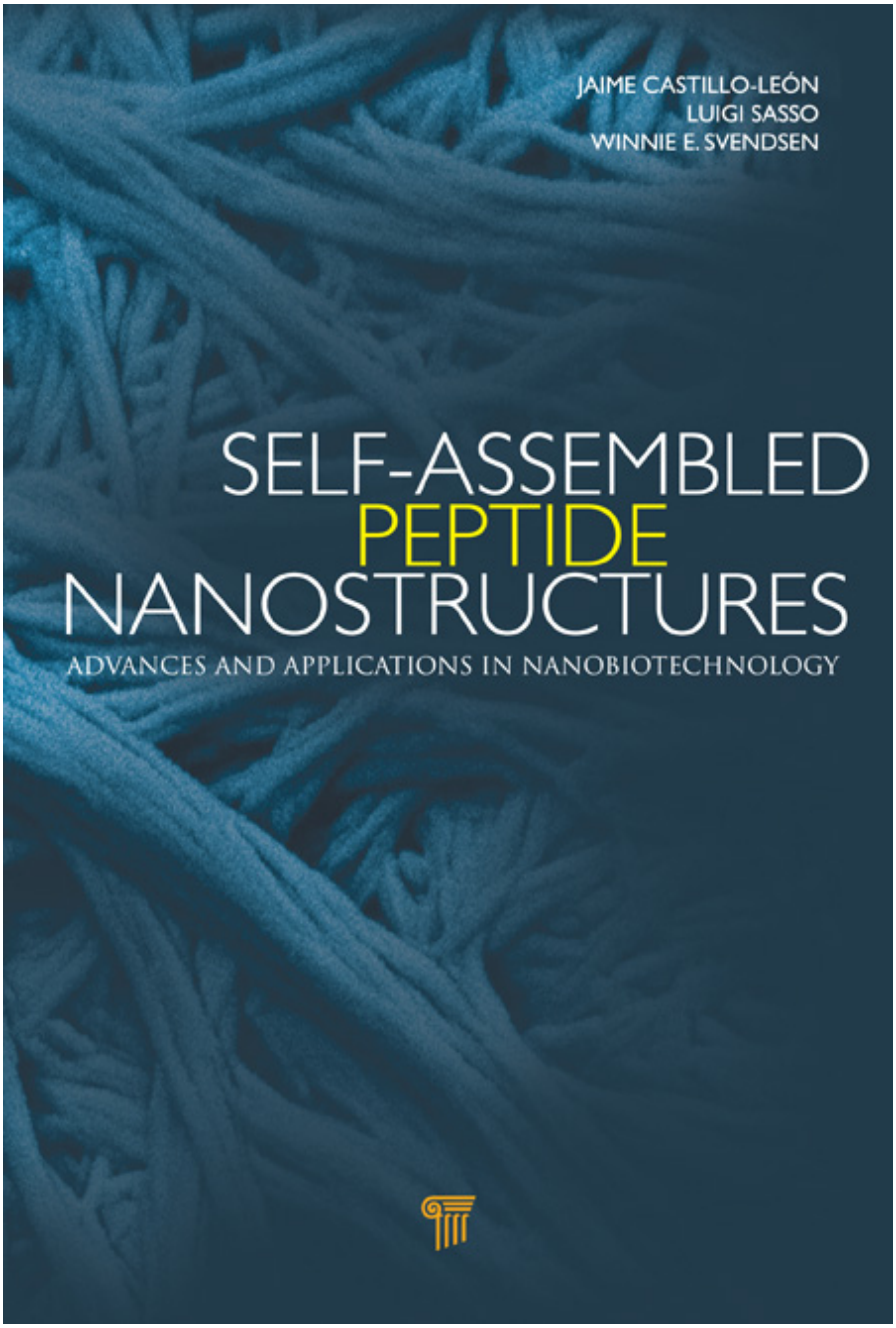
JAIME CASTILLO-LEÓN
LUIGI SASSO
WINNIE E. SVENDSEN
SELF-ASSEMBLED
PEPTIDE
NANOSTRUCTURES
ADVANCES AND APPLICATIONS IN NANOBIOTECHNOLOGY

C.10 Publication XI

Diphenylalanine: a short molecule with a big impact

(By Jaime Castillo-León, Luigi Sasso, Winnie Svendsen, Nano Bio Integrated Systems Group (NaBIS)
DTU Nanotech, Technical University of Denmark)

The self assembling peptide diphenylalanine can be used to create functionalised nanostructure applications like contrast imaging, photo thermal therapy, drug delivery or biosensor fabrication.

Diphenylalanine (FF), the core recognition motif of Alzheimer's β-amyloid polypeptide is a small aromatic dipeptide able to self-assemble into 3D nanostructures under very mild conditions (room temperature, aqueous conditions) without the need of specialized equipment. This self-assembled peptide plays a potential role in the formation of amyloid fibers involved in Alzheimer's disease. However, despite this negative connection with neurological diseases, diphenylalanine has found a long list of applications in different areas ranging from electrochemistry and biomedicine to applications in clean-room fabrication processes.

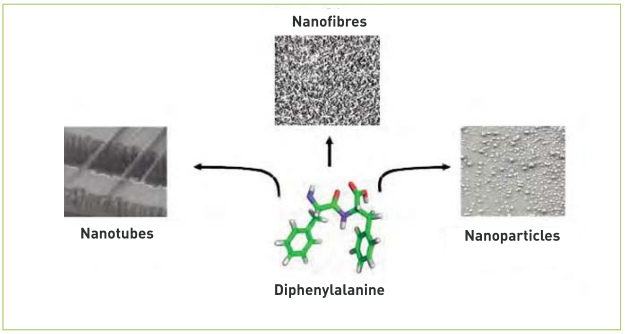

Around eight years ago Professor Ehud Gazit and Meital Reches at Tel-Aviv University described a simple method to obtain peptide nanotubes by using diphenylalanine [1]. This method proved to be fast, facile and low-cost compared with other methods used for the fabrication of more traditionally used nanostructures such as carbon nanotubes or silicon nanowires. Since then, a constantly increased number of scientific publications dedicated to the study, characterization and application of this short dipeptide have been reported [2, 3].

Why use diphenylalanine? One of the more obvious answers to this question is the fact that, as mentioned before, this building block is able to self-organize into 3D nanostructures in a very fast way at room temperature. Gorbitz reported the visualization of peptide structures a few seconds after mixing a solution of the dissolved peptide in 1,1,1,3,3,3-hexafluoro-2-propanol [4]. Recently the on-chip fabrication of nanotubes and nanoparticles was reported, which allows the synthesis of nanostructures with a more uniformly defined size [5]. A second advantage is that different types of structures can be obtained by changing the synthesis conditions. In this way, nanotubes, nanofibres o nanoparticles can be easily obtained.

Dyphenilalanine nanostructures have been structurally, electrically and chemically characterized [6-9]. The fabricated nanostructures can be decorated with a variety of functional molecules such as enzymes, metallic or magnetic nanoparticles, fluorescent molecules or quantum dots, among others [10]. This gives researchers the opportunity to obtain functionalized biological nanostructures with potential to be used in different applications like contrast imaging, photo thermal therapy, drug delivery or biosensor fabrication to mention a few.

It was recently shown that diphenylalanine nanotubes are extremely resistant to the bombardment of fluoride ions in a microfabrication process call reactive ion etching. This property was used for the fabrication of silicon nanowires using diphenylalanine peptide tubes as etching mask [11]. This fabrication method was faster, cheaper and reduces the use of chemical reagents during the process.

Preliminary toxicity studies involving the growth of cells in the presence of diphenylalanine peptide nanostructures demonstrated that cells such as PC-12, HeLa or Chinese ovary cells can grow on top of nanowires or hydrogels fabricated with the short peptide [12, 13]. However, since these nanostructures have been suggested as candidates for the development of drug delivery systems and for tissue reparation experiments, a detailed study is necessary in order to obtain a more clear insight of the toxicity and immune response generated by these nanostructures.

It is also necessary to mention that despite all these advantages, there are several challenges that need to be confronted when working with these nanostructures. These challenges involve their low conductivity, their manipulation, their solubility in liquid solutions and the intriguing different behaviours between nanotubes and nanowires as has been reported in several publications [6, 14].

Applications. Since the publication of the first report on the synthesis of diphenylalanine nanotubes an increased number of studies involving the use of these biological nanostructures in bionanotechnological